

FACILITY FORM 602

**N 69-14670**  
(ACCESSION NUMBER)

**107**  
(PAGES)

**CR 98210**  
(NASA CR OR TMX OR AD NUMBER)

(THRU)

**1**  
(CODE)

**17**  
(CATEGORY)



**Alexandria Division**  
AMERICAN MACHINE & FOUNDRY COMPANY

DEVELOPMENT OF  
LIGHT WEIGHT MAGNESIUM ALLOYS FOR  
LOW TEMPERATURE APPLICATIONS

Final Summary Report

March 21, 1966 through March 25, 1967

Contract No. NAS 8-11168

March 20, 1967

H. W. Leavenworth, Jr.  
F. J. Dunkerley

AMERICAN MACHINE & FOUNDRY COMPANY  
ALEXANDRIA DIVISION  
1025 NORTH ROYAL STREET  
ALEXANDRIA, VIRGINIA

GEORGE C. MARSHALL SPACE FLIGHT CENTER  
NATIONAL AERONAUTICS AND SPACE ADMINISTRATION  
HUNTSVILLE, ALABAMA

## ACKNOWLEDGEMENT

This report was prepared by the Alexandria Division of the American Machine & Foundry Company under Contract No. NAS 8-11168, "Development of Light Weight Magnesium Alloys for Low Temperature Applications", for the George C. Marshall Space Flight Center of the National Aeronautics and Space Administration. The work was administered under the technical direction of the Propulsion and Vehicle Engineering Laboratory, Engineering Materials Branch of the George C. Marshall Space Flight Center with Dr. Karl J. Pschera acting as project manager.

Acknowledgement is given to Hugh F. Develin, Richard C. Bond and Lyle R. Mullen who assisted in the experimental aspects of the magnesium alloy development, to Elizabeth C. Hoskins for performing the chemical analyses of the alloys, and to Dr. Elihu A. Schatz for supervising the reflectance measurements.

## TABLE OF CONTENTS

	<u>Page</u>
1.0 INTRODUCTION	1
1.1 Program Planning	1
2.0 TECHNICAL REVIEW OF PROGRAM COMPLETED DURING THE PERIOD 20 MARCH 1966 THROUGH 20 MARCH 1967	4
2.1 Selection of Alloying Compositions	4
2.2 Melting and Casting	9
2.3 Fabrication, Cast Billet to Sheet Technology	22
2.3.1 Metallography Review of Matrix IV and Matrix V	23
2.3.2 Metallography Studies of Second Generation Alloys	31
2.4 Mechanical Properties - Ambient and Cryogenic Temperatures	43
2.4.1 Tensile Testing	43
2.4.2 Notch/Unnotched Tensile Strength	58
2.4.3 Weldability and Tensile Strength	58
2.5 Coatings Development	60
2.5.1 Commercial Coatings	61
2.5.2 Coating Developed in AMF Laboratory	64
2.5.2.1 Corrosion Resistant Chemical Conversion Coating, FSC-1	64
2.5.2.2 High Reflectance Coating Technology	65
2.6 X-Ray Studies	76
2.7 Machinability	76
2.8 Electrical Resistivity	78
2.9 Thermal Conductivity	79
2.10 Extrusion of Thin-Wall Tubing	80
2.11 Final Tensile Properties	83
2.11.1 Final II4 As-Rolled Properties and Thermal Stability	85
2.11.2 Mechanical Properties of Heat Treated Material	85
2.11.3 Cryogenic Testing of II4	86



## LIST OF FIGURES

<u>Figure</u>		<u>Page</u>
1.	Task Schedule	3
2.	The Original Statistical Alloying Plan for Selecting Alloying Compositions.	5
3.	Modification of Matrix I	6
4.	Alloying Compositions for the Preparation of 50 Pound Matrix	7
5.	Macrographs of Fractures Showing Results Obtained When Various Amounts of Hexachlorobenzene were Added to Matrix IV and Matrix V Alloys just Prior to Casting.	10
6.	Melting Crucible and Top Showing Entrance Port for Adding Alloying Elements to the Melt.	11
7.	Schematic Drawing of Foundry Facility for Melting 50 Pound Heats of Magnesium Alloys.	13
8.	Melting Facility for the 50 Pound Magnesium Pilot Melts	14
9.	Design of the Small-Ingot Casting Mold Showing Initial Dimensions of the Sprue and Runner.	15
10.	Opened View of Small Cast Iron Permanent Mold Showing An Enlarged Runner and the Final Ingate Design.	16
11.	Scale-Up Permanent Mold	17
12.	Opened View of a Nodular Iron Permanent Mold for Producing Three Inch Thick Ingots of Magnesium-Lithium Alloys	18
13.	Photomicrograph of Alloy ZLK972	20

<u>Figure</u>		<u>Page</u>
14.	Pilot Lot Ingot of Alloy II 4, Melt Number 4-8-2	21
15.	Photomicrograph of Alloy IV 2 As Cast	24
16.	Photomicrograph of IV 2 Alloy as Rolled	24
17.	Photomicrograph of IV 7 Alloy as Cast	25
18.	Photomicrograph of IV 7 Alloy as Rolled	25
19.	Photomicrograph of IV 9 Alloy as Cast	26
20.	Photomicrograph of IV 9 Alloy as Rolled	26
21.	Photomicrograph of V6 Alloy as Cast	27
22.	Photomicrograph of V6 Alloy as Rolled	27
23.	Photomicrograph of V7 Alloy as Cast	28
24.	Photomicrograph of V7 Alloy as Rolled	28
25.	Photomicrograph of V8 Alloy as Cast	29
26.	Photomicrograph of V8 Alloy as Rolled	29
27.	Photomicrograph of II 4 Alloy Rolled at 450 <sup>o</sup> F	32
28.	Photomicrograph of II 4 Alloy Rolled at 500 <sup>o</sup> F	33
29.	Photomicrograph of II 4 Alloy Rolled at 500 <sup>o</sup> F and Solution Heat Treated for 1 Hour at 600 <sup>o</sup> F.	34
30.	Photomicrograph of II 4 Alloy Rolled at 750 <sup>o</sup> F	35
31.	Photomicrograph of ZLH972 Alloy Rolled at 500 <sup>o</sup> F and Solution Heat Treated 1/2 Hour at 600 <sup>o</sup> F	36

<u>Figure</u>		<u>Page</u>
32.	Photomicrograph of ZLH972 Alloy Rolled at 500 <sup>o</sup> F and Solution Heat Treated for 1 Hour at 600 <sup>o</sup> F	37
33.	Photomicrograph of ZLH972 Alloy Rolled at 750 <sup>o</sup> F	38
34.	Photomicrograph of 1A6 Alloy Rolled at 500 <sup>o</sup> F and Solution Heat Treated for 1/2 Hour at 600 <sup>o</sup> F.	39
35.	Same Specimen as Shown in Figure 34, But at Higher Magnification.	40
36.	Photomicrograph of 1A6 Alloy Rolled at 500 <sup>o</sup> F and Solution Heat Treated for 1 Hour at 600 F.	41
37.	The Effect of Aging Time on the Mechanical Properties of Alloy II4	44
38.	The Effect of Testing Temperature on the Strength of Alloy II 4	45
39.	The Effect of Testing Temperature on the Percent Elongation of Alloy II 4	46
40.	The Effect of Aging Time at 200 <sup>o</sup> F on the Mechanical Properties of Alloy ZLH 972	47
41.	The Effect of Testing Temperature on the Strength of Alloy Z LH 972	48
42.	The Effect of Testing Temperature on the Percent Elongation of Alloy ZLH 972	49
43.	The Effect of Aging Time on the Mechanical Properties of Alloy 1A6	50
44.	The Effect of Testing Temperature on the Mechanical Properties of Alloy 1A6	51

<u>Figure</u>		<u>Page</u>
45.	The Effect of Testing Temperature on the Percent Elongation of Alloy IA6	52
46.	Welded Panels of Alloy IA6 Showing A Test Panel That Broke Upon Impact in an Area Outside the Weld.	59
47.	Spectral Total Reflectance (vs. MgO) of Coated Magnesium-Lithium Alloy ZLH972 from the Ultra-violet to the Infrared Region.	63
48.	Coated Specimens after One Month Exposure to the Marine Atmosphere.	66
49.	Spectral Total Reflectance of ZnO-Potassium Silicate.	69
50.	Spectral Total Reflectance of TiO <sub>2</sub> -Potassium Silicate	70
51.	Spectral Total Reflectance of TiO <sub>2</sub> -Lithium Aluminum Silicate	71
52.	Absolute Spectral Reflectance of a TiO <sub>2</sub> -Potassium Silicate Coating	73
53.	Absolute Spectral Reflectance of TiO <sub>2</sub> -Potassium Silicate, TiO <sub>2</sub> -Lithium Aluminum Silicate, and ZnO-Potassium Silicate Coatings	75
54.	Tubing of Alloys II4 and IA6	81
55.	Photomicrographs of Extruded Tubing of Alloys II4 and IA6	82
56.	Properties of As-Rolled Alloy II4 After Exposure to 150°F for Various Time Intervals.	84

Figure

Page

- |     |  |    |
|-----|--|----|
| 57. | Properties of Alloy II4 Solution Heat Treated Three Hours at 625°F and Heated at 150°F for Various Time Intervals. | 87 |
| 58. | Properties of Alloy II4 Solution Heat Treated Three Hours at 650°F and Heated at 150°F for Various Time Intervals. | 88 |
| 59. | Properties of Alloy II4 Solution Heat Treated Three Hours at 675°F and Heated at 150°F for Various Time Intervals. | 89 |

## ABSTRACT

The thirty-three month research program to develop light weight magnesium alloy(s) for cryogenic applications at subatmosphere temperatures as low as  $-423^{\circ}\text{F}$  has been completed. In this final twelve month period of the program all of the major goals of the research contract have been attained, as briefly summarized here.

Three alloys, having the nominal compositions,

II 4 - Mg + 1 Zr + 3 Th + 6 Zn + 5 Cd + 6 Ag + 7 Li

IA 6 - Mg + 3 Th + 9 Li + 2 Zn + 4 Al + 4 Ag + 1 Mn

ZLH 972 - Mg + 9 Zn + 7 Li + 2 Th

were found, when properly processed and heat-treated, to satisfy the major strength-ductility goals of the contract as well as most of the other specified fabrication characteristics. Specifically, II 4 either 1) as rolled initially at  $675^{\circ}\text{F}$  for ingot breakdown followed by finish rolling at  $450^{\circ}\text{F}$ , or, 2) as solution heat-treated at  $650^{\circ}\text{F}$  followed by thermal stabilizing aging at  $150^{\circ}\text{F}$ , exhibits tensile strength in excess of 45,000 psi (at  $68^{\circ}\text{F}$ ), yield strengths of more than 35,000 psi (at  $68^{\circ}\text{F}$ ) and minimum ductility values of 15%. These strength values are of course increased at  $-452^{\circ}\text{F}$ , with the expected reduction in ductility to the 8% minimum value required. Alloy IA 6 similarly, by rolling at  $260^{\circ}\text{F}$ , followed by solution heat treatment at  $600^{\circ}\text{F}$ , water quenching and then aging at  $200^{\circ}\text{F}$ , will yield the required strength properties. However, this composition was ultimately judged marginal because the long aging times needed to obtain the required 15% and 8% ductility at  $68^{\circ}$  and  $-452^{\circ}\text{F}$  respectively, often resulted in degradation of the strength properties below the goal limits. ZLH 972 alloy, when rolled at  $450^{\circ}\text{F}$ , heat-treated at  $600^{\circ}\text{F}$ , quenched and aged at  $200^{\circ}\text{F}$ , yields satisfactory strength and ductility properties as required but because of its sensitivity to embrittlement and tendency toward hot shortness at the usual hot working temperatures ( $600^{\circ}$  -  $675^{\circ}\text{F}$ ), its value as a commercial alloy is believed limited. Thus, on the basis of these goal-oriented deductions, the major emphasis has gradually shifted throughout the closing phase of this program to a comprehensive metallurgical study of the II 4 alloy.

All three alloys exhibit better than 90% welding efficiency by conventional MIG or TIG methods, are readily machinable, can be readily chemically milled, respond well to all conventional metal-forming operations (except that ZLH 972 is not readily extruded), and have notch/unnotched tensile ratios of 1.0 and 0.9 at  $68^{\circ}$  and  $-452^{\circ}\text{F}$  respectively. Other physical-mechanical properties of all



these alloys, and especially the II 4 composition, are also presented to implement their prospective commercial exploitation.

An adherent fused-salt chemical conversion coating was developed both for corrosion protection and as a paint base. Corrosion data in sea water indicate the coating has excellent sea environment corrosion protection characteristics. Furthermore, high reflectance coatings were readily applied to the conversion coated alloys to substantiate the prospective use of these alloys for aerospace structures.

## 1.0 INTRODUCTION

The purpose of this program was to develop a wrought magnesium alloy with improved thermal stability at 150°F and having the following mechanical properties and fabricating characteristics as goals at both ambient and cryogenic temperatures:

- a) 45,000 psi ultimate tensile strength at ambient temperature;
- b) 35,000 psi, 0.2% offset, yield strength at ambient temperature;
- c) 15% elongation (in 2") at ambient temperature;
- d) No deterioration of these properties to -452°F except elongation which may be a minimum of 8%;
- e) A notched/unnotched tensile ratio ( $K_t = 10$ ) of 1.0 or greater at ambient temperature, and 0.9 at -452°F;
- f) A weld joint efficiency of 80% or more at ambient temperature and weldability by MIG or TIG techniques equal to or greater than that of AZ 31B;
- g) For the melting and processing phase of the program, emphasis was placed upon obtaining high quality ingots and final wrought products free of dross.

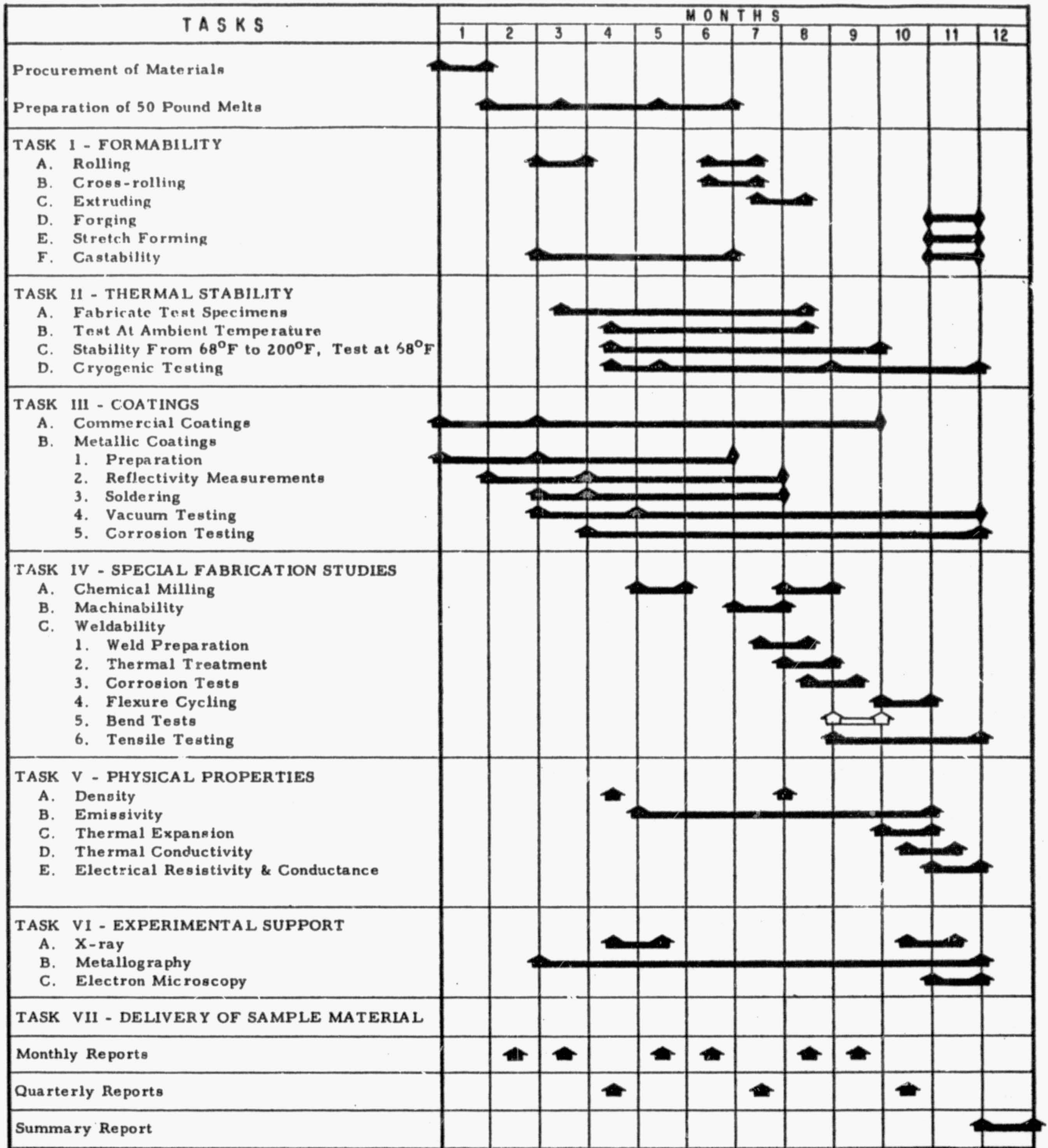
Three compositions were developed during the previous term of the present contract which went far in achieving the earlier goals. However, since these compositions were selected on the basis of limited mechanical property data, and because the wrought process procedures were not as thoroughly evaluated as desired, two major objectives of this final twelve month extension were to obtain additional strength property data on variously heat-treated sheet stock of the developed alloy(s) and to more comprehensively study and establish the optimum hot rolling practice for producing the alloy(s) in wrought sheet form. Additional objectives were: 1) to improve the long term thermal stability of the selected alloy(s) without detracting from the mechanical property goals, 2) to develop a coating not only to provide corrosion protection during handling and/or fabrication, but at the same time, to provide a suitable base for a thermal-radiator type coating to control the temperature of vehicles exposed to the extremes of darkness and bright solar energy in aerospace environments. Other concurrent objectives included obtaining general physical properties of the finalized alloy(s), evaluation of the response of the alloy(s) to extrusion-fabrication, and finally, obtaining some experimental evidence of their castability.

### 1.1 Program Planning

The results of the experimental program, implementing the above objectives during this final twelve month extension to Contract NAS 7-11168 originated more than thirty months ago, are presented in this Final Summary report. Emphasis is placed on data covering the period from March 20, 1966 to March 20, 1967, although appropriate summary data from the previous twenty-one month period

of the subject contract have often been introduced.

A chart reflecting the entire program schedule and planning is shown in Fig. 1. This chart does reflect modifications from the schedule proposed at the beginning of this contract period because events beyond our control often dictated the overlapping of the various phases of the program.



LEGEND:

SCHEDULE EVENT ▲

TIME SPAN ▬

EVENT COMPLETED ▬

MODIFIED FORECAST ◇

Figure 1. Task Schedule

## 2.0 TECHNICAL REVIEW OF PROGRAM COMPLETED DURING PERIOD FROM 20 MARCH 1966 THROUGH 20 MARCH 1967

During this entire thirty-three month program more than 100 different compositions were melted, cast into ingot shapes in cast-iron molds, hot rolled to 0.100"-0.150" thickness sheet, and thence studied comprehensively to establish their physical metallurgical and mechanical-physical property characteristics within the ambient and cryogenic temperature range. Initial compositions during the early months of the program were selected from three basic alloying systems, according to the matrix plan shown in Fig. 2, intended to evaluate alloying-element interaction as regards property effects on an economical and statistically sound basis.

### 2.1 Selection of Alloying Compositions

None of the alloys in Matrix I approached the ambient temperature strength requirements of the program so this alloy system was modified as shown in Matrix IA, Fig. 3. For example, the most promising of these compositions was alloy II4 (Mg - 1 Zr - 3 Th - 5 Cd - 6 Zn - 6 Ag - 7 Li) which had a tensile strength that varied from 36,000 psi to 51,000 psi at ambient temperature depending upon prior thermal-mechanical treatments. The remaining alloys studied during the course of the original program were cadmium and thorium variations of alloy II4.

Additional refinements to alloy II4 involved varying the lithium from 7 to 14% along with various amounts of aluminum, zinc, and silver; plus a further evaluation of magnesium-9% lithium alloys with various amounts of manganese, aluminum, zinc and silver. The composition of these preliminary melts is shown in Matrices IV, V, and VI in Figure 4. This development is exemplification of the initial approach to melt and cast all the alloys in each matrix for screening purposes and then to modify the composition of the most promising alloy for final optimization of mechanical properties. This approach worked well for Matrix II and Matrix IA, and a good comparison was made between the properties of these alloys. On the other hand, a great deal of time was spent on fabrication studies of 18 alloys from Matrix I and Matrix III without promising results. In order to eliminate time wasted in processing alloys with little change of meeting the contractual goals, the plan of approach was changed slightly. In the new approach, three alloys were selected from each matrix for processing, and, based upon the mechanical properties of these three alloys, the remaining alloys in the matrix were either eliminated from the program, processed as originally planned, or modified in composition to incorporate the latest scientific alloying principles developed during the course of the program.

MATRIX I

Basic Alloy - Pure Mg

	0.05 Li	0.2 Li	1.0 Li
.25 Mn	1 3 Al 6 Zn	2 8.5 Al 3 Zn	3 12 Al 1 Zn
.75 Mn	4 12 Al 3 Zn	5 3 Al 1 Zn	6 8.5 Al 6 Zn
1.5 Mn	7 8.5 Al 1 Zn	8 12 Al 6 Zn	9 3 Al 3 Zn

MATRIX II

Basic Alloy - Mg + 1 Zr + 3 Th

	5 Cd	10 Cd	20 Cd
2 Zn	1 2 Ag 2 Li	2 4 Ag 7 Li	3 6 Ag 12 Li
6 Zn	4 6 Ag 7 Li	5 2 Ag 12 Li	6 4 Ag 2 Li
12 Zn	7 4 Ag 12 Li	8 6 Ag 2 Li	9 2 Ag 7 Li

MATRIX III

Basic Alloy - Mg + 1 Zr

	0 Nd	1.5 Nd	3 Nd
0 Th	1 2 Zn 2 Ag	2 6 Zn 4 Ag	3 9 Zn 6 Ag
3 Th	4 9 Zn 4 Ag	5 2 Zn 6 Ag	6 6 Zn 2 Ag
5 Th	7 6 Zn 6 Ag	8 9 Zn 2 Ag	9 2 Zn 4 Ag

Figure 2. The Original Statistical Alloying Plan for Selecting Alloying Compositions



MATRIX IA

Basic Alloy - Mg - 3 Th - 9 Li

	$\frac{1}{2}$ Mn	$\frac{1}{2}$ Mn	1 Mn
1 Zn	1 0 Al 4 Ag	2 4 Al 2 Ag	3 2 Al 1 Ag
2 Zn	4 2 Al 2 Ag	5 0 Al 1 Ag	6 4 Al 4 Ag
4 Zn	7 4 Al 1 Ag	8 2 Al 4 Ag	9 0 Al 2 Ag

Figure 3. Modification of Matrix I

MATRIX IV

Basic Alloy Mg + 2 Th

	1 Al	3 Al	6 Al
3 Zn	1 1 Ag 12 Li	2 2 Ag 9 Li	3 0 Ag 7 Li
5 Zn	4 0 Ag 9 Li	5 1 Ag 7 Li	6 2 Ag 12 Li
7 Zn	7 2 Ag 7 Li	8 0 Ag 12 Li	9 1 Ag 9 Li

MATRIX V

Basic Alloy Mg + 2 Th + 9 Li

	$\frac{3}{4}$ Mn	$\frac{1}{2}$ Mn	$\frac{1}{4}$ Mn
0 Zn	1 1 Ag 3 Al	2 2 Ag 4.5 Al	3 0 Ag 6 Al
2 Zn	4 0 Ag 4.5 Al	5 1 Ag 6 Al	6 2 Ag 3 Al
4 Zn	7 2 Ag 6 Al	8 0 Ag 3 Al	9 1 Ag 4.5 Al

MATRIX VI

Basic Alloy Mg + 2 Th

	8 Li	12 Li	14 Li
2 Al	1 6 Cd 6 Ag	2 12 Cd 4 Ag	3 2 Cd 2 Ag
4 Al	4 2 Cd 4 Ag	5 6 Cd 2 Ag	6 12 Cd 6 Ag
6 Al	7 12 Cd 2 Ag	8 2 Cd 6 Ag	9 6 Cd 4 Ag

Figure 4. Alloying Compositions for the Preparation of 50 Pound Melts

The alloys from Matrix IV, Matrix V and Matrix VI selected for initial testing were:

- IV 2 (Mg - 2 Th - 2 Ag - 3 Al - 9 Li - 3 Zn)
- IV 7 (Mg - 2 Th - 2 Ag - 1 Al - 7 Li - 7 Zn)
- IV 9 (Mg - 2 Th - 1 Ag - 6 Al - 9 Li - 7 Zn)
- V 6 (Mg - 2 Th - 2 Ag - 3 Al - 9 Li - 2 Zn - 0.25 Mn)
- V 7 (Mg - 2 Th - 2 Ag - 6 Al - 9 Li - 4 Zn - 0.75 Mn)
- V 3 (Mg - 2 Th - 0 Ag - 3 Al - 9 Li - 4 Zn - 0.50 Mn)
- VI 2 (Mg - 2 Th - 4 Ag - 2 Al - 12 Li - 12 Cd)
- VI 5 (Mg - 2 Th - 2 Ag - 4 Al - 12 Li - 6 Cd)
- VI 8 (Mg - 2 Th - 6 Ag - 6 Al - 12 Li - 2 Cd)

The refinements to alloy II 4 made prior to selecting the first alloy for scale-up melting consisted of the following modifications to the basic composition:

- II 4 Mg + 1 Zr + 3 Th + 6 Zn + 5 Cd + 6 Ag + 7 Li
- II 4 A Mg + 1 Zr + 2 Th + 6.3 Zn + 5 Cd + 4.85 Ag + 9 Li
- II 4 B Mg + C<sub>6</sub>Cl<sub>6</sub> + 2 Th + 6 Zn + 2.5 Cd + 6 Ag + 8 Li
- II 4 C Mg + C<sub>6</sub>Cl<sub>6</sub> + 2 Th + 6 Zn + 5 Cd + 0 Ag + 9 Li
- II 4 D Mg + C<sub>6</sub>Cl<sub>6</sub> + 2 Th + 8 Zn + 0 Cd + 0 Ag + 7 Li
- II 4 E Mg + 2 Th + 6 Zn + 5 Cd + 0 Ag + 9 Li

Alloy II 4 A was a repeat of a modification to alloy II 4 that was developed earlier in the program and showed good strength and elongation values. Alloys II 4 B, C and D were designed to show the effect of varying the solute concentrations, with special emphasis placed upon eliminating silver from the family of alloys. Alloy II 4 E was selected to show the effect of eliminating hexachlorobenzene from alloy II 4 C, a 9% lithium alloy.

In each case the alloy was prepared in sheet form in 10-lb. lots and submitted to screening tests, before possible modification scale-up to 50-lb. lots and subsequent evaluation. On the basis of this approach, work on the present extension began with the preparation of 50-lb. lots of alloy sheet, followed by the comprehensive physical property studies of the three following nominal compositions, referred to subsequently as "Second Generation Alloys":

II 4 Mg + 1 Zr + 3 Th + 6 Zn + 5 Cd + 6 Ag + 7 Li

ZLH 972 Mg + 9 Zn + 7 Li + 2 Th

IA 6 Mg + 3 Th + 9 Li + 2 Zn + 4 Al + 4 Ag + 1 Mn

The technical aspects of every phase of alloy development from melting to ultimate property studies of the final composition(s) are presented in the following sections.

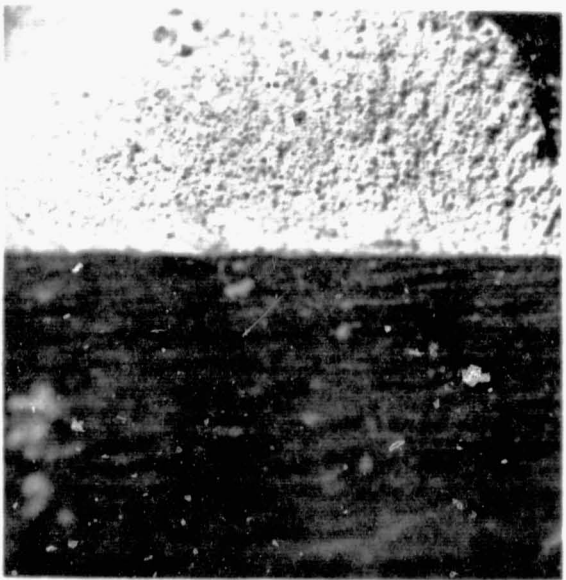
## 2.2 Melting and Casting

One of the important discoveries of the initial program was the fact that neither zirconium nor commercial grade silicon could satisfactorily effect grain refinement in magnesium alloys that contain more than 7% lithium. Chill casting was also not effective in producing a fine grain structure for alloys containing a large percentage of lithium. Similarly, the most common techniques of superheating used historically for grain refining the AZ series of magnesium alloys were not practical for lithium alloys. As a first approach those alloys not containing zirconium were grain refined with hexachlorobenzene, according to the present day foundry practice for AZ magnesium alloys. Typical results obtained are shown by the macrographs of fractures, Fig. 5, when various amounts of hexachlorobenzene were added to melts of the Matrix IV and Matrix V alloys just prior to casting. The resultant castings were characterized by a uniform, fine-grained structure; and the addition of three grams of hexachlorobenzene per ten pounds of melt appeared to be optimum.

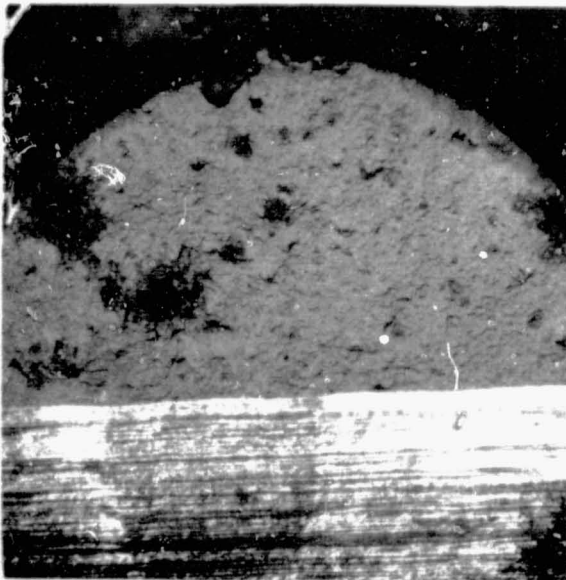
The initial crucible-furnace design is shown in Fig. 6. The strip chart recorders and temperature controllers appear in the background. All 10-lb. compositions were made in this type of closed iron crucible argon atmosphere furnace. Care should be taken in small crucible melting to fill the crucible only to about two-thirds of its molten-metal capacity to assure a greater volume of argon cover gas over the molten metal at all times during melting. The melting practice developed with this small furnace was applied to the operation of the 50-lb. melt furnace developed on the earlier program, and the former



Fracture of alloy V-6 bar made with an addition of 2g. of hexachlorobenzene per 10 lb. of melt. The melt was single screened and the dark particles are dross. Note the fine grained texture of the fracture which is shown at 5X.



Fracture of alloy V-7 bar made with an addition of 3g. of hexachlorobenzene per 10 lb. of melt. The melt was double screened and the dark areas are holes caused by the pulling out of material during fracture. The very fine grained texture of the fracture is shown at 5X.



Fracture of alloy IV-7 bar made with an addition of 3g. of hexachlorobenzene per 10 lb. of melt. The melt was not screened and the large dark areas are dross. The fine grained texture of the fracture is shown at 5X.

Figure 5.

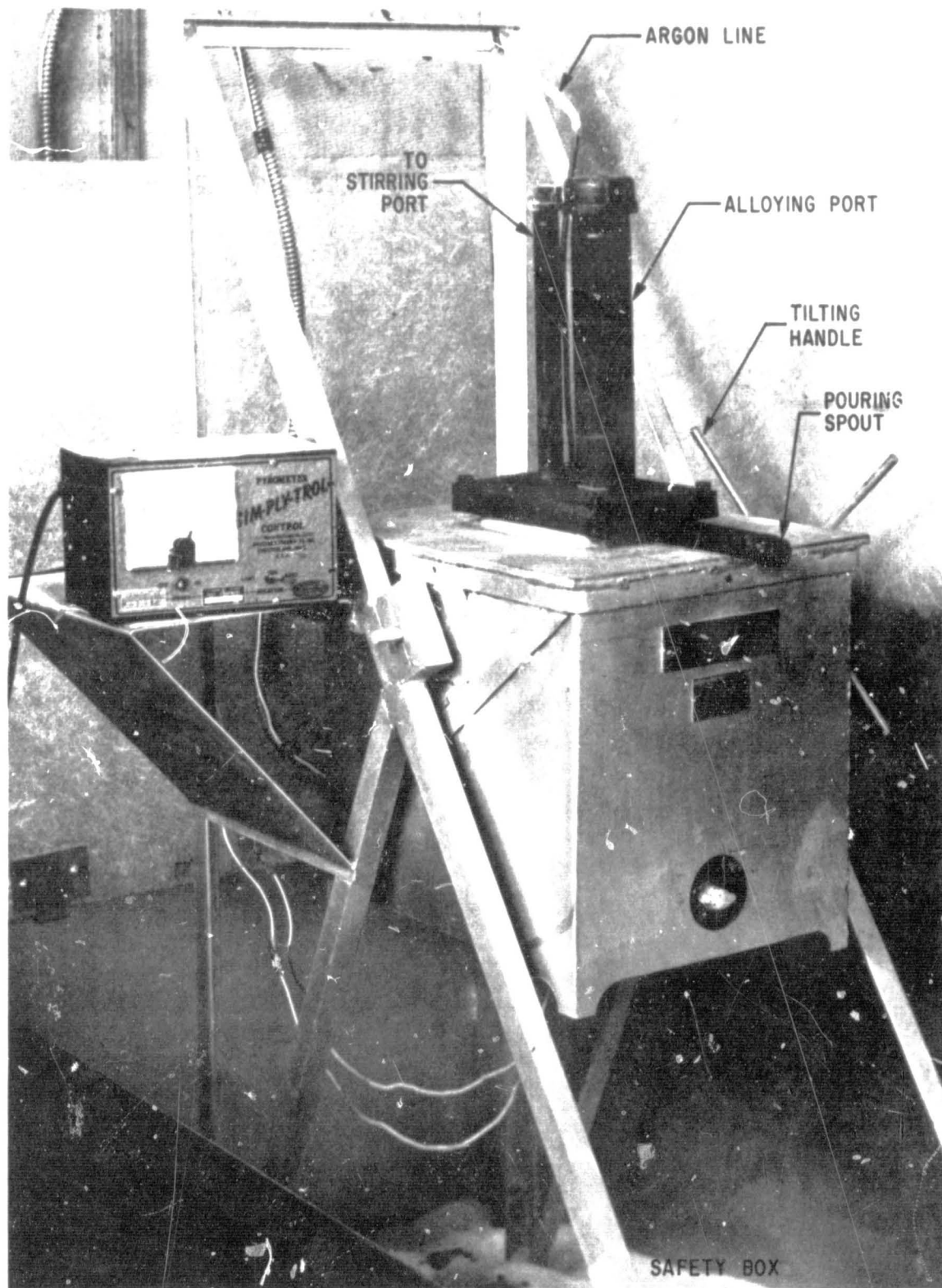


Figure 6 Melting Crucible and Top Showing Entrance Port for Adding Alloying Elements to the Melt



will be presented here in summary form. A sketch of the melting and casting technique used to make the 50-lb. melts is shown in Fig. 7 and a picture of the melting furnace with one of the crucibles in position is shown in Fig. 8. The melting procedure involves adding the pure magnesium charge to the melting crucible and sealing and flushing with purified argon before heating. After reaching the melting temperature the alloying elements are added through the alloying port and stirred into the melt by "puddling". As was done during preparation of the preliminary melts, lithium, thorium, zirconium and manganese are added as master alloys in order to obtain good recovery values. Hexachlorobenzene is added to melts of the ZLH 972 and I A 6 alloys while zirconium is added to alloy II 4 for grain refinement. The grain refiner is always added last just after adding lithium.

The 10-pound melts were cast into the permanent mold shown in Figs. 9 and 10. The preliminary melts of magnesium-lithium alloys that contained a large percentage of aluminum appeared to be sluggish, and the castings did not completely fill the mold. A fracture of each casting runner revealed some dross inclusions in the first castings. To alleviate the dross problem the mold sump was enlarged to accommodate a larger pair of concentric screens and recessed to prevent any molten metal from bypassing the screens. The runner diameter was also increased slightly for improved fluidity.

The 50-lb. melts were cast into the nodular cast-iron mold shown in Figs. 11 and 12. Various mold coatings were tried throughout the program, the most satisfactory being any one of several graphite-water glass formulations available from any foundry supply house. In all cases the mold was sprayed with several thin coats of mold coat, with the mold at 500°F-600°F prior to each melting campaign. The pouring practice developed for casting all ingot billets used for rolling stock was as follows:

The crucibles were prepared by cleaning them with 20% HCl followed by a 10% phosphoric acid treatment and bake-out at 250°F. The unalloyed magnesium charge was added to the crucibles at ambient temperature, and the crucible tops were securely bolted in place prior to flushing the chamber with gettered argon and heating to the melting temperature. A chromel-alumel thermocouple controlled the temperature next to the furnace windings at 1450°F  $\pm$  5°F which resulted in the molten metal being maintained at the temperature of 1350°F.

After reaching the melting temperature, the alloying elements were added to the melt through a port in the top of the crucible. For alloy ZLH 972, the following sequence was used: zinc, magnesium-thorium master alloy, magnesium-lithium master alloy, and, finally, the grain refiner. For grain refining hexachlorobenzene was added to alloys ZLH 972 and I A 6 while zirconium, in the form of a master alloy, was used in alloy II 4. For all three alloys the grain refiner was added after the melt temperature returned to a constant value near

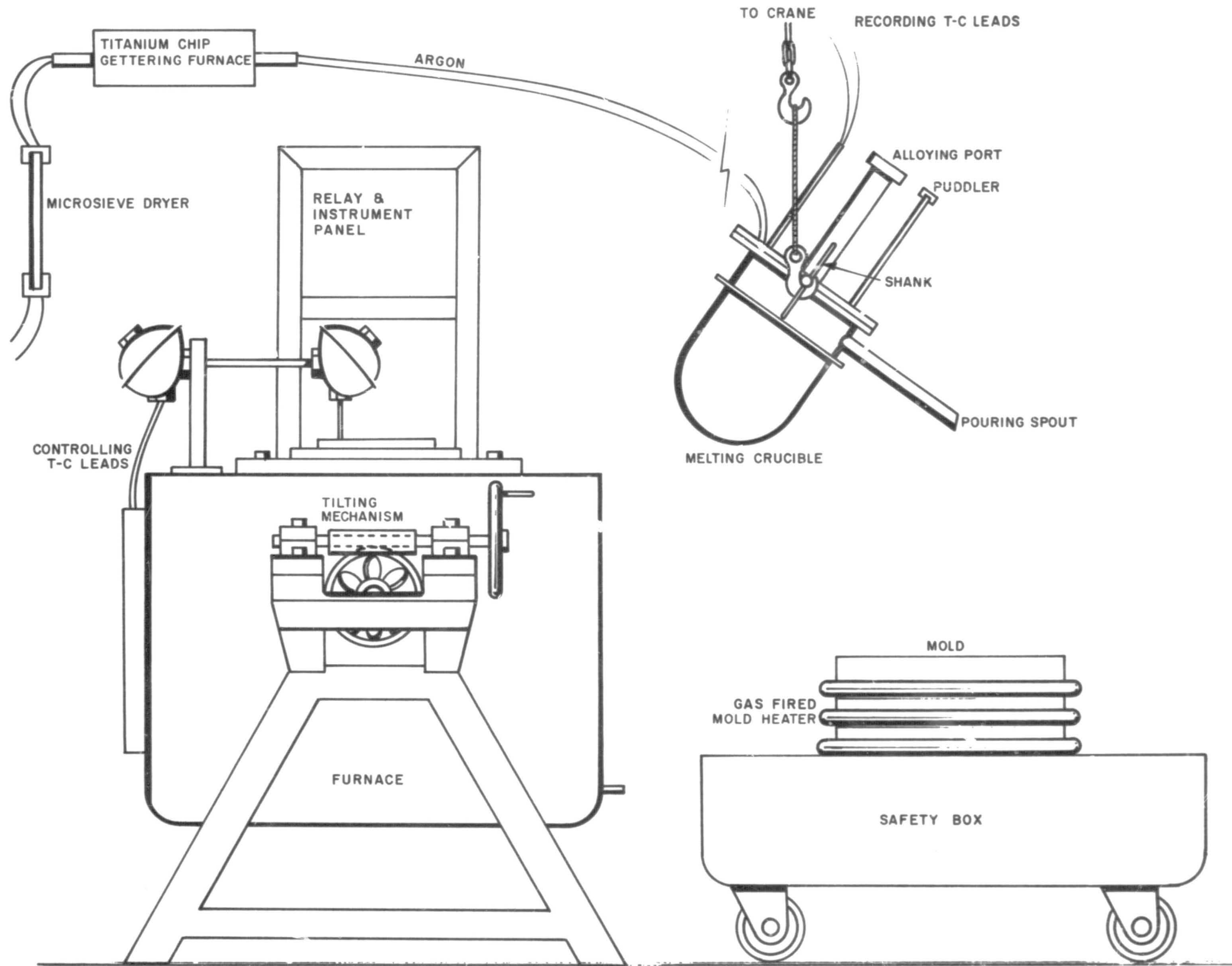


Figure 7. Schematic drawing of foundry facility for melting 50 pound heats of magnesium alloys.

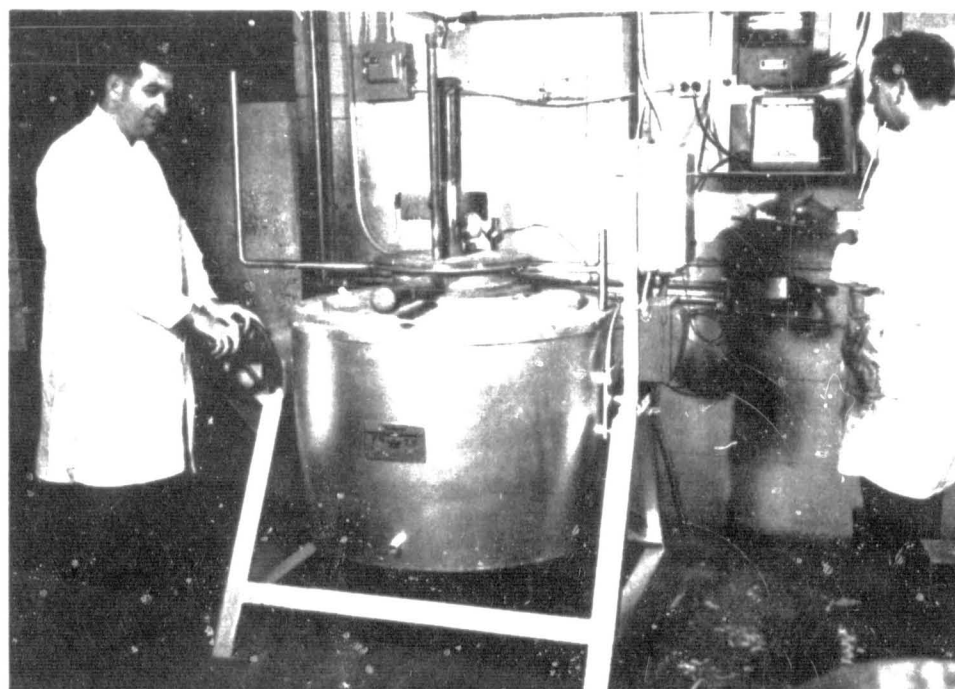


Figure 8. Melting Facility For The 50 Pound Magnesium Pilot Melts

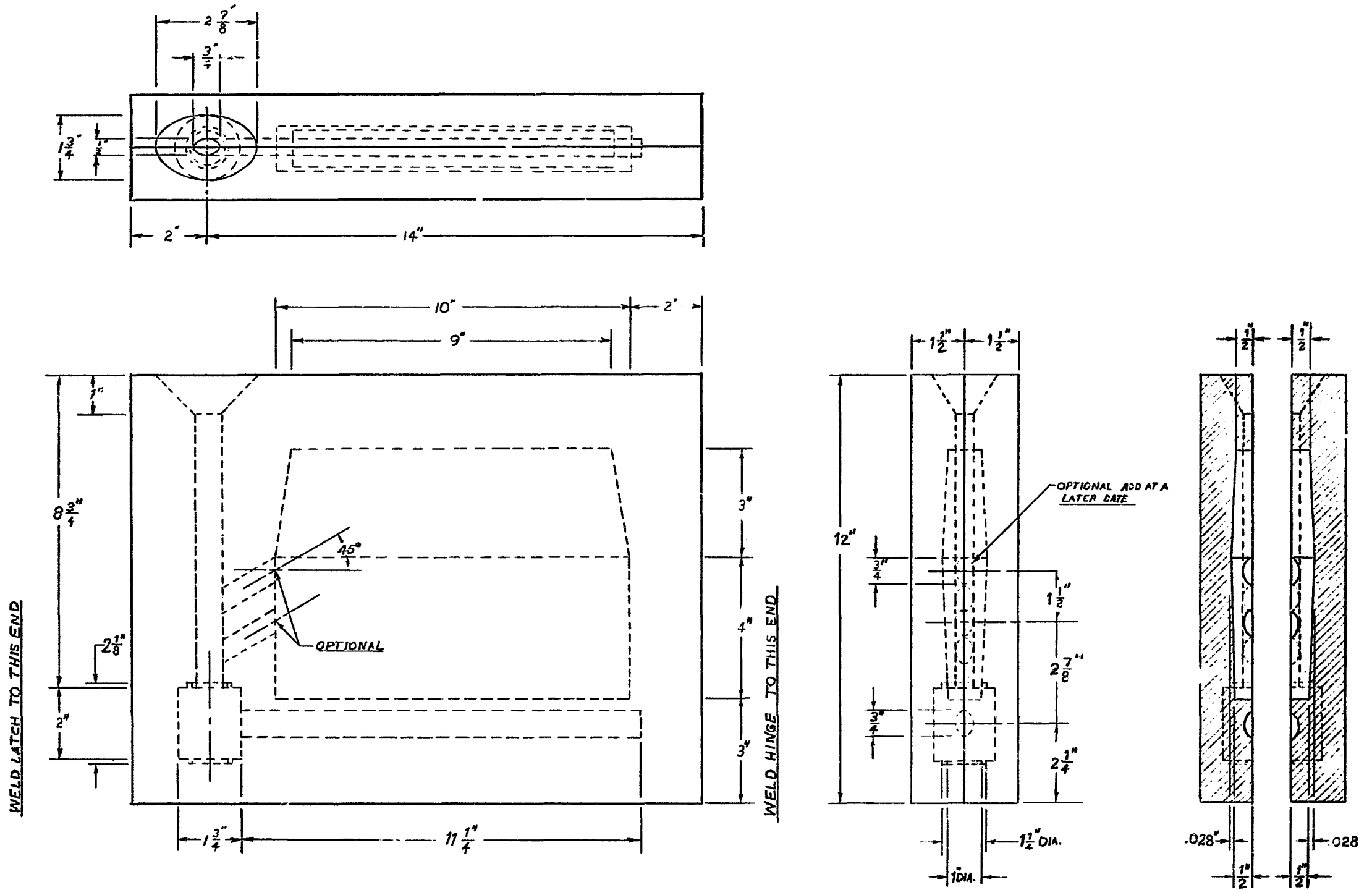


Figure 9. Design of the small-ingot permanent casting mold showing initial dimensions of the sprue and runner. A bottom ingate was added after trial castings. Note: The side tapers are exaggerated in the drawing for illustration.

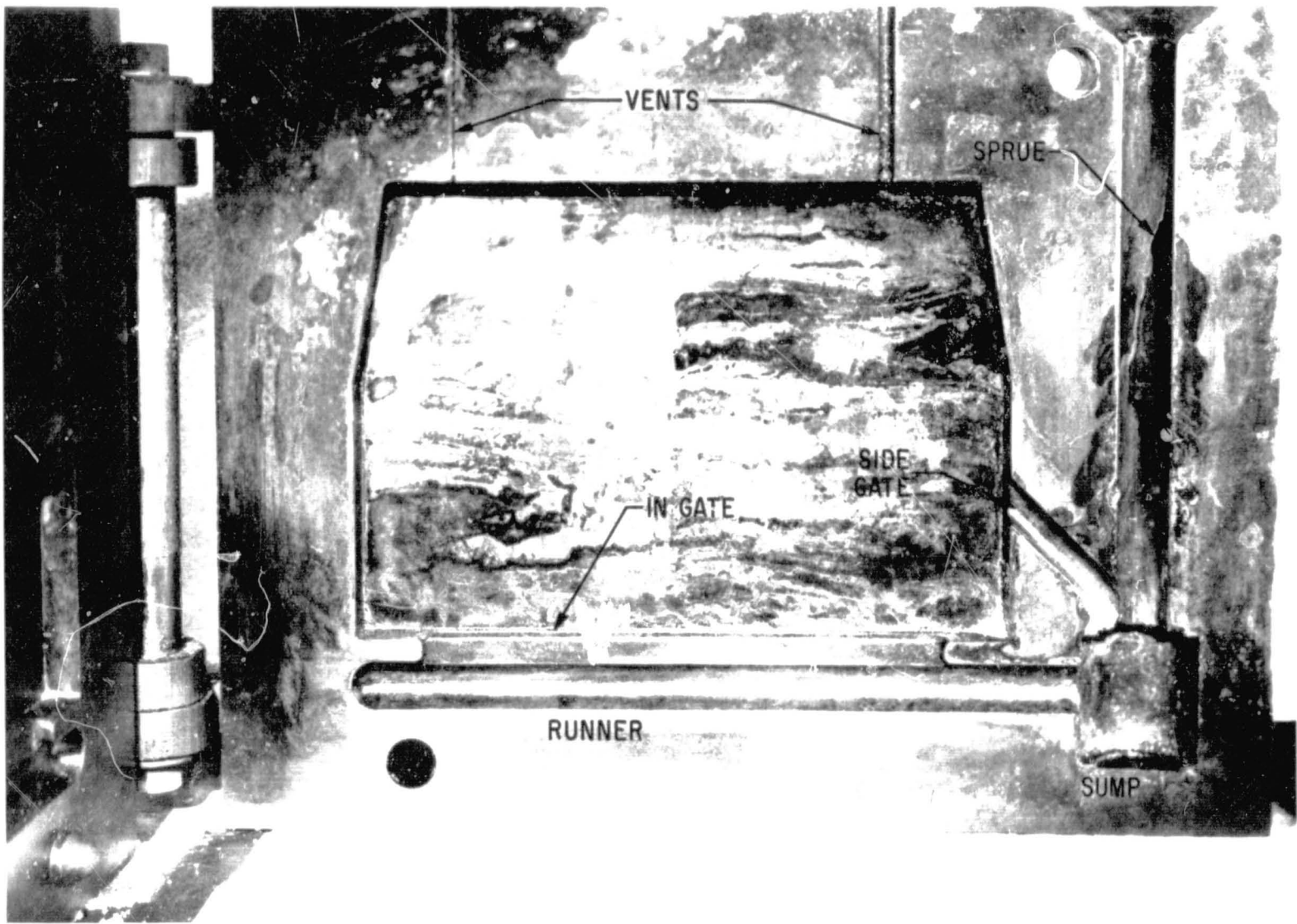


Fig. 10. Opened view of small cast iron permanent mold showing an enlarged runner and the final ingate design. The side gate was blocked off for most of the melts and inserts were used in the cavity to vary the size of the preliminary ingots for research purposes.

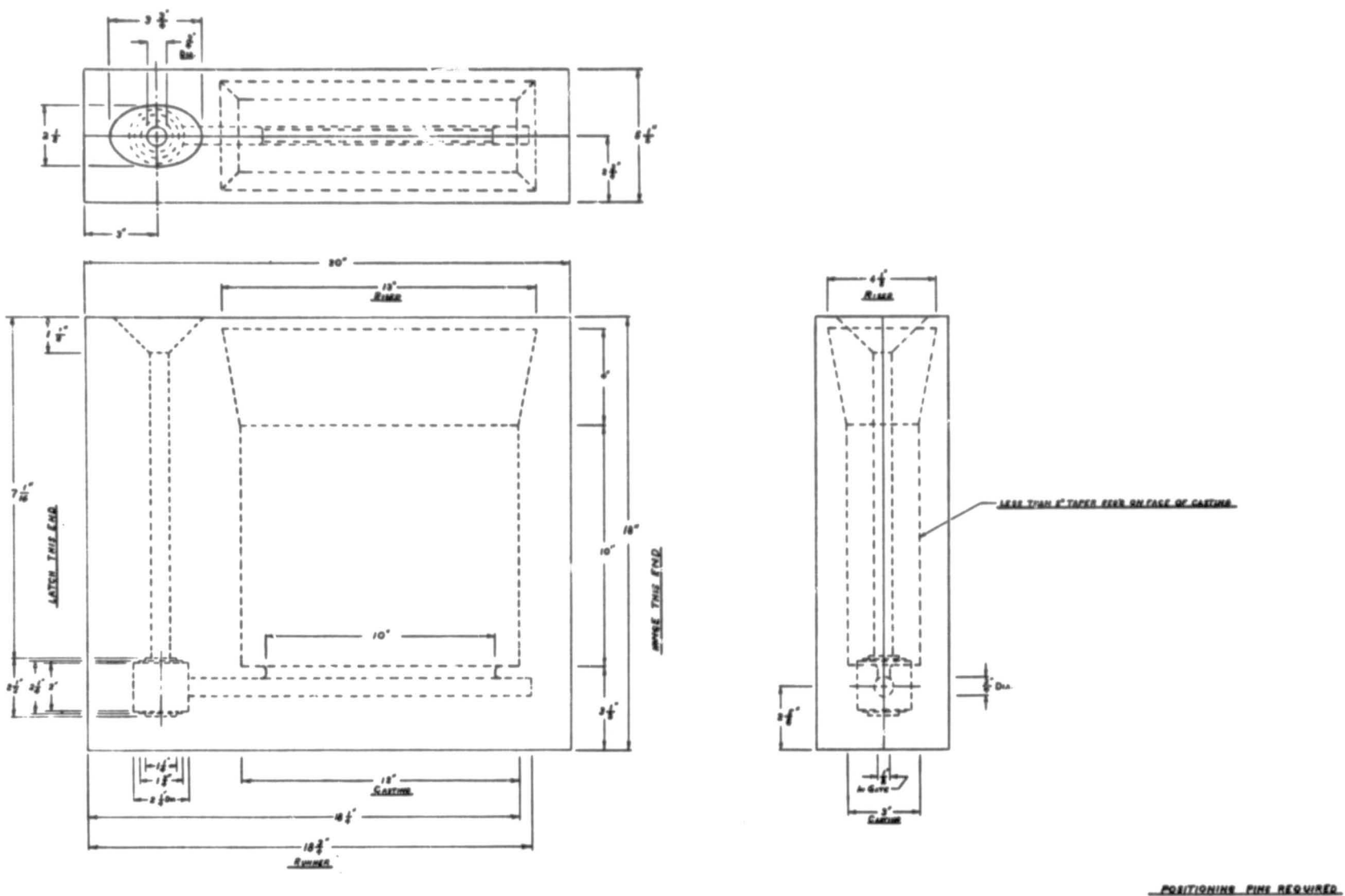


Figure 11. Scale-Up Permanent Mold

The design for the permanent mold used to produce the 50-lb. lots of each alloy is shown above. The sprue-to-runner-to-gate ratio was chosen to choke the molten stream of metal before it entered the mold cavity and thus reduce turbulence to a minimum. The sump is designed to incorporate concentric screens which will prevent dross from entering the mold cavity. The draft in the sides of the mold cavity is to provide for easy removal of the casting. Nodular iron was chosen for the mold material because of its superior machinability, stability and uniform quality.



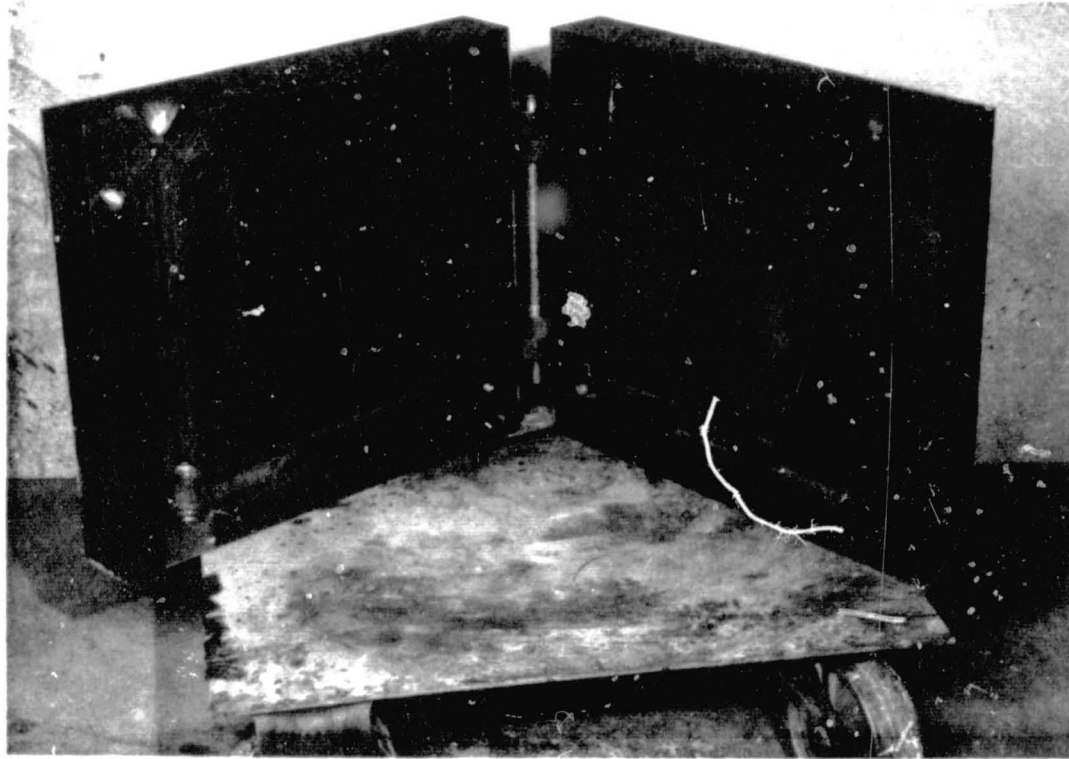


Figure 12. Opened View Of A Nodular Iron Permanent Mold For Producing Three Inch Thick Ingots Of Magnesium-Lithium Alloys

the pouring temperature.

After making final preparations and recording the melt temperature and the surface temperature of the mold, the melting crucible is lifted from the furnace by an overhead crane and lowered to the height of the mold where the cap is removed from the pouring spout. Removing the cap allows argon to escape ahead of the flowing liquid metal so that it can act as a protective blanket and, at the same time, flush the mold with argon ahead of the teemed metal.

During the melting sequence the permanent mold was heated to 500°F with a gas-air flame and immediately prior to casting, the mold was opened and a perforated screen containing (fluffed) steel wool was placed in the sump. The mold was closed and the molten metal teemed into a choked sprue until the mold would no longer accept molten alloy. After removing the casting from the mold the runners and sprues were fractured for a visual inspection of the quality of the metal. For all castings made by this procedure, the runner material was free of dross and the sprues appeared exceptionally clean. The castings themselves were cut into sections and no visible flaws or dross could be found.

While most of the castings were removed from the mold as soon as the metal was completely solidified, one casting of alloy ZLH 972 was allowed to cool slowly in the mold. This metal was extremely difficult to roll but was finally reduced to wrought sheet by a series of light reductions at 450°F. Specimens of this material were solution heat treated for three hours at 600°F and quenched rapidly. Fig. 13 is a photomicrograph of the cross sectional area of one of these specimens and shows that both a  $\alpha$  magnesium matrix and the white  $\beta$  phase contain numerous precipitates which did not go into solution at 600°F and which undoubtedly caused the rolling difficulties. As a standard practice, it is recommended that the compositions involved in this program be removed from the mold as quickly as it is practical to do so.

Using these procedures, castings were made of all three alloys, one of which is shown in Fig. 14 with the mold coating still adhering to the surface. The runners were usually fractured from these castings and the surface inspected for dross. In general, the final pouring operation for any final composition was made with a sprue and sump which would accommodate enough extra screening to insure that the metal would be choked in the sprue. The purpose of this provision is to permit no turbulence to occur in the teemed metal after it has passed through the sump screening. This, in turn, minimizes drossing and oxide inclusions in the final ingot billet.

The entrapped melting dross, variation in chemical composition, and resulting low tensile strength values obtained from materials made from the early melts were caused by a lengthy melting practice. A slow furnace heating rate, a sluggish rate of temperature recovery after making the master alloy additions, and time taken to double check all temperatures, contributed to the

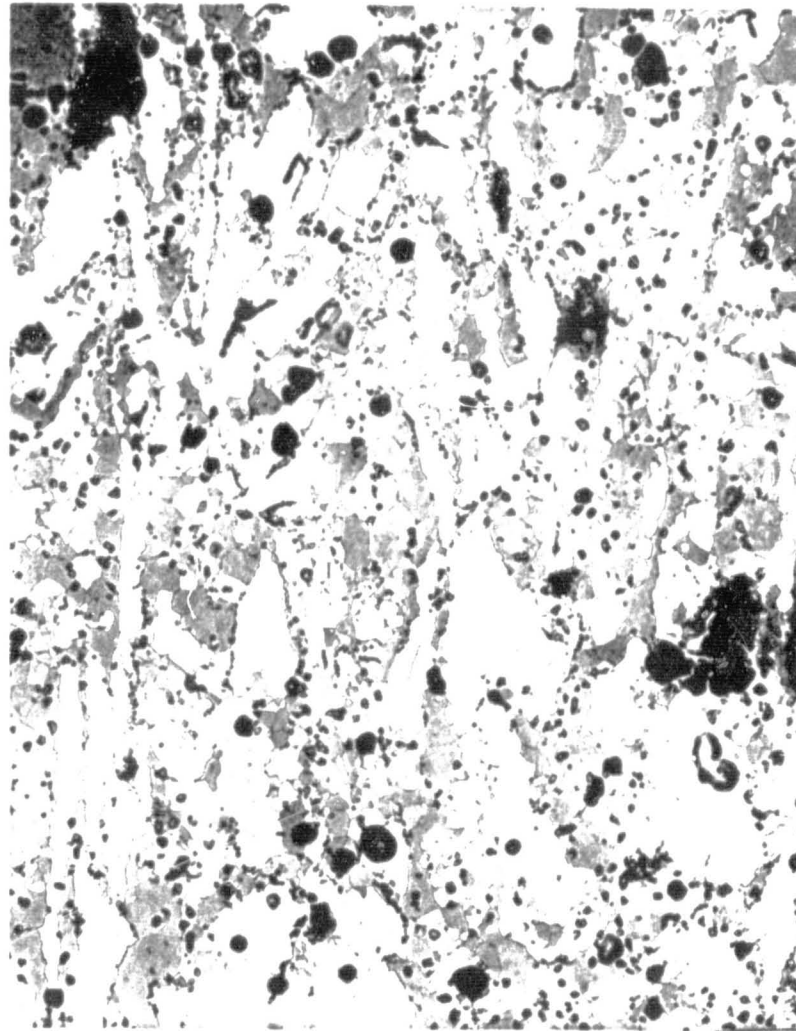


Figure 13

Alloy ZLH 972

100 X  
Electrolytically Polished  
and Etched

This specimen was rolled at 450°F, solution heat treated for 3 hours at 600°F and received no artificial aging. There appears to be large precipitates in the grain boundaries of the  $\alpha$  matrix and a few within the  $\alpha$  grains themselves or in the  $\beta$  phase.

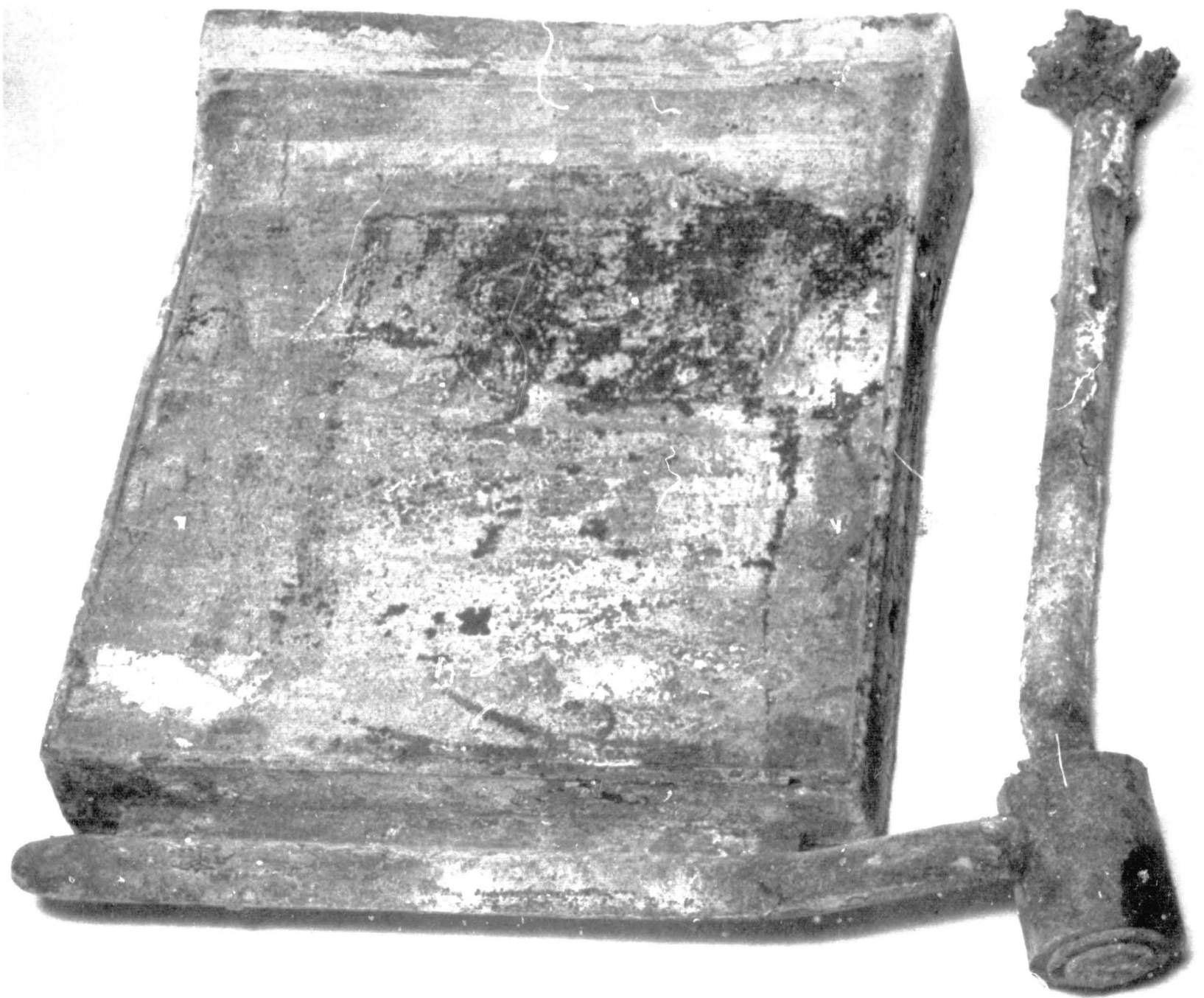


Figure 14. Pilot Lot Ingot of Alloy II 4, melt number 4-8-2, as it appeared just after being removed from the hot mold. The sprue, sump, runner, gating and hot top can be clearly seen in the photograph.

deterioration of the melts. The practice of melting pure magnesium in an initially cold pot and adding the alloying elements, as master magnesium hardeners, through a port in the top of the enclosed pot, was considered essential, as was the practice of rechecking and recording all temperatures. Any improvements in the melting procedure had to be made by changing the design of the furnace to shorten the melting time as much as possible. This was accomplished by replacing the original nichrome winding with Kanthal wire, and adding heavier conductors capable of passing 100 amperes. As a result of these changes the melting time was considerably shortened and the total time required to obtain a completed ingot from a cold, empty pot was 2-1/2 hours. This included adding a pure magnesium charge, bolting and leak checking the top, flushing the system with purified argon, bringing the initial charge up to temperature, making the alloying additions, heating and preparing the mold, puddling while the melt temperature returned to normal, and finally casting the ingot. After the first ingot was made, industrial practice was adhered to as much as possible, i. e., the weight of hot metal remaining in the pot was determined and additions were then made to the molten heel and hot pot for the next pour without lost time caused by a lengthy shutdown.

The newer procedures were perfected to the point where metal was poured smoothly, the mold consistently filled, and sound ingots were consistently obtained. This procedure produced ingots free of dross inclusions and without any trace of gas or shrinkage voids. During subsequent testing, described later in the report, none of the test specimens made from these ingots failed because of entrapped melting dross, and the results of chemical analyses performed on sections cut from such ingots showed excellent recovery values with the possible exception of thorium. The results of wet chemical analysis of thorium have not been consistent, showing either 0% or 1.6% for the II4 alloy, although X-ray fluorescence has shown the presence of thorium in every case.

### 2.3 Fabrication, Cast Ingot Billets to Sheet Technology

The initial castings were rolled at 450°F, 500°F, and 750°F with most of the material rolled at the lowest temperature. Alloy IA 6 rolled so well it was decided to reduce the rolling temperature to 260°F. Preliminary tests indicated that this procedure resulted in improved mechanical properties, so most of the IA 6 specimens were rolled at 260°F. The rolling temperature could not be reduced below 450°F for alloys II4 and ZLH 972 without producing cracks. Thirty percent reductions were made between reheating for each alloy. Surface depletion of lithium during rolling was completely eliminated by heating the rolling stock in either a eutectic mixture of 56% KCl-44% LiCl salt for the 750°F rolls, or in an oil bath for rolling at the lower temperatures. Care was taken to keep the salt mixture hot when it was not in use so that it would not absorb moisture. It was discovered early in the program that lithium depletion was promoted whenever the salt absorbed moisture. Heating the specimens in

either the salt or the oil bath insured an accurate and uniform temperature. A few specimens of each alloy were rolled to 0.010" foil without difficulty, but almost all of the material was rolled to 0.100" sheet. One specimen of each alloy was hammer forged to foil thickness at its lowest rolling temperature (i. e., 450°F for alloys II 4 and ZLH 972, and 260°F for alloy IA 6) to obtain some measure of their forging and forming characteristics.

A review of the experimental rolling practices employed indicated that the rolling procedure was too slow to be practical commercially. Therefore, development of a rolling procedure involving few rolling passes and hence more rapid reduction of billet to sheet was undertaken to enhance the commercial exploitation of this wrought alloy. It was established that a faster rolling procedure had to be developed for the II 4 alloy. The tensile strength was rather surprisingly found to increase as the rolling temperature increased; an ultimate tensile strength of 48,800 psi was obtained at 675°F after a total reduction of 95%, while a reduction of 85% in cross sectional area resulted in a tensile strength of 45,000 psi. A repeat of the earlier, faster rolling technique at 675°F, followed by two final passes of .007" in thickness-reduction-per-pass at 450°F, was selected as a practical rolling practice for these alloys. The final, lower temperature rolling involved preheating the metal for three minutes in an oil bath, and for no more than two minutes between passes. This procedure prevented over-aging and resulted in a thin adherent surface coating of oxide and oil on the wrought sheet product, which protected the metal from excessive oxidation-degradation during subsequent storage.

Other rolling experiments involving cross rolling at 400°F and at room temperature, subsequent to the initial rapid reduction of 1" thickness material to 0.150", were also conducted for the II 4 alloy. Very interestingly, it was found that after the hot rolling reduction at 675°F, both the tensile strength and the hardness of the II 4 alloy were not changed by rolling at either 400°-450°F or at room temperature, even though the elongation of the alloy did increase from less than 5% to more than 25% in 2". This indicated clearly that this alloy is not sensitive to work-hardening when cold-worked. Hence, the alloy should respond favorably to any forming operation involving deformation, such as spinning, shear-forming, bending, stretch forming, etc.

### 2.3.1 Metallography Review of the Matrix IV and Matrix V Alloys

For discussion purposes the as-cast structures of the initial six alloys of Matrices IV and V are compared with their as-rolled structures in Figs. 15 through 27. All of the as-rolled photomicrographs show the effect of cross rolling. Cross rolling alloy IV 2 completely broke up the elongated  $\beta$  phase in the as-cast structure in the lamellar structure shown in Fig. 16, which turned



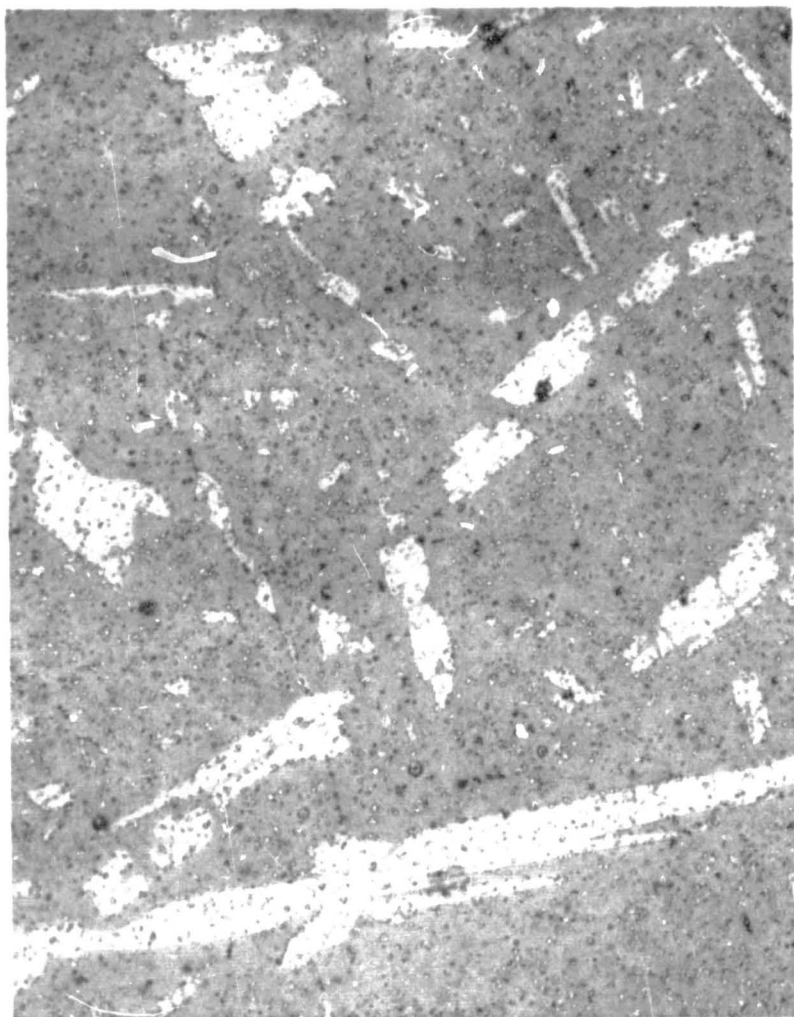


Figure 15.  
Alloy IV 2

250 X  
As Cast

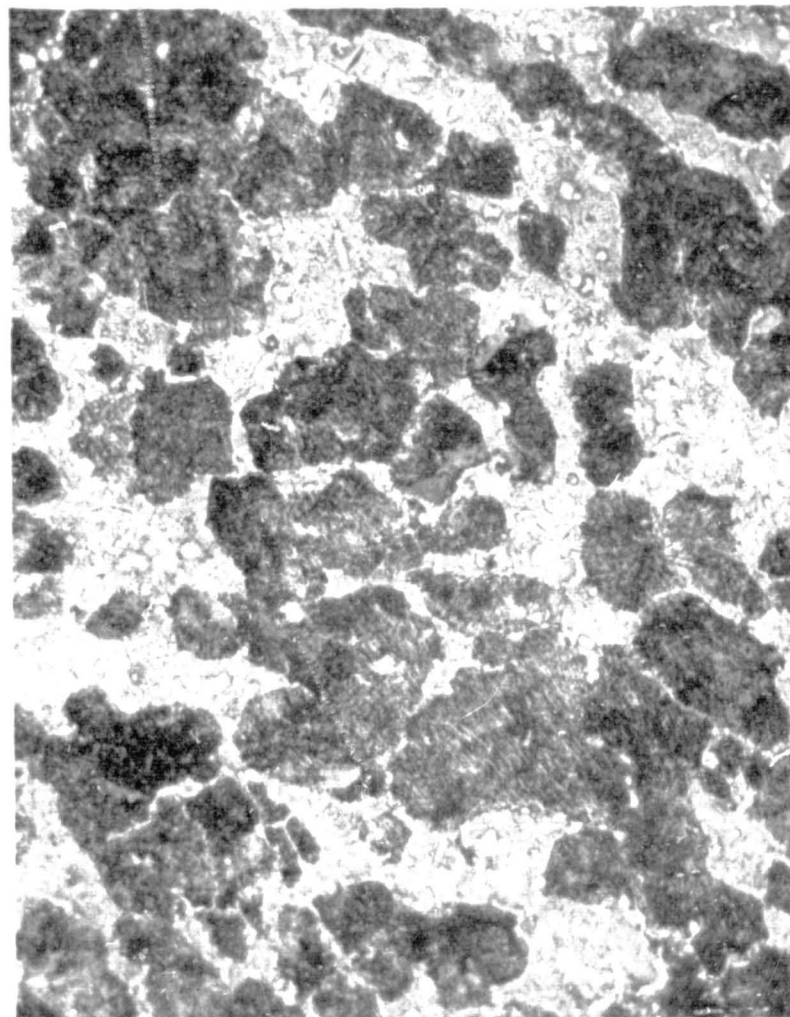


Figure 16.  
Alloy IV 2

250 X  
As Rolled

The lamellar structure shown in Figure 11 is brittle resulting in no elongation in the as-rolled condition. Solution heat treating this structure at 800°F and aging at 200°F raised the elongation to 17% but also reduced its tensile strength.



Figure 17.  
Alloy IV 7

250 X  
As Cast

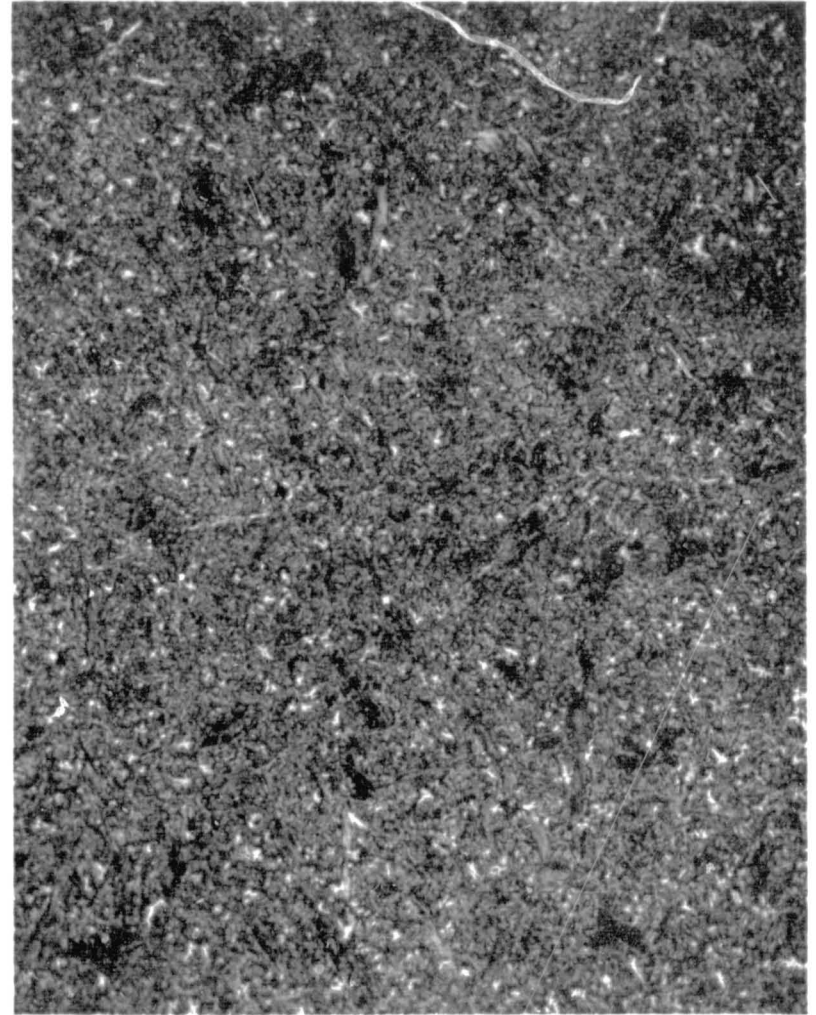


Figure 18.  
Alloy IV 7

250 X  
As Rolled

The large amount of  $\beta$  phase shown in Figure 12 is unusual for an alloy that contains only 7% lithium. This second phase was broken up by hot working at 800°F as shown in Figure 13 and an elongation value of 30.6% was obtained for a specimen with this structure.



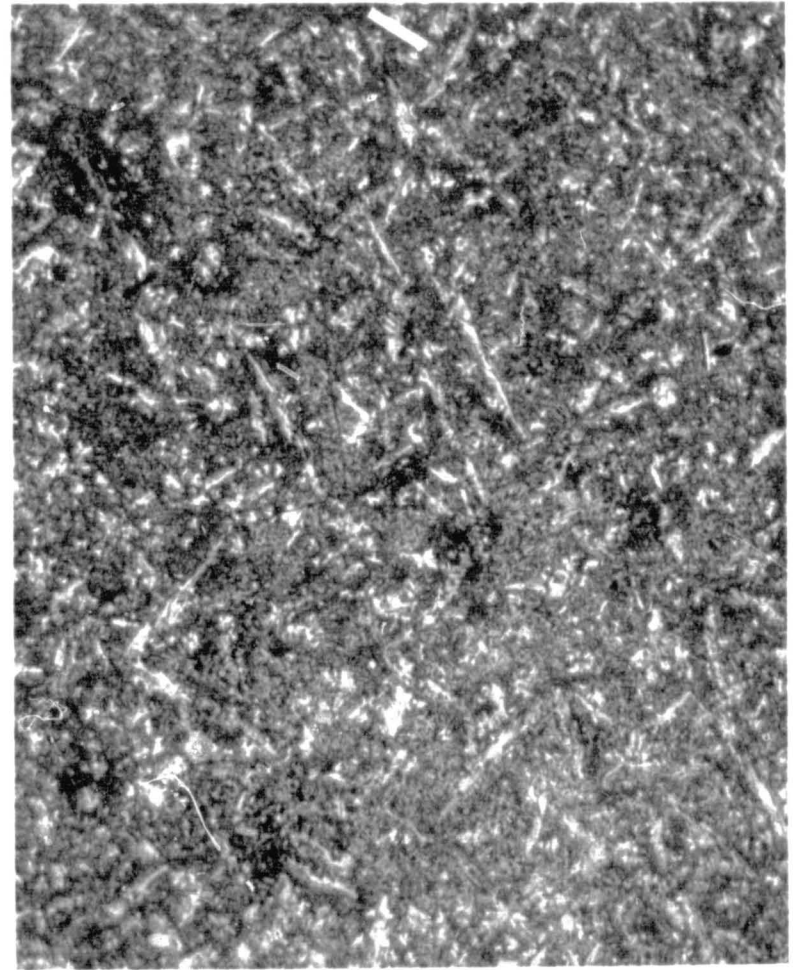
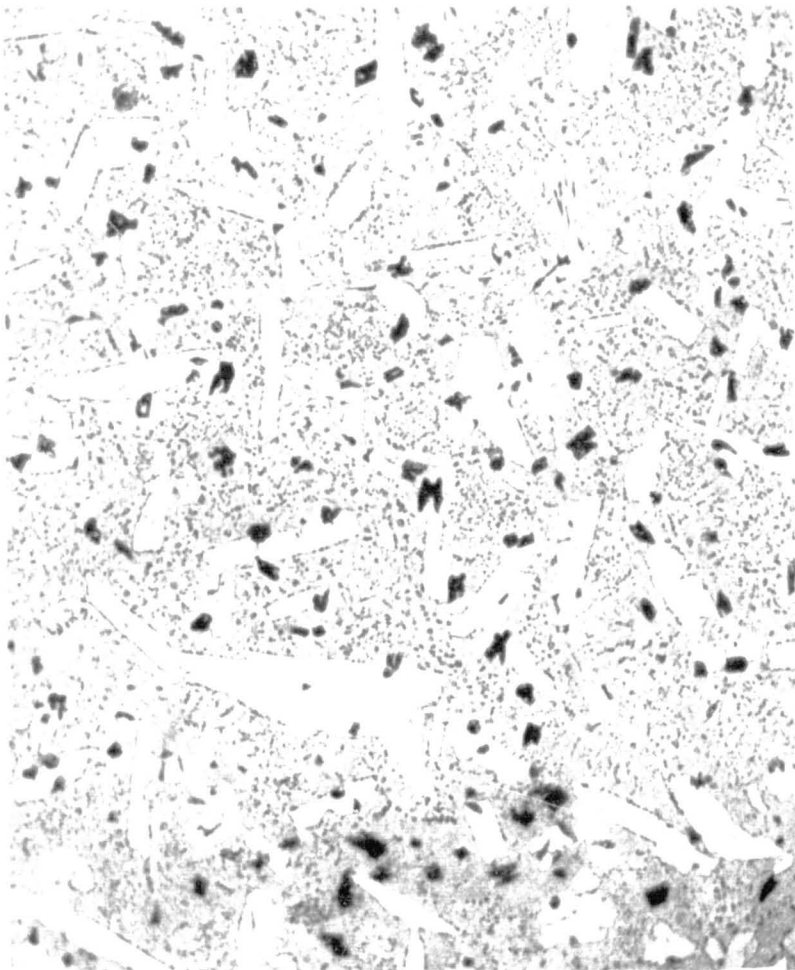


Figure 19  
Alloy IV 9

250 X  
As Cast

Figure 20  
Alloy IV 9

250 X  
As Rolled

The structure shown in Figure 20 had good ductility at ambient temperature but was surprisingly brittle at low temperatures. This lack of ductility was probably caused by a brittle matrix as the  $\beta$  phase in Figure 19 appears to be free from brittle precipitates. The small black particles in Figure 19 were not caused by hexachlorobenzene and are too large for nucleant grain refinement.

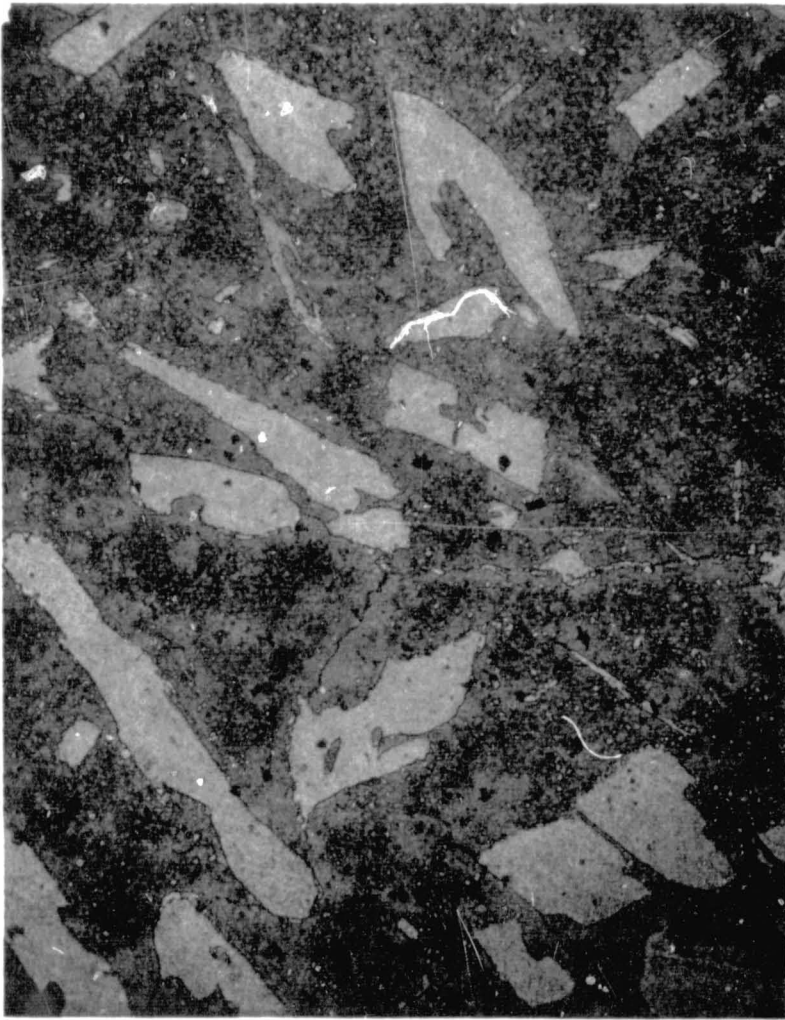


Figure 21  
Alloy V 6

250 X  
As Cast

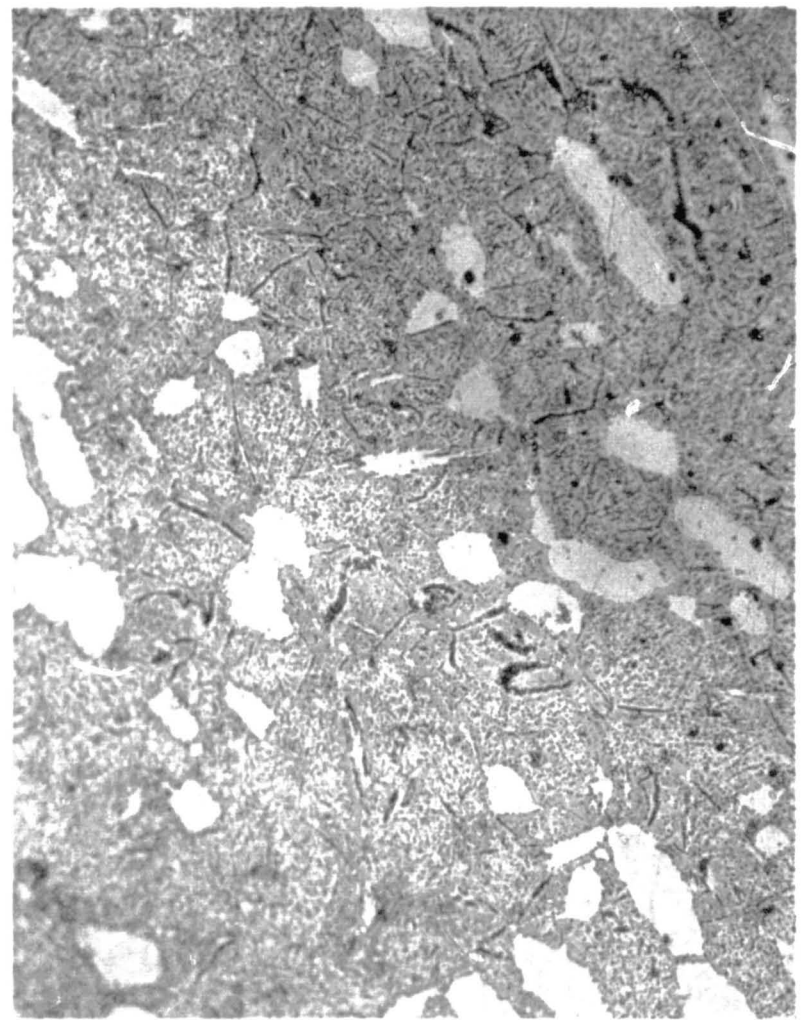


Figure 22  
Alloy V 6

250 X  
As Rolled

Alloy V 6 was rolled at 800°F and although the structure shown in Figure 22 resulted in good properties, the size and distribution of the  $\beta$  phase is not uniform. Subsequent research indicated that much better properties could have been obtained by rolling this alloy at a much lower temperature.

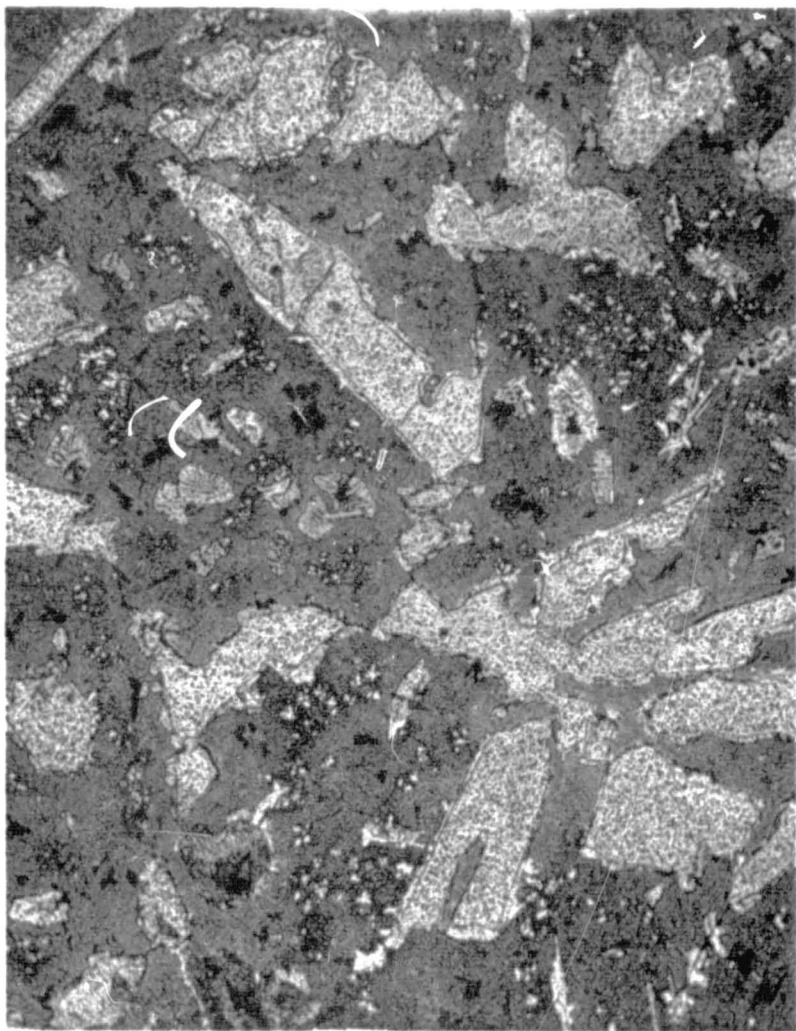


Figure 23  
Alloy V 7

250 X  
As Cast

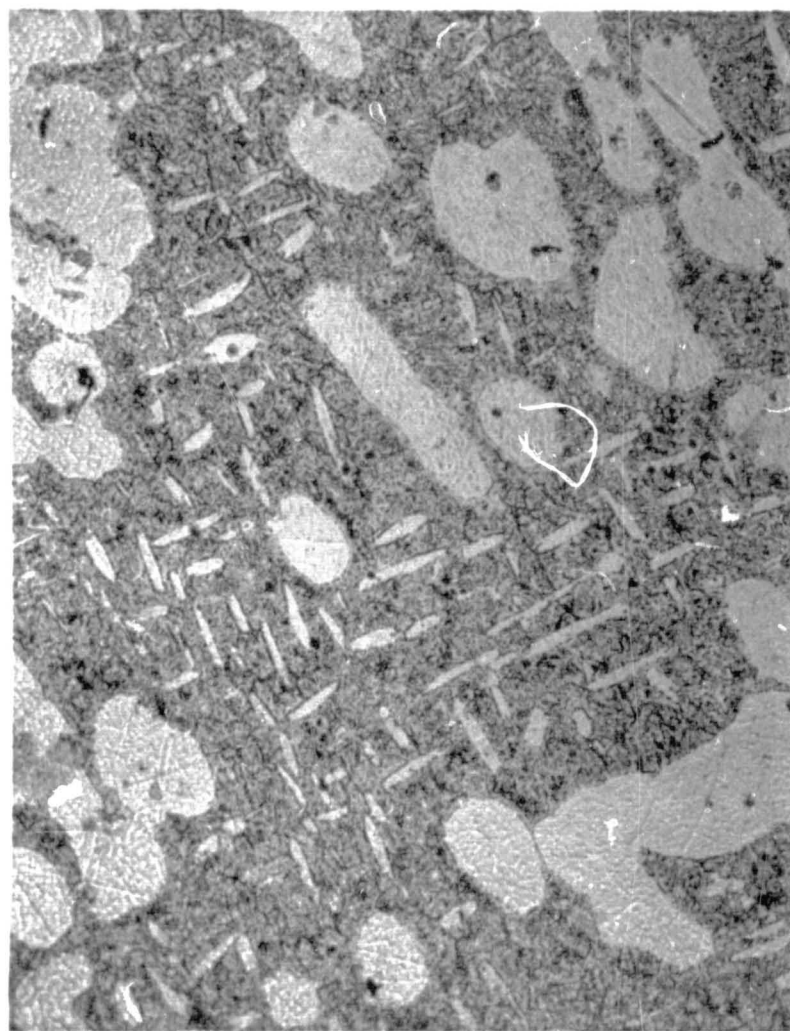


Figure 24  
Alloy V 7

250 X  
As Rolled

The structure in Figure 24 indicates that this alloy, like alloy V 6 should have been rolled at a lower temperature. The wide spacing between the needle-like  $\beta$  phase is too large to obtain good mechanical properties. The large areas of  $\beta$  were almost unaffected by rolling at 800°F further indicating that a lower rolling temperature could have been advantageous.





Figure 25  
Alloy V 8

250 X  
As Cast

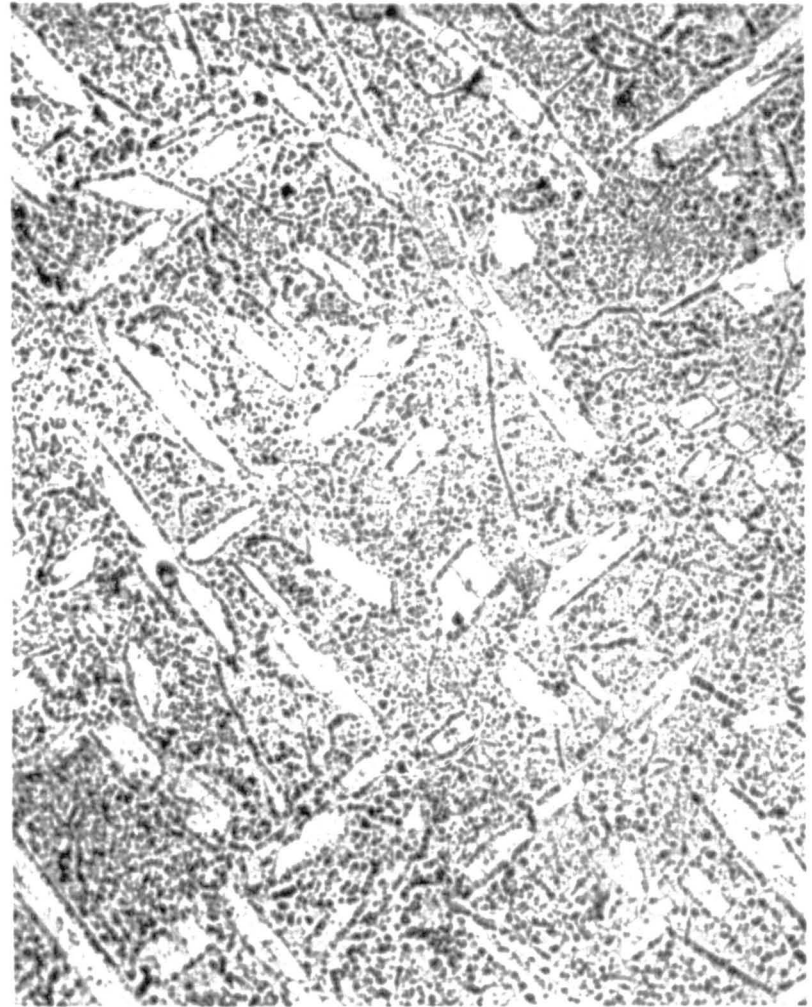


Figure 26  
Alloy V 8

250 X  
As Rolled

Intermetallic compounds have enveloped the  $\beta$  phase in Figure 26 making cross slip between phases difficult. Further development of this alloy does not seem warranted.

out to be the most brittle as-rolled structure tested during the program. The as-cast structure of alloy IV 7 shows an unusually large amount of the ductile  $\beta$  phase for an alloy that contains only 7% lithium. Hot working at 800°F greatly reduced the amount of the ductile  $\beta$  phase shown in the as-cast photo micrograph in Fig. 18, and explains, in part, why this alloy became harder after a high temperature heat treatment; although, at the same time, 30% elongation was obtained in the as-rolled condition. The as-cast and as-rolled structures of alloy IV 9 are compared in Figs. 19 and 20. The ductile  $\beta$  phase was broken up by hot working, and elongated equally in both directions of rolling. This type of structure resulted in good low temperature ductility in previous specimens, but alloy IV 9 was very brittle at -320°F. This surprising lack of ductility must have been caused by a brittle matrix because no brittle precipitates are apparent in the bcc  $\beta$  phase. Note that uniform black particles can be seen throughout the as-cast structure of alloy IV 9. These particles were not caused by hexachlorobenzene. The size of the particles in Fig. 19 appear to be too large for nucleant grain refinement and appear to be dispersed throughout the matrix and the  $\beta$  phase.

The structures of the Matrix V alloys are shown in Figs. 21 through 26, and are characterized by larger amounts of  $\beta$  phase in the as-rolled condition. This accounts for the improved ductility of these alloys over the Matrix IV alloys. Some coring can be seen in the as-cast structure of alloy V 6 in Fig. 21, and a continuous precipitate is present in the grain boundaries in the as-rolled condition. The alloy Mg - 2 Th - 2 Ag - 3 Al - 9 Li - 2 Zn - 0.25 Mn was the most promising of the preliminary alloys. The structure in Fig. 22 indicates that much better properties could have been obtained by rolling this alloy at a much lower temperature. The size and distribution of the  $\beta$  phase could have been more uniform had the rolling temperature been lower, and the continuous precipitate in the grain boundaries might have been eliminated. Subsequent research on the three alloys ultimately selected for scale-up to 50-lb. pilot melts further indicated that alloy V 6 should have been rolled in the 450° to 500°F temperature range. These results were the basis for the continued rolling procedure studies reported below.

Coring is also present in the as-cast structure of alloy V 7, shown in Fig. 23, with a great deal of intermetallic compound precipitation in the  $\beta$  phase. Alloy V 7 and IV 9 are similar in composition, with the latter alloy having more zinc and the former containing manganese. Evidently the manganese promotes precipitation in the  $\beta$  phase, a function contrary to its role as a solid solution hardener. The as-rolled structure shows  $\beta$  phase elongated in both directions of rolling, and precipitation in the  $\beta$  phase somewhat reduced but still present in quantity. The relatively large spacing between the  $\beta$  phases probably accounts for the mediocre ductility of this alloy indicating again that a lower rolling temperature should increase its ductility and probably the strength as well. The as-cast structure of alloy V 8 shows no coring and elongated  $\beta$  phase. The as-rolled structure in Fig. 26 shows the  $\beta$  phase elongated in both directions of rolling and

very coarse intermetallic compounds precipitated in the matrix. Intermetallic compounds have also enveloped the  $\beta$  phase making cross slip between phases difficult. Attempts to strengthen this alloy further are expected to meet diminishing returns on time invested.

### 2.3.2 Metallographic Studies of Second Generation\* Alloys

Metallographic studies were made of the brittle behavior of magnesium-lithium alloys in the T4 condition for the three second generation alloys. Specimens of each alloy which were rolled 90% at 450°F and 750°F were heated for  $\frac{1}{2}$  hour and 1 hour at 600°F for these studies. Photomicrographs of the alloys are shown in Figs. 27 through 36. Metallographic preparation of these magnesium-lithium specimens was difficult because of surface activity. The procedure used to prepare the specimens was to rough polish them by standard techniques, and to final polish them with a Vibromet polisher using Buehler 40-6440AB Magomet polishing compound in an aqueous solution of lithium hydroxide. The etchant was:

Ethylene glycol	75 ml
Water	25 ml
Nitric acid	1 ml

To avoid pitting, metallographic preparation should be continuous up until a good photomicrograph has been obtained.

Photomicrographs of alloy II4 rolled at successively higher temperatures from 450° to 750°F, are shown in Figs. 27 through 30. Isolated areas of the white  $\beta$  phase appear in the microstructure after rolling at 450° and 500°F, while a needle-like  $\beta$  structure appears after rolling at 750°F. It is this needle-like structure that contributed to the excellent ductility of alloy II4 in the initial program and attempts were made to duplicate it. The structure developed at 750°F is needle-like but too coarse to obtain exceptionally high ductility together with good tensile strength. These photomicrographs indicate that better properties can be obtained by rolling alloy II4 in the 600° to 700°F temperature range. Heating in this temperature range can promote lithium depletion as it did earlier in the program and a great deal of effort was used to find a suitable oil or neutral salt in which to heat the rolling stock between passes. One salt, an inexpensive nitrite-nitrate mixture called Aeroheat 300, made by the American Cyanamid Co., was found to be inert to magnesium-lithium alloy. But it was discovered late in the program and time did not permit tensile specimens to be rolled in this temperature range. The properties obtained from material rolled at 450°F were excellent and it would have been interesting to compare these properties with

---

\*Second generation alloys - designation of three compositions selected at beginning of the present 12-month extension of contract NAS 8-11168 for study during contract period 20 March 1966 to 20 March 1967.

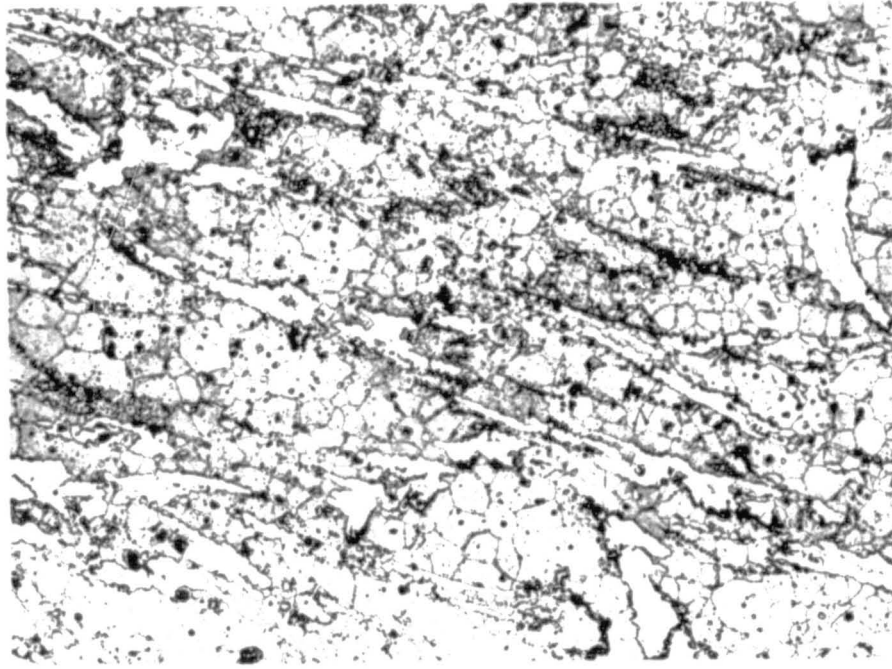


Figure 27. Alloy II 4 100 X

This specimen was rolled at 450°F, solution heat treated for one hour at 600°F, and aged one hour at 200°F. There is no evidence of aging after this short aging time.

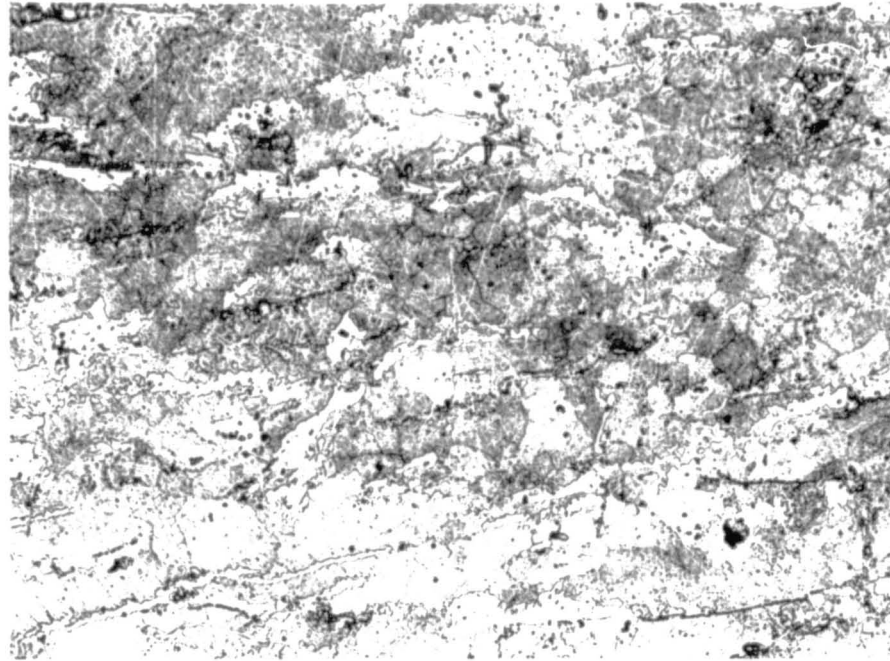


Figure 28.

Alloy II 4

100X.

This specimen was rolled at 500°F and solution heat treated for  $\frac{1}{2}$  hours at 600°F. The photomicrograph shows a two phase  $\alpha + \beta$  structure with the white  $\beta$  phase elongated in the direction of rolling. Very little of the ductile, lithium-rich  $\beta$  phase has segregated to the grain boundaries.



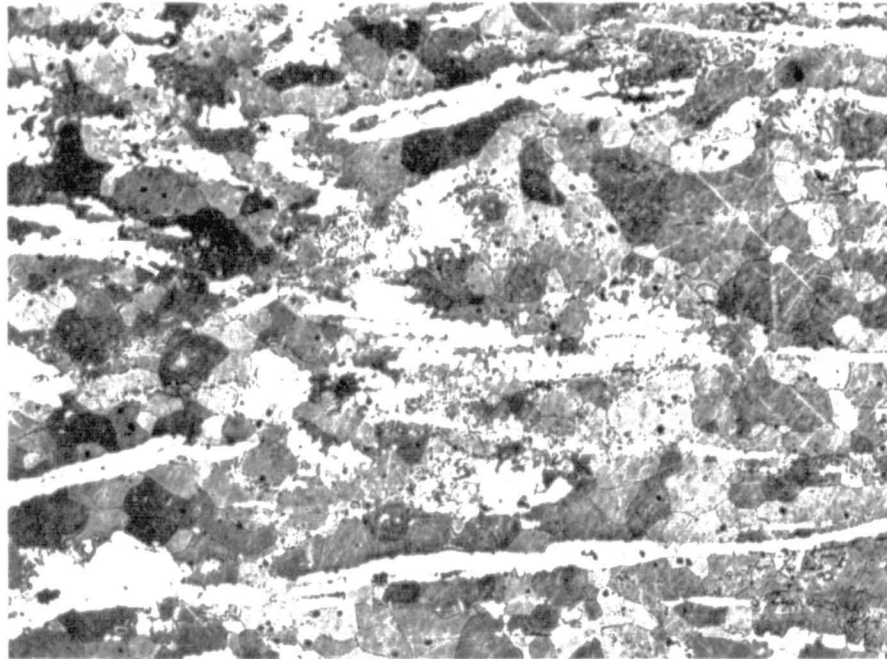


Figure 29. Alloy II 4 100X

This specimen was rolled at 500°F and solution heat treated for 1 hour at 600°F. The photomicrograph shows a two phase  $\alpha + \beta$  structure with the white  $\beta$  phase elongated in the direction of rolling. Fewer precipitates appear in the  $\beta$  phase after 1 hour at temperature, but enough lithium segregation to greatly enhance the ductility has not taken place.

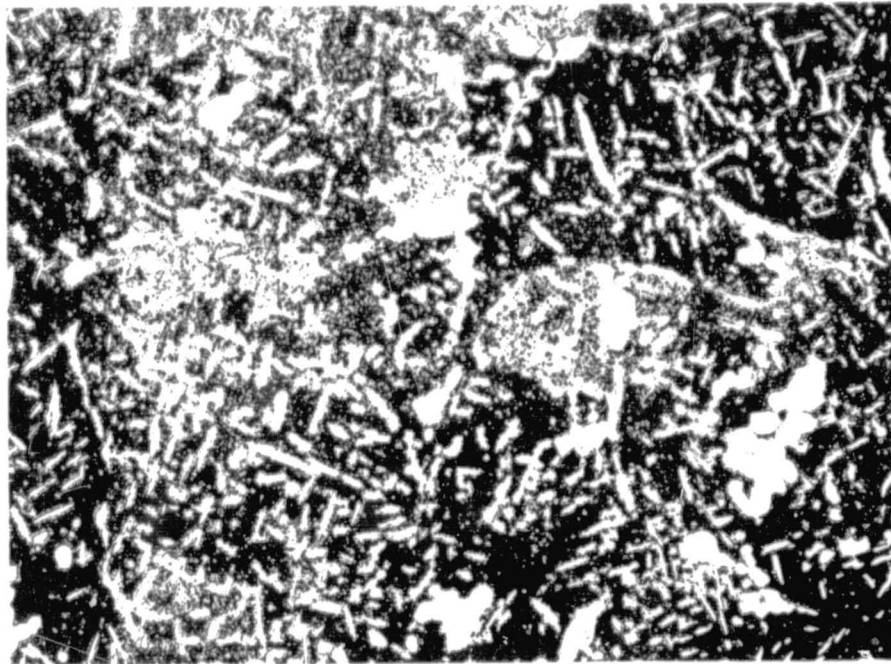


Figure 30. Alloy II 4 100 X

This specimen was rolled at 750°F, solution heat treated for 3 hours at 600°F, and aged 16 hours at 200°F. The  $\epsilon$  phase appears as random needles in the matrix which, in the past, has resulted in very ductile material. This structure is undoubtedly too coarse for outstanding values for elongation (16% was obtained) indicating that the optimum rolling temperature may lie between 450°F and 750°F.

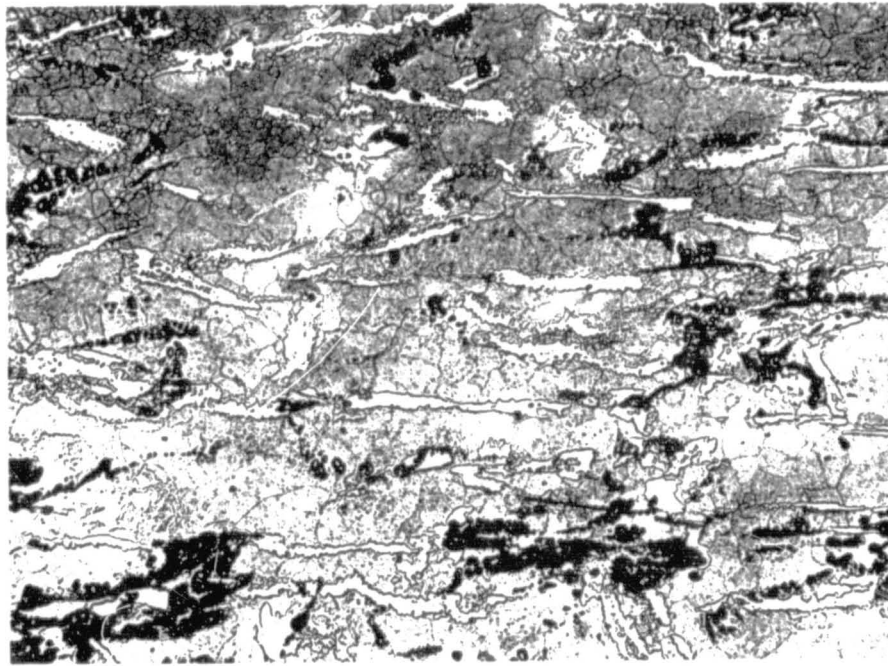


Figure 31. Alloy ZLH 972 100X

This specimen was rolled at 500°F and solution heat treated  $\frac{1}{2}$  hour at 600°F. The white  $\beta$  phase, elongated in the direction of rolling, appears to contain fewer precipitates than the  $\beta$  phase in alloy II 4.

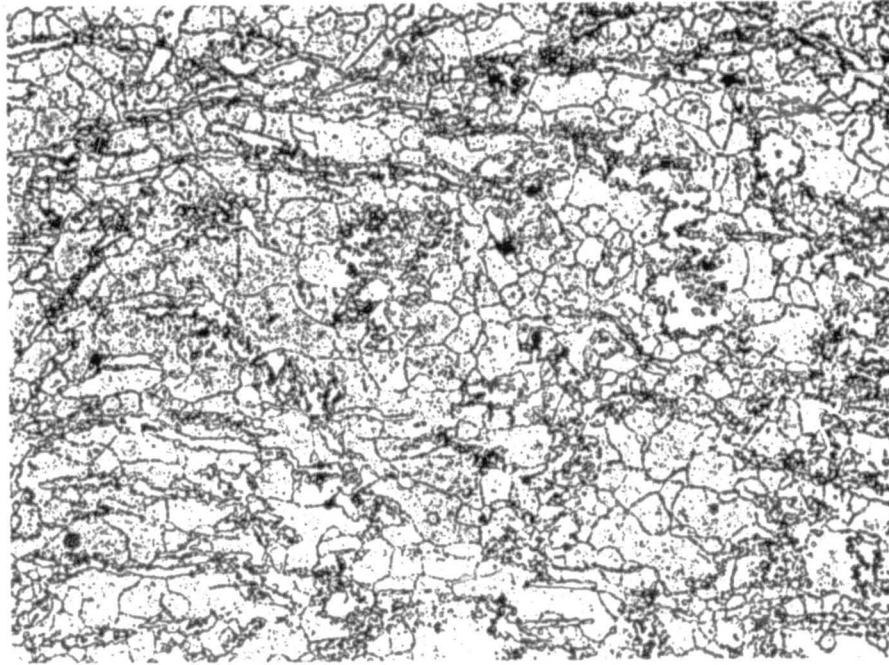


Figure 32. Alloy ZLH 972 100X

This specimen was rolled at 500°F and solution heat treated for 1 hour at 600°F. This structure appears more equiaxed than the one shown in Figure 39 and more lithium has segregated to the grain boundaries.

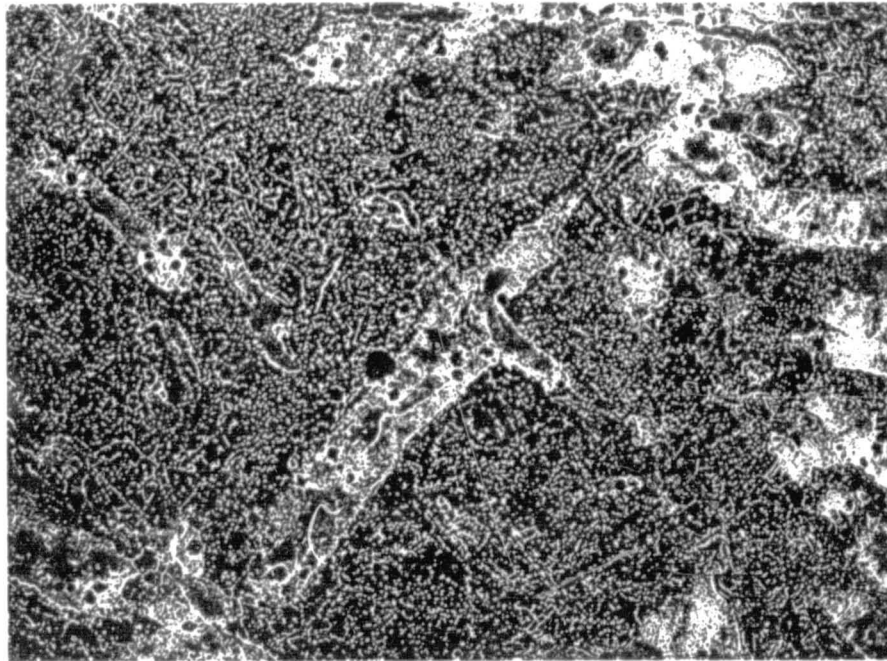


Figure 33. Alloy ZLH 972 100X

This specimen was rolled at 750<sup>o</sup>F, solution heat treated for 3 hours at 600<sup>o</sup>F, air quenched, and was not superficially aged. The large  $\beta$  phase contains a great many precipitates and an almost continuous network of the second phase appears in the grain boundaries.

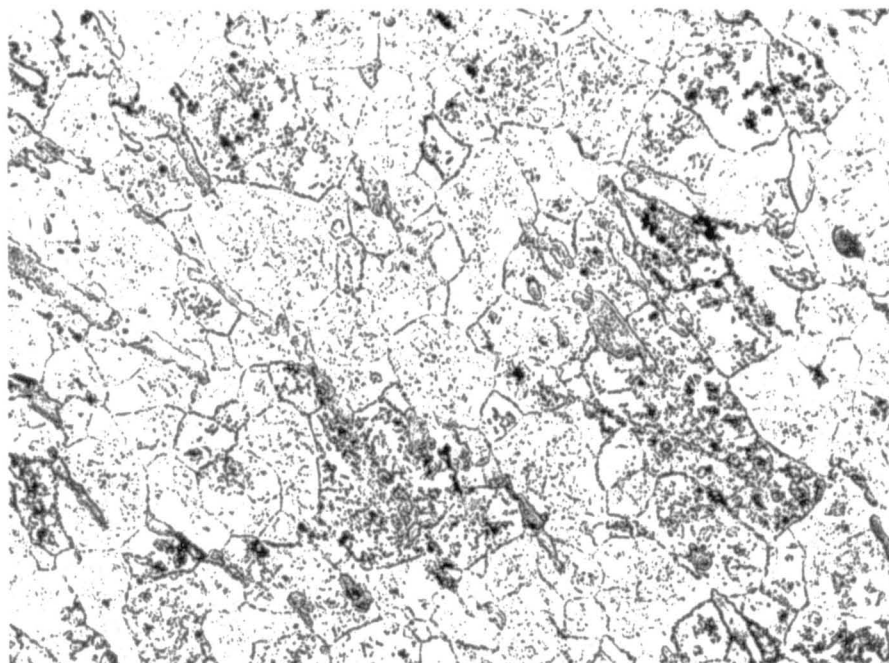


Figure 34. Alloy IA 6 100X

This specimen was rolled at 500°F and solution heat treated for  $\frac{1}{2}$  hour at 600°F. The elongated  $\beta$  phase appears rough at this magnification and a great deal of precipitation can be seen in the matrix. The time at temperature was not long enough to dissolve these fine particles.



Figure 35. Alloy IA 6 2000X

This specimen is the same as the one discussed in Figure 18 but shown here at a much higher magnification. The rough appearance of the  $\beta$  phase is caused by very fine precipitates, assumed to be  $MgLi_2Al$ .



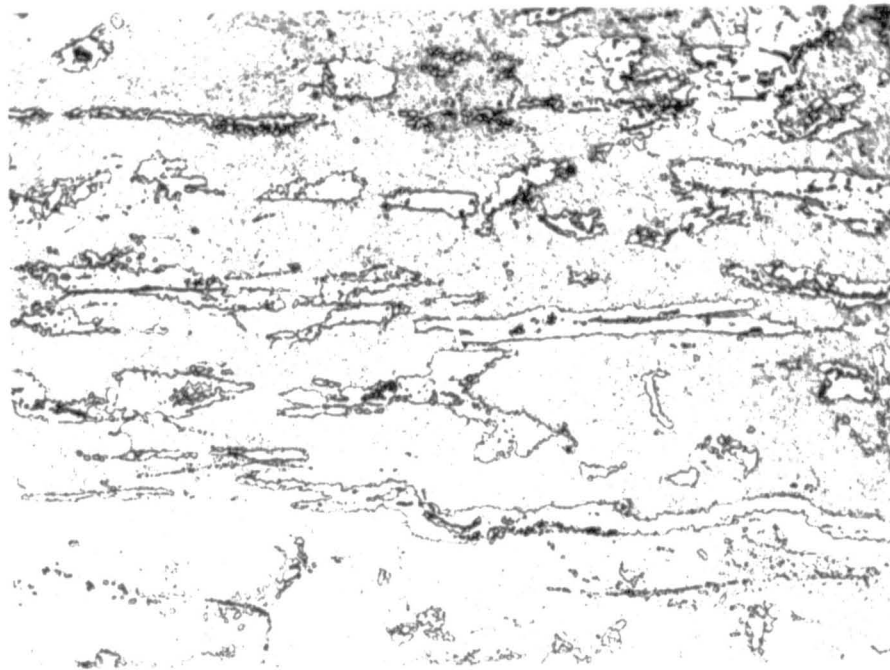


Figure 36. Alloy IA 6 100X

This specimen was rolled at 500°F and solution heat treated for 1 hour at 600°F. Fine precipitates have dissolved in the matrix and the  $\beta$  phase appears cleaner.



those obtained after rolling at 650°F.

Photomicrographs of alloy ZLH 972 which was rolled at successively higher temperatures are shown in Figs. 31 through 33. The specimen that was rolled at 750°F and solution heat treated for 3 more hours at 600°F shows a great deal of precipitation in the  $\beta$  phase, which accounts for its brittle behavior in the solution heat treated condition. Rolling at a lower temperature elongated the  $\beta$  phase in the direction of rolling, and this phase appears clean and free from precipitates in Fig. 31. Solution heat treating this specimen for 3 hours at 600°F, as shown in Fig. 32, resulted in the formation of another phase within the  $\beta$  phase, which has not been identified and which evidently contributed to the stability of this alloy.

Photomicrographs of alloy IA 6 are shown in Figs. 34 and 35. Rolling this alloy at 750°F resulted in a material with excellent ductility and poor strength at ambient temperature, but with very high strength at -452°F. Rolling at 260°F greatly increased the ambient temperature strength, with a reduction in ductility. The brittleness in the T4 condition was not as pronounced as in alloys II 4 and ZLH 972 indicating that this brittleness is associated with high lithium, together with high zinc, content.

According to Jones and Hogg<sup>3</sup> the T4 brittleness in  $\beta$  magnesium alloys is caused by a continuous network around the grain boundaries which forms when the alloys contain silver or copper. Three of the modified II 4 alloys studied earlier in the program did not contain silver, while most of the others did. No correlation was found between brittleness and increased silver content. Clark<sup>2</sup> stated that the cause of embrittlement after solution treatment is obscure and suggested that traces of sodium may be responsible. Very high purity Mg-Li master alloys were used to prepare the melts for this program and the fact that ductility can be recovered makes this hypothesis doubtful. Jones and Hogg could not see precipitation in the  $\beta$  phase after a solution treatment and reported a general coarsening of the grains. An examination of the  $\beta$  phase shown at high magnification in Fig. 35 reveals that this coarsening is actually a dispersion of very fine precipitates which are coherent with the  $\beta$  phase. The precipitate is assumed to be  $MgLi_2X$ , where X can be either Zn or Al. Aging within the  $\beta$  phase occurs by the rejection of lithium to form  $MgLiX$  and  $LiX$  with overaging occurring when these compounds lose their coherency with the matrix.

## 2.4 Mechanical Properties, Ambient-Cryogenic Temperature

This section is a compilation of the significant mechanical properties data obtained over the term of the contract for the wrought alloys. Data are presented for various heat-treating conditions, notched and unnotched, as range welded, etc. Throughout these studies, standard flat tensile specimens, six inches long with 2 1/2 inches of reduced area, were used. A concentration factor of  $K_t = 10$  was used for the notched specimens which had radii of  $0.0015 \pm 0.0005$  inches at the root of the notch. The welded specimens were made by welding panels, and then making tensile specimens from these panels. Welds were made both longitudinal and transverse to the direction of rolling. The specimens were machined with the longitudinal parallel and the transverse welds perpendicular to the applied load.

All specimens were tested in a 20,000 pound capacity Instron testing machine equipped with a continuous load-elongation recorder. A specially constructed cryostat, Cryogenic Inc. Model 307-1, was used for testing at low temperatures. Specimens were tested at ambient temperature,  $-108^{\circ}\text{F}$  (dry ice and acetone),  $-320^{\circ}\text{F}$  (liquid nitrogen), and  $-452^{\circ}\text{F}$  (liquid helium); with the specimens exposed to the cryogen. All specimens were pulled at a rate of 0.1 inch per minute, with the strip chart recorder set at 1.0 inch per minute. These speeds gave a magnification factor of 10 which was found convenient for all specimens except the very ductile ones (i. e., those with elongations greater than 30%, where the load-elongation curves were rather long). Calculating the percent elongation values directly from the strip chart gave results which were considered too large. Therefore, all elongation values tabulated in this report were obtained by marking the specimens prior to testing and measuring the total change in length after the test.

### 2.4.1 Tensile Testing

The results of short time tensile testing are presented graphically in Figures 37 to 45 and are summarized in Tables 1, 2 and 3. In every case, rolling at the lowest temperature possible without producing edge cracking resulted in the highest ultimate tensile strength. This was especially true for alloy IA 6 where a  $260^{\circ}\text{F}$  roll increased the optimum tensile strength from about 25,000 psi (measured earlier in the program), to an average value of about 43,000 psi.

The aging curves in Figure 37 show that the II4 alloy was unstable after one-hour solution heat treatment and that a three-hour solution heat treatment increased its stability considerably. Time did not permit an extensive investigation of the mechanism for this increase in stability but the photomicrograph shown in Figure 32 reveals another phase developing within

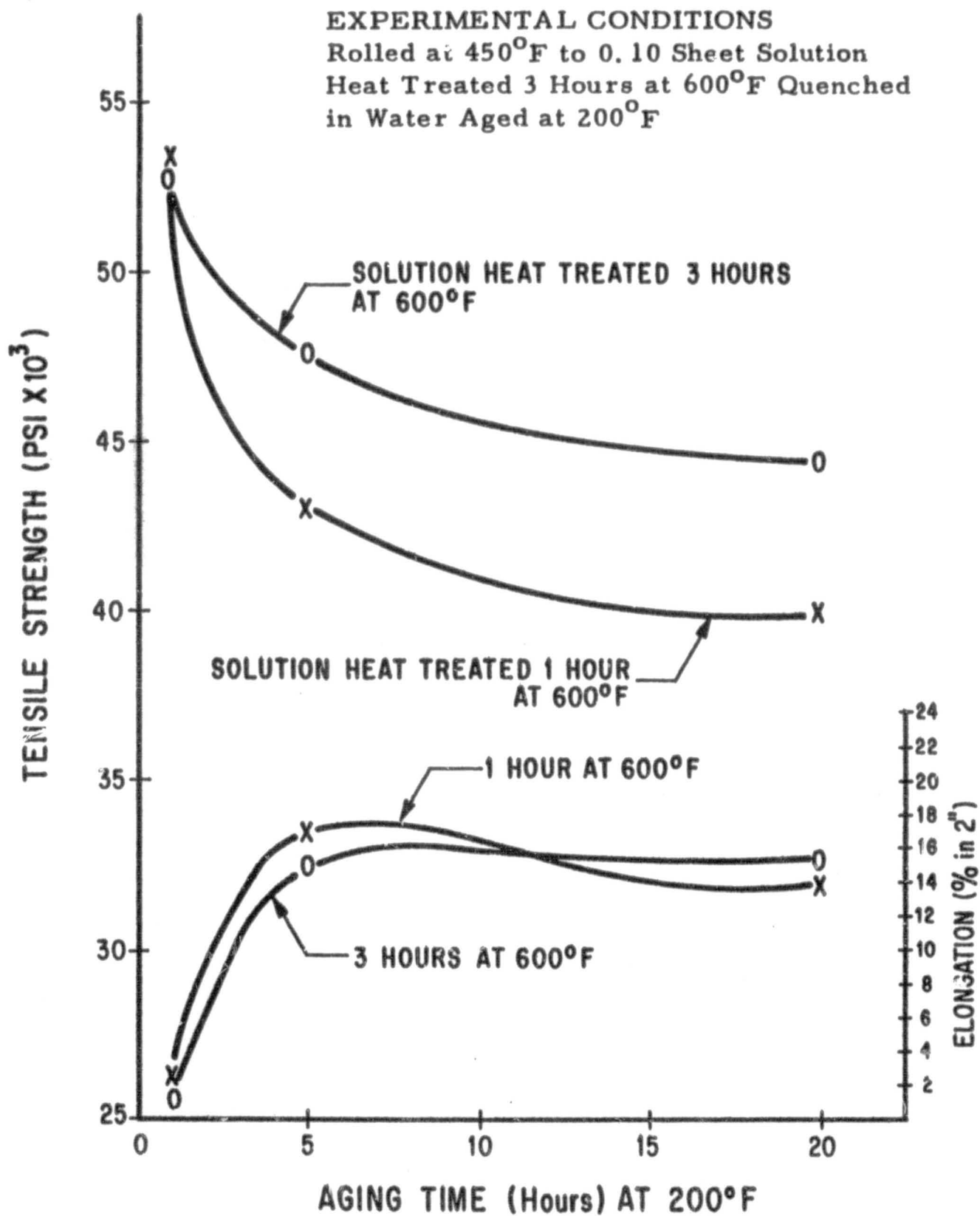


Figure 37. The Effect of Aging Time on the Mechanical Properties of Alloy II 4

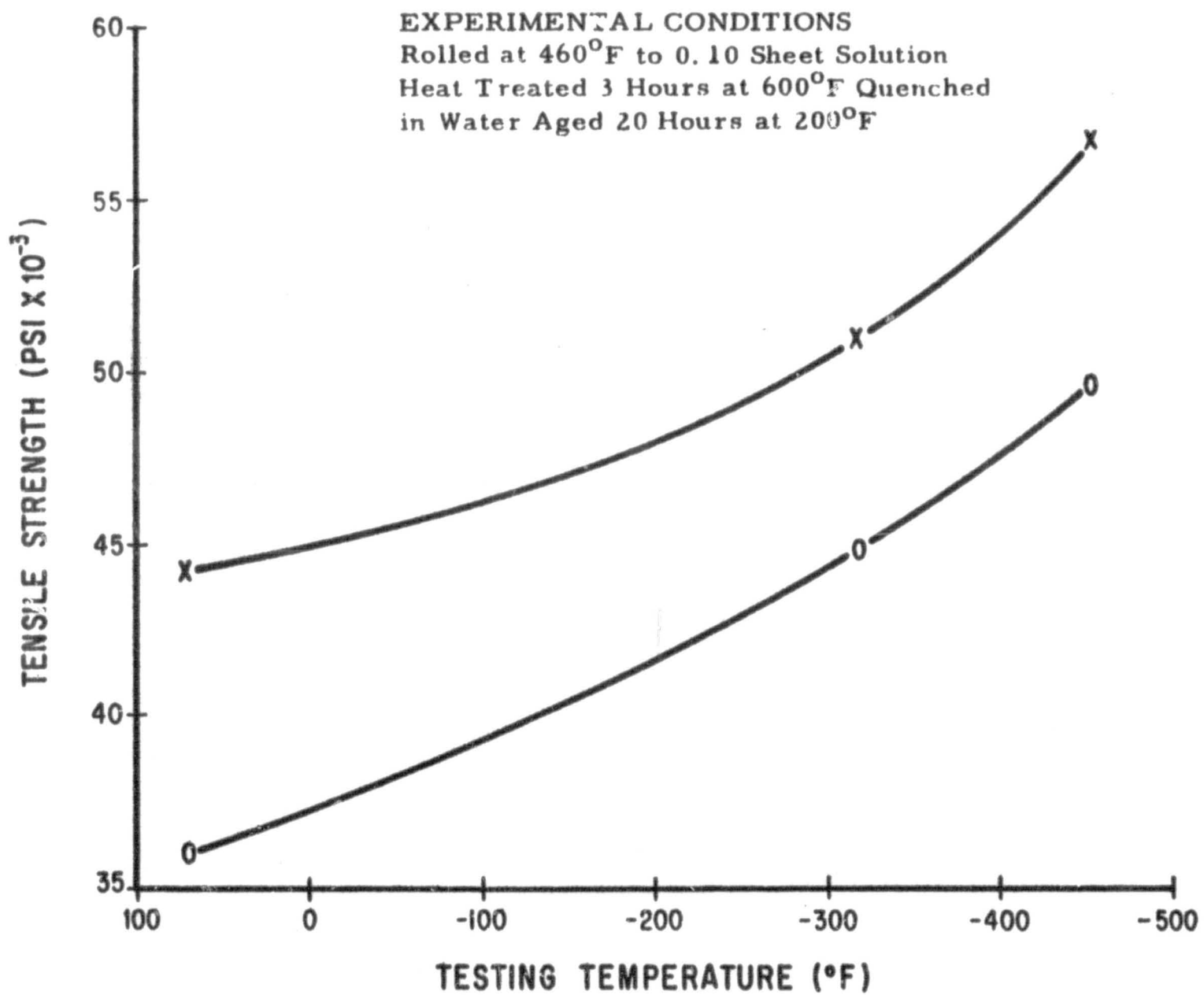


Figure 38 The Effect of Testing Temperature on the Strength of Alloy II 4

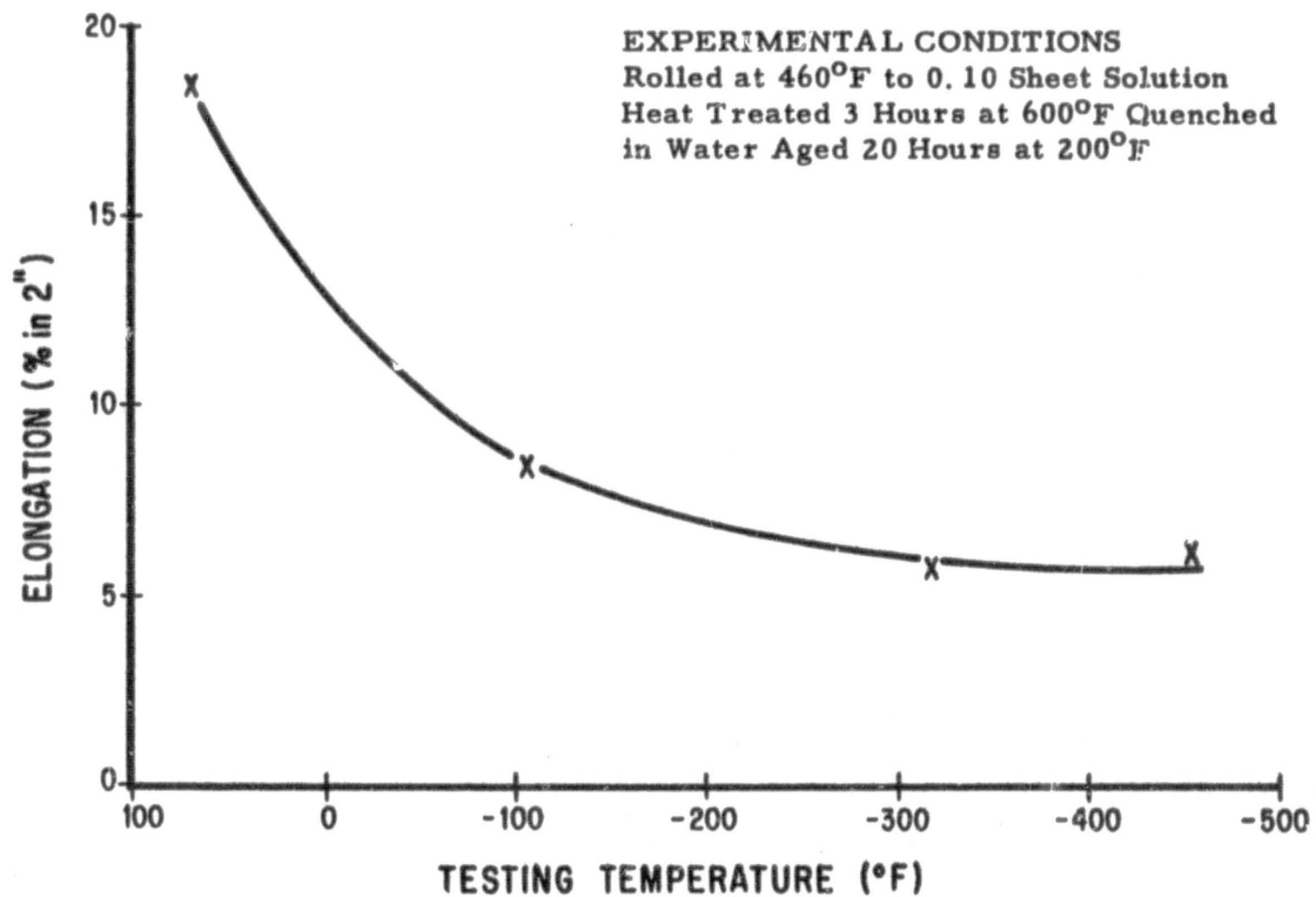


Figure 39. The Effect of Testing Temperature on the Percent Elongation (in 2'') of Alloy II 4

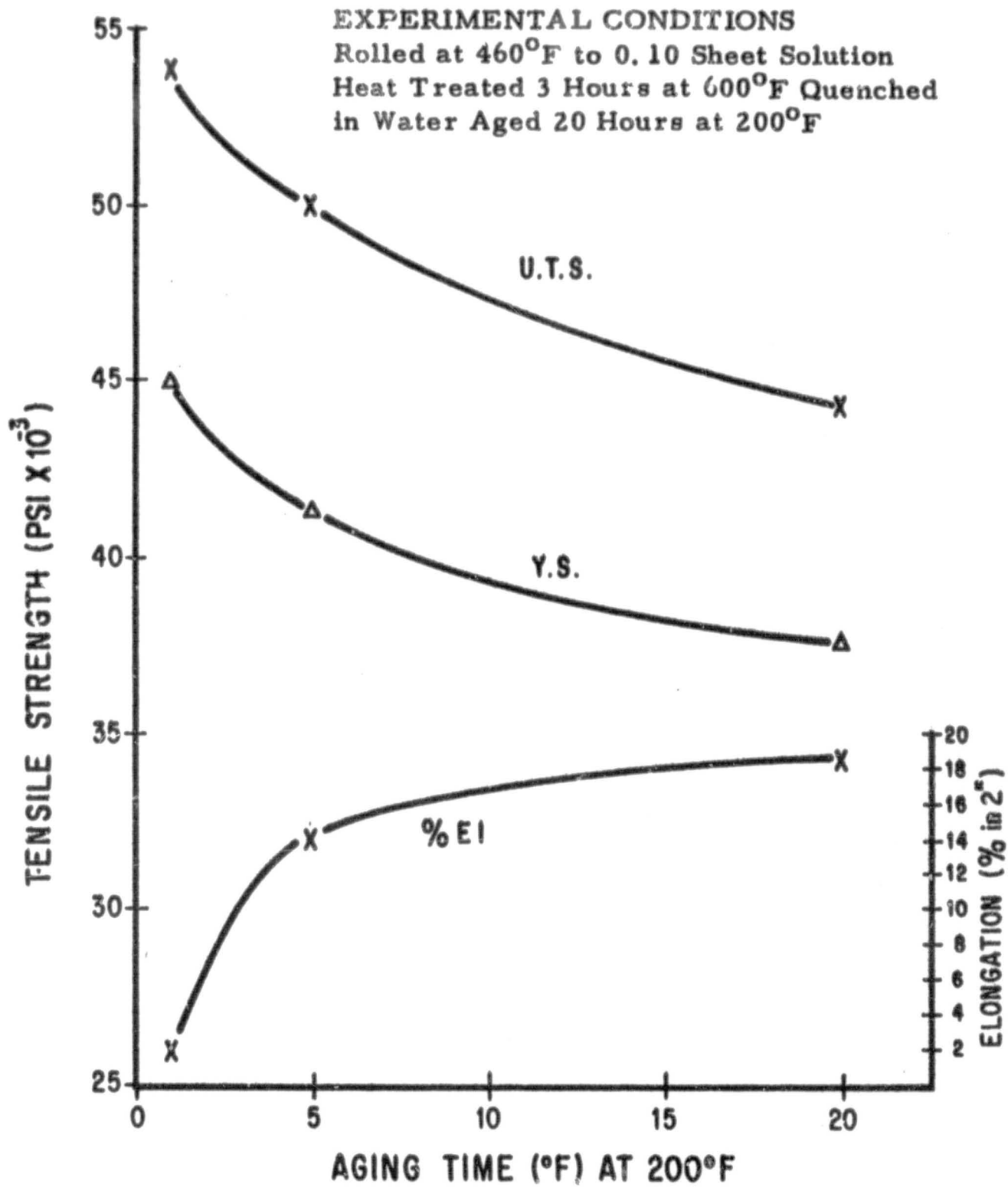


Figure 40 The Effect of Aging Time at 200°F on the Mechanical Properties of Alloy ZLH 972

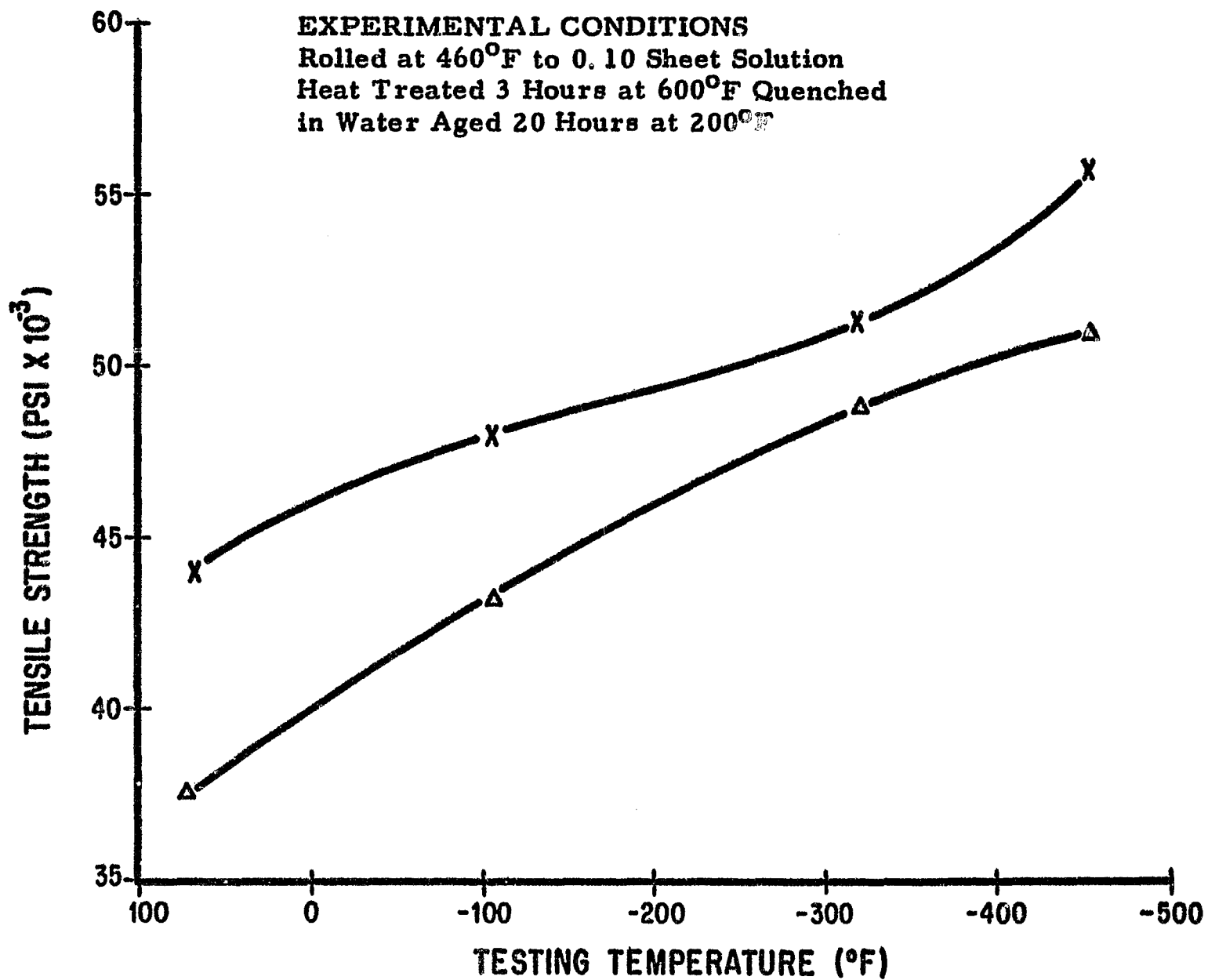


Figure 41. The Effect of Testing Temperature on the Strength of Alloy ZLH 972

**EXPERIMENTAL CONDITIONS**  
Rolled at 460°F to 0.10 Sheet Solution  
Heat Treated 3 Hours at 600°F Quenched  
in Water Aged 20 Hours at 200°F

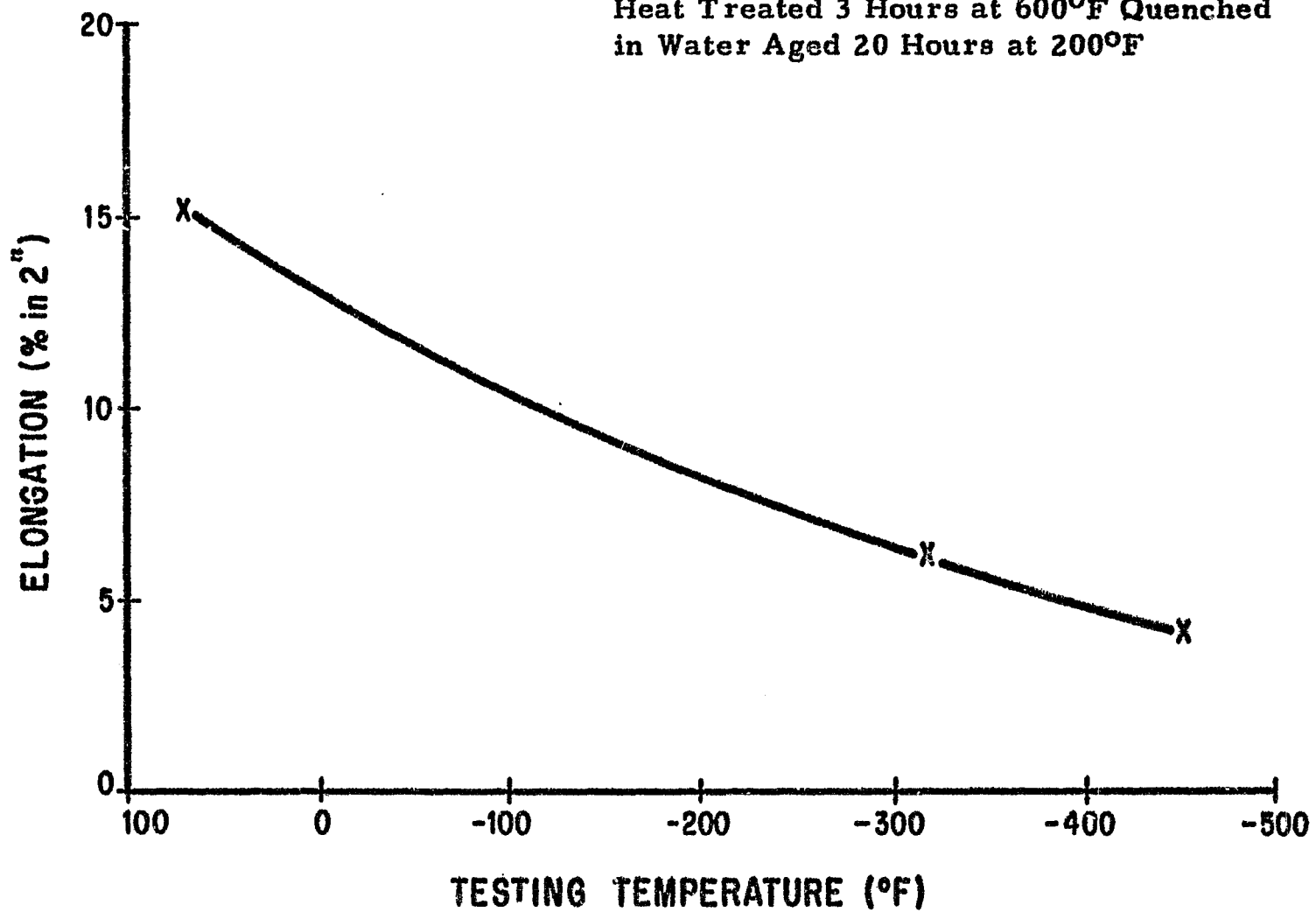


Figure 42. The Effect of Testing Temperature on the Percent Elongation (in 2'') of Alloy ZLH 972



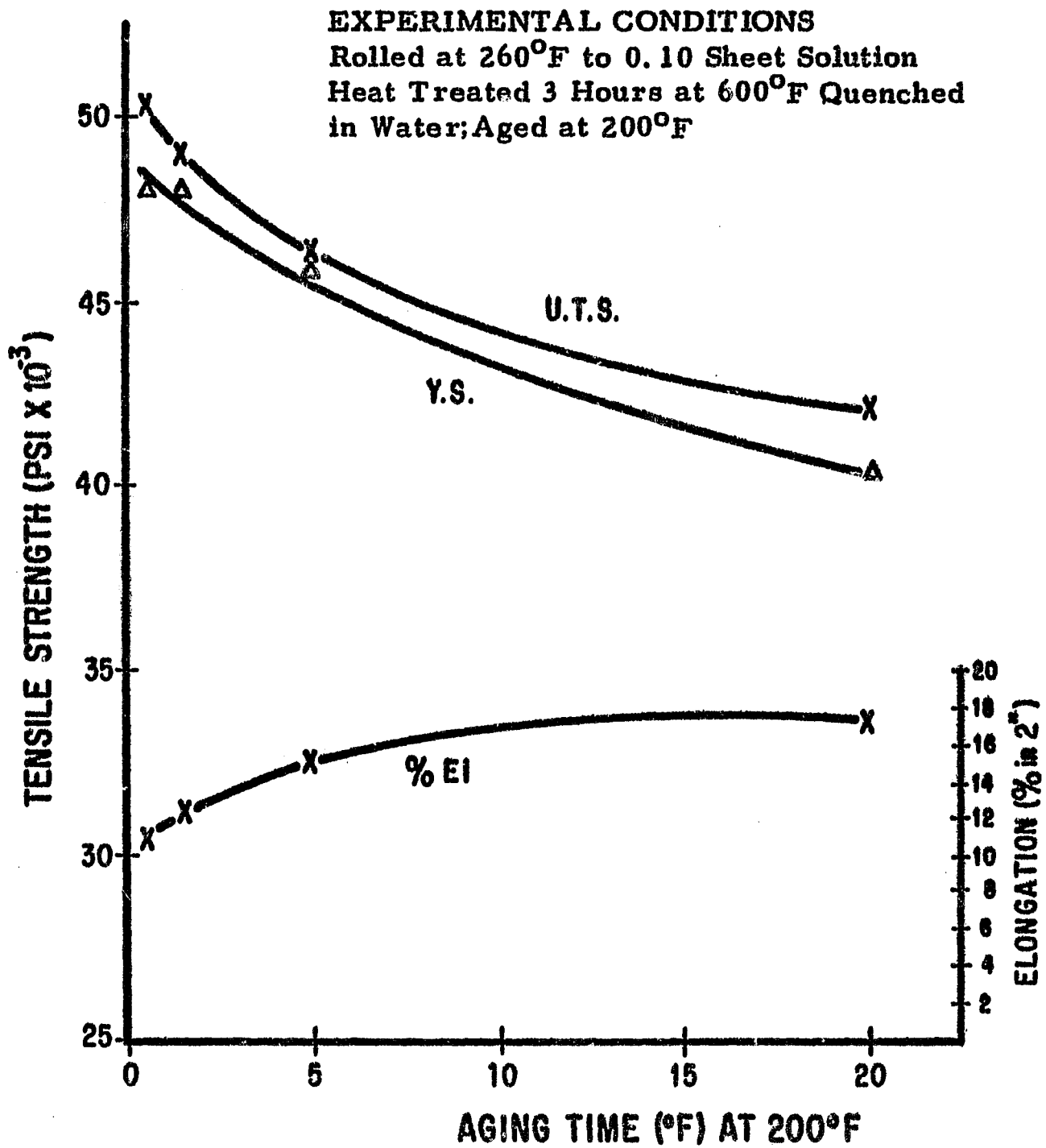


Figure 43. The Effect of Aging Time on the Mechanical Properties of Alloy IA 6

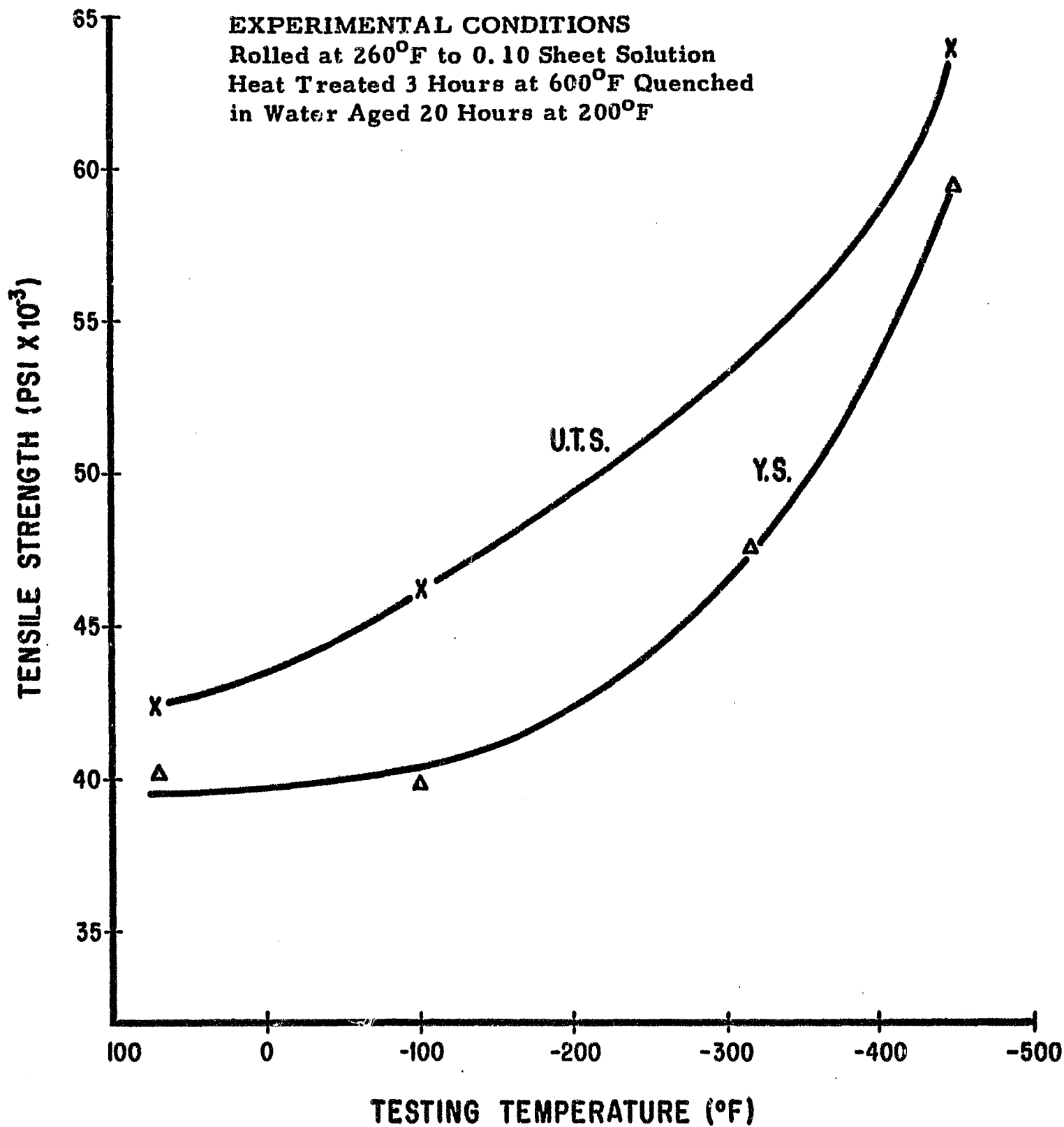


Figure 44. The Effect of Testing Temperature on the Mechanical Properties of Alloy IA 6

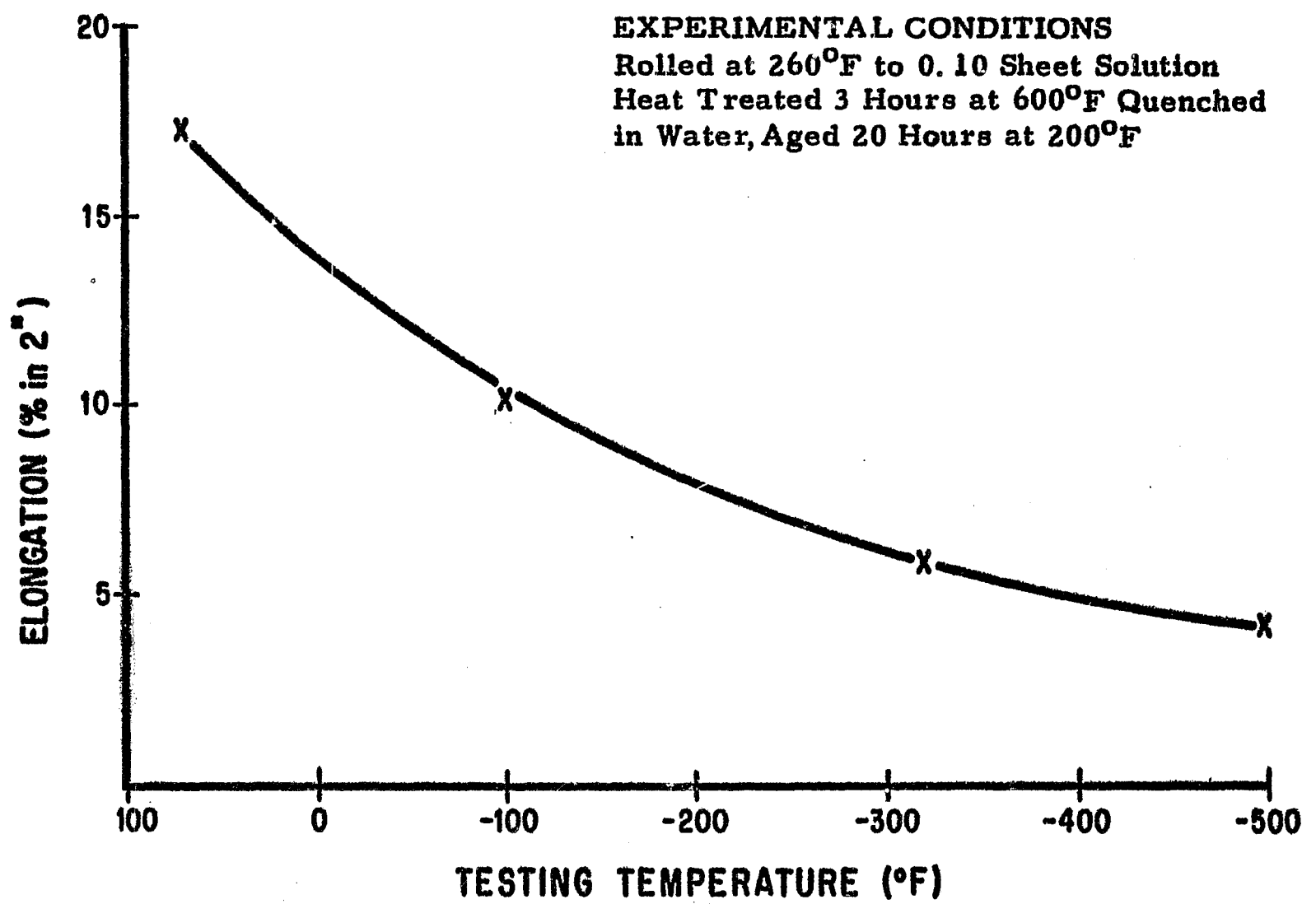


Figure 45. The Effect of Testing Temperature on the Percent Elongation of Alloy IA 6

Rolling Temp. °F	S.H.T.		Aging		Hardness Re	U. T. S. psi	0.2% Y. S. psi	El. % in 2"	Testing Temp. °F	Remarks
	Temp. °F	Time Hrs.	Temp. °F	Time Hrs.						
750						44, 100	40, 300	18.3	68	As Rolled (average)
750	600	3	200	16	92	38, 400	35, 400	16	68	
750	600	3	200	16	93	39, 800	37, 000	12	68	
750	600	3	200	20	90	38, 900	34, 600	19	68	
750	600	3	200	20	89	37, 700	33, 400	25	68	
450	800	1	200	1	83	32, 800	27, 000	16	68	
450	800	1	200	1	84	33, 200	28, 000	15.8	68	
450					93	47, 600	-	0.5	68	As Rolled
450	600	1	200	1	99	51, 300	-	0	68	
450	600	1	200	1	99	53, 200	50, 600	2.7	68	
450	600	1	200	5	89	43, 000	36, 500	17.0	68	
450	600	1	200	20	84	40, 000	34, 000	13.7	68	
450	600	2	200	5	90	45, 500	37, 000	14.0	68	
450	600	2	200	20	89	43, 000	34, 500	12.0	68	
450	600	3	200	1	97	52, 800	49, 900	2.0	68	
450	600	3	200	5	93.5	47, 600	40, 500	15.0	68	
450	600	3	200	20	89	42, 500	34, 200	16.0	68	
450	600	3	200	20	88	44, 000	36, 000	16.0	68	
450	600	3	200	20	90	45, 500	37, 000	14.8	68	
450	600	3	200	20	89	44, 200	36, 200	14.6	68	
450	600	3	200	20	88	43, 600	35, 300	15.0	68	
450	600	3	200	20	88	44, 200	36, 000	15.3	68	
450	600	3	200	20	90	45, 600	37, 400	15.0	68	
750	600	3	200	20	90	54, 500	48, 800	2	-320	
450	600	3	200	20	90	53, 000	46, 300	6.0	-320	
450	600	3	200	20	87	48, 000	42, 800	7.0	-320	
450	600	3	200	20	88	52, 000	46, 000	5.3	-320	
450	600	3	200	20	88	51, 000	45, 000	6.3	-320	
750	600	3	200	20	88	51, 000	45, 000	6.5	-320	
450	600	3	200	20	89	58, 900	51, 500	4.0	-452	
450	600	3	200	20	90	60, 000	52, 200	3.2	-452	
450	600	3	200	20	87	54, 000	47, 000	5.0	-452	
450	600	3	200	20	87	53, 500	47, 200	4.3	-452	
750	600	3	200	16	89	61, 000	-	1	-452	
750	600	3	200	16	70	56, 700	48, 200	10	-452	
750	600	3	200	16	89	41, 500	-	-	68	Notched/Unnotched = 1.06
750	600	3	200	16	88	46, 400	-	-	-452	Notched/Unnotched = 0.78
450	600	3	200	20	88	44, 300	-	-	68	Notched/Unnotched = 1.0
450	600	3	200	20	89	41, 500	-	-	68	Notched/Unnotched = 0.95
450	600	3	200	20	90	50, 300	-	-	-452	Notched/Unnotched = 0.89
750	600	3	200	20	88	40, 000	32, 000	3	68	Transverse Weld
750	600	3	200	20	78	33, 000	28, 000	11	68	Transverse Weld
750	600	3	200	20	89	33, 600	-	1	68	Longitudinal Weld
450	600	3	200	20	89	47, 200	-	1	68	Transverse Weld, 106% Efficient
450	600	3	200	20	88	43, 000	37, 300	5	68	Transverse Weld, 96.8% Efficient
450	600	3	200	20	87	39, 500	34, 500	4	68	Longitudinal Weld, 88.6% Efficient
450	600	3	200	20	87	40, 000	35, 000	5	68	Longitudinal Weld, 90% Efficient

The Measured Average Density of Alloy II 4 is 1.82 gm/cc

Table 1

Rolling Temp. °F	S. H. T.		Aging		Hardness Re	U. T. S. psi	0.2% Y. S. psi	El. % in 2"	Testing Temp. °F	Remarks
	Temp. °F	Time Hrs.	Temp. °F	Time Hrs.						
750	600	3			87	39,700	37,300	16	68	As Rolled
750	600	3	200	16	76	28,000	24,400	35	68	
750	600	3	200	16	77	30,200	28,000	31	68	
750	600	1	200	20	89	30,500	24,400	20	68	
900	600	1	200	2	92	43,200	37,200	9	68	As Rolled
450	600	1	200	5	90	43,000	36,000	12	68	
450	600	1	200	20	86	43,000	36,400	12	68	
450	600	1	200	5	88	43,500	36,000	16	68	
450	600	1½	200	20	88	46,000	45,000	13.5	68	
450	600	3	200	1	78	27,500	23,000	36.6	68	
450	600	3	200	1	98	54,000	45,000	2	68	
450	600	3	200	5	94	50,100	41,300	14	68	
450	600	3	200	20	89	46,000	38,200	17	68	
450	600	3	200	20	89	42,100	37,600	17	68	
450	600	3	200	20	88	40,800	35,400	25	68	
450	600	3	200	20	90	46,500	39,000	16	68	
450	600	3	200	20	90	45,100	37,800	17	68	
450	600	3	200	20	89	47,400	37,000	11.5	-108	
450	600	3	200	20	90	51,100	40,300	9	-108	
450	600	3	200	20	89	49,500	37,800	9	-108	
450	600	3	200	20	88	46,700	36,800	8	-108	
450	600	3	200	20	87	44,800	36,200	5	-108	
450	600	3	200	20	88	51,200	49,200	5.0	-320	
450	600	3	200	20	88	50,100	49,000	6.0	-320	
450	600	3	200	20	89	53,300	48,000	4.0	-320	
450	600	3	200	20	88	50,000	47,900	5.0	-320	
450	600	3	200	20	88	51,400	50,000	4.0	-320	
450	600	3	200	20	89	51,200	49,000	4.8	-320	
450	600	3	200	20	87	57,500	54,000	5	-452	
450	600	3	200	20	88	56,000	52,700	6	-452	
450	600	3	200	20	88	52,000	49,200	6.3	-452	
450	600	3	200	20	90	58,700	51,700	5.8	-452	
450	600	3	200	20	87	50,000	48,700	6	-452	
450	600	3	200	20	90	58,600	50,300	6	-452	
450	600	3	200	20	88	57,500	50,000	8.5	-452	
750	600	3	200	16	90	35,100	-	-	68	Notched/Unnotched .78
750	600	3	300	16	88	48,200	-	-	-452	Notched/Unnotched .89
450	600	3	200	20	88.5	40,200	-	-	68	Notched/Unnotched .895
450	600	3	200	20	89	43,000	-	-	68	Notched/Unnotched .96
450	600	3	200	20	90	50,000	-	-	-452	Notched/Unnotched .896
450	600	3	200	20	87	42,000	37,800	5	68	Transverse Weld, 93.5% Efficient
450	600	3	200	20	88	41,000	26,000	6	68	Longitudinal Weld, 92% Efficient
450	600	3	200	20	88	28,000	26,000	2	68	Transverse Weld, Dross in Weld

The Measured Average Density of Alloy ZL1072 is 1.81 gm/cc

Table 2

<u>Rolling</u> <u>Temp.</u> <u>°F</u>	<u>Temp.</u> <u>°F</u>	<u>Time</u> <u>Hrs.</u>	<u>Temp.</u> <u>°F</u>	<u>Time</u> <u>Hrs.</u>	<u>Hardness</u> <u>Re</u>	<u>U. T. S.</u> <u>psi</u>	<u>0.2% Y.S.</u> <u>psi</u>	<u>El.</u> <u>% in 2"</u>	<u>Testing</u> <u>Temp.</u> <u>°F</u>	<u>Remarks</u>
750					79	28,200	25,000	30.8	68	As Rolled, Coarse Grained
750	850	1	200	½	74	24,700	21,800	50	68	Coarse Grained
750	850	1	200	½	76	25,800	23,000	15	68	Coarse Grained
500	600	1	200	1	78	28,900	25,700	32	68	
500	600	1	200	2	78	26,500	23,200	30.4	68	
260	600				78	34,000	31,500	37	68	As Rolled
260	600	1	200	1	88	40,200	40,000	17	68	
260	600	3	200	1	88	39,500	38,500	19	68	
260	600	3	200	1½	88	40,000	39,000	18	68	
260	600	3	200	2	81	38,000	38,000	15	68	
260	600	3	200	2	84.5	37,300	37,200	17	68	
260	600	3	200	2	90	39,200	39,200	17	68	
260	600	3	200	20	81	36,000	35,000	20	68	
260	600	3	200	½	91	50,600	48,000	11	68	
260	600	3	200	1½	90	49,000	48,000	12.3	68	
260	600	3	200	5	88	46,400	46,000	15.5	68	
260	600	3	200	20	87	43,000	37,800	16	68	
260	600	3	200	20	86	42,500	42,000	16	68	
260	600	3	200	20	86	43,500	43,000	15.5	68	
260	600	3	200	20	85	39,500	39,000	18	68	
260	600	3	200	20	86	40,500	39,500	17	68	
260	600	3	200	20	87	42,700	39,600	20	68	
260	600	3	200	20	89	52,200	46,300	8.2	-108	
260	600	3	200	20	87	46,000	40,100	8.5	-108	
260					85	42,800	36,500	13.0	-108	
260	600	3	200	20	85	44,000	38,400	6.0	-108	
260					88	49,100	40,100	14.0	-108	
260	600	3	200	20	88	49,100	42,100	8.0	-108	
260	600	3	200	20	85	42,600	36,400	13.0	-108	
260	600	3	200	20	86	43,500	37,700	10.5	-108	
450	600	1	200	1	80.5	49,000	42,600	14	-320	
450	600	1	200	2	82	48,100	42,000	14	-320	
260	600	3	200	20	88	58,800	49,800	7	-320	
260	600	3	200	20	88	53,100	47,500	4	-320	
260	600	3	200	20	87	46,700	42,500	-	-320	Broke in Pin Area
260	600	3	200	20	86	49,000	42,600	5.0	-320	
260	600	3	200	20	88	53,500	-	-	-320	Broke in Pin Area
260	600	3	200	20	89	55,300	50,100	7.0	-320	

Table 3

Table 3 (cont'd)

260	600	3	200	20	88	60,700	60,000	4	-452	
260	600	3	200	20	90	70,200	66,000	2	-452	
260	600	3	200	20	89	64,300	61,200	3	-452	
260	600	3	200	20	88	64,400	61,200	3	-452	
260	600	3	200	20	88	65,700	-		-452	Brake in Pin Area
260	600	3	200	20	87	61,000	60,000	4	-452	
260	600	3	200	20	86	59,300	50,200	8.5	-452	
260	600	3	200	2	85	38,400	-	-	68	Notched/Unnotched = 0.91
260	600	3	200	20	89	43,600	-	-	68	Notched/Unnotched = 1.03
260	600	3	200	20	80	44,000	-	-	68	Notched/Unnotched = 1.04
260	600	3	200	20	87	58,200	-	-	-452	Notched/Unnotched = 0.91
260	600	3	200	20	88	58,800	-	-	-452	Notched/Unnotched = 0.92
260	600	3	200	20	86	26,000	22,400	12.5	68	Transverse Weld, 61.7% Efficient
260	600	3	200	20	86	27,700	23,300	6.6	68	Transverse Weld, 65.5% Efficient
260	600	3	200	20	88	34,200	29,400	8	68	Transverse Weld, 81% Efficient
260	600	3	200	20	89	33,900	29,200	9	68	Longitudinal Weld, 80.5% Efficient

The Measured Average Density of Alloy 1 A 6 is 1.57 gm/cc



the unstable  $\beta$  phase. This may account for this higher stability. As expected from a longer high temperature heat treatment, the grains were more equiaxial and the ends of the elongated  $\beta$  phase were rounded, showing a tendency for this second phase to become spherical. The matrix grain size remained small because of the addition of 2 and 3% thorium for stability.

All three alloys could be air cooled from 600°F to obtain optimum properties, but this rate of quench was marginal, and many of these specimens were too soft for testing. In the interest of uniformity all specimens tested at the end of the program were quenched in water resulting in hardness of Re 100 for alloys II4 and ZLH 972 and about an average of Re 95 for alloy IA 6.

After the solution heat treatment and prior to aging, alloys II4 and ZLH 972 were hard and brittle whereas alloy IA 6 retained some ductility, approximately 11%. During the first few hours of aging, the strength and hardness of alloys II4 and ZLH 972 dropped quickly and then became more stable as aging proceeded. The percent elongation of these two alloys increased sharply after a few hours of aging while the increase in ductility of alloy IA 6 was less drastic. No obvious correlation is evident between this initial brittleness and initial change in mechanical properties after aging. Part of the initial drop in strength properties must be attributed to stress relieving, but attempts to determine if the hardness of the alloys would decrease drastically after very short aging (i. e. essentially stress relieving) and then increase upon further aging failed to change the shape of the aging curves, indicating that stress relieving is not the entire mechanism.

Alloys II4 and ZLH 972 have a relatively large amount of lithium and zinc, close to 1:1 ratio, while alloy IA6 contains three times as much lithium as zinc. The other strengthening elements in alloy IA6 are aluminum, manganese and silver. These results indicate that initial brittleness is caused by a compound in the lithium-rich  $\beta$  phase, such as  $MgLi_2Zn$ , which overages very quickly; and that  $MgLi_2Al$ , or a similar compound, has a less embrittling effect. The aging curves were not extended long enough to determine which of the alloys is more stable, but this should be done along with x-ray diffraction studies in order to contribute to a more thorough understanding of the aging mechanism in these alloys.

For the specimens given the optimum thermal-mechanical treatments, the ambient temperature tensile strength of alloy II4 varied between 42,500 and 45,600 psi, with corresponding elongation values 16 and 15%. Under the same conditions alloy ZLH 972 varied from 40,800 to 46,500 psi and from 25 to 16% elongation. Alloy IA 6 varied from 39,500 psi to 43,500 psi with the elongation varying between 20% and 15.5%. Except for the one specimen that

had a low tensile strength of 40,000 psi, alloy ZLH 972 very closely approached the ultimate tensile strength goals of the program. No problem was encountered in meeting the yield strength goals, but the average elongation values for all three alloys were only slightly better than the 15% goal. The strength of each alloy increased with decreasing temperature with alloy IA 6, reaching a maximum tensile strength of 70,200 psi at  $-452^{\circ}\text{F}$ . All three alloys had usable ductility at  $-452^{\circ}\text{F}$  although the goal of 8% was only sporadically obtained.

In addition to the ultimate tensile strength, yield strength (0.2% offset) and % elongation (within 2"), the modulus of elasticity was obtained for each alloy. When the modulus of elasticity was calculated directly from the slope of the load vs. elongation curves, recorded automatically on the strip charts, values of 7 to  $7.2 \times 10^6$  were obtained at ambient temperature. These values were considered to be too high and they were not listed in Tables 1, 2 or 3. Instead, corrections were made for relaxation effects, and these new values ranged from  $6.5 \times 10^6$  at ambient temperature to  $8.2 \times 10^6$  at  $-452^{\circ}\text{F}$ . The method used for calculating the elastic modulus, and the very slight changes in the slope of the curves did not permit a comparison to be made between the elastic modulus of each alloy.

#### 2.4.2 Notched/Unnotched Tensile Strength

Notched tensile specimens ( $K_t = 10$ ), were tested at ambient temperature and at  $-452^{\circ}\text{F}$ . The alloys developed in the initial 12-month program were notch sensitive but, with the longer aging times developed for the second generation alloys in the current program, the specimens became less sensitive to notches. All specimens were close to a notched/unnotched ratio of 1.0 at ambient temperature, and 0.9 at  $-452^{\circ}\text{F}$ , i. e. they achieve the contractual goal from a notch sensitivity standpoint. The average ultimate tensile strengths were used for the unnotched strength values which accounts for the variations obtained for notch sensitivity.

#### 2.4.3 Weldability, Tensile Strength

For most magnesium alloys an increase in alloy content increases the solidification range but lowers the shrinkage and the solidus and liquidus temperatures. For alloys containing both aluminum and zinc, the aluminum content aids weldability, and zinc induces hot shortness and resulting weld cracking. Thorium, which provides creep strength at elevated temperatures, usually greatly enhances weldability.

All three alloys developed in this program were easy to weld using the TIG method with an a-c machine that contained a high frequency arc stabilizer. A picture of a typical welded panel is shown in Figure 46. All weld beads were

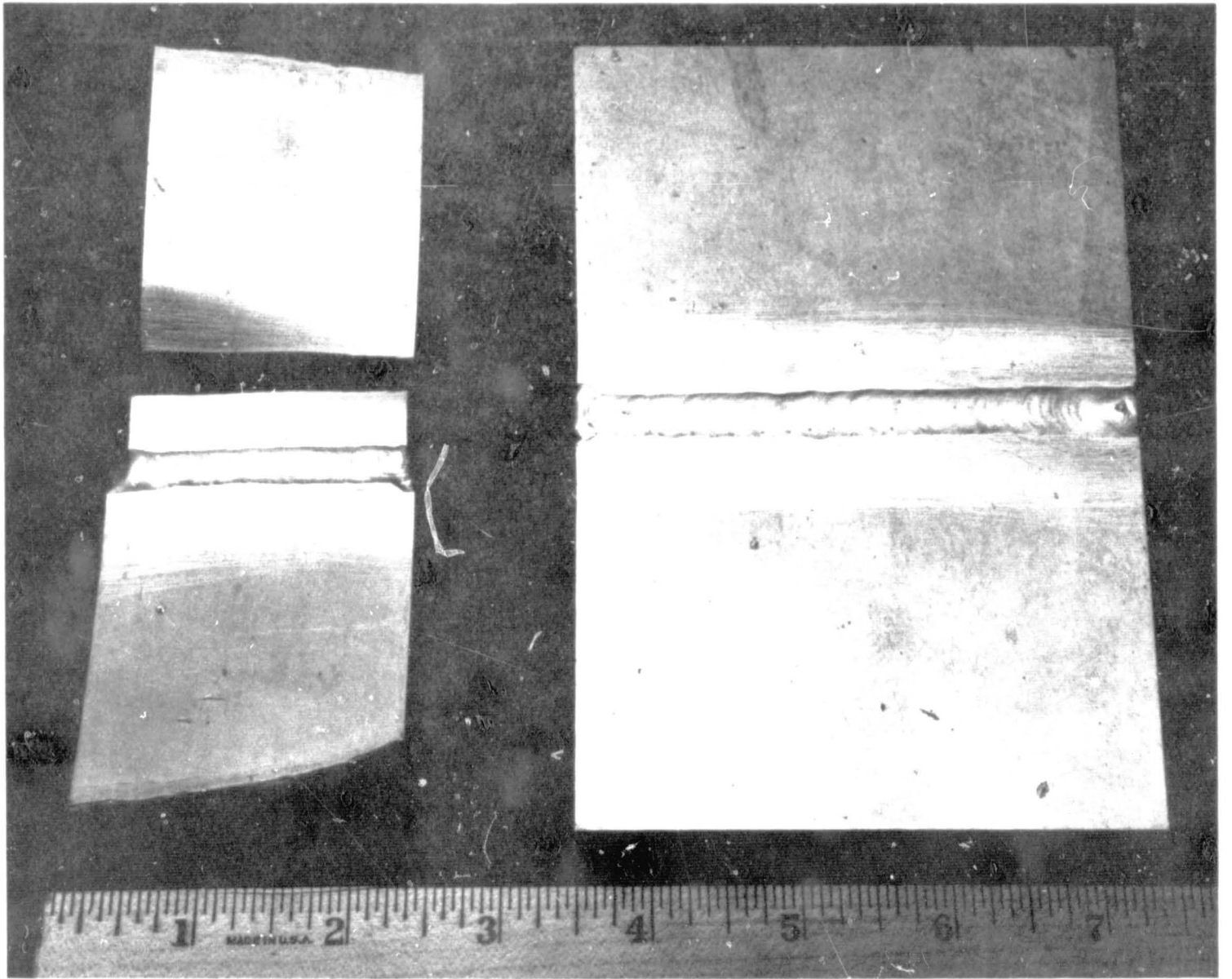


Figure 46. Welded Panels Of Alloy 1A6 Showing A Test Panel That Broke Upon Impact In An Area Outside The Weld.

removed from the surface by machining. The specimens tested and recorded in Tables 1, 2 and 3 were welded by using filler rods made of the parent material. A few specimens were welded using other weld rod material but the welds were poor and were not included in the testing program. At the beginning of the program considerable trouble was encountered in obtaining dross-free welds but this problem was solved by using an excess amount of cover gas and by cleaning the filler rods just prior to welding.

Although none of the specimens developed cracks, the weld joint efficiency of alloy IA 6 was the poorest of the three alloys under development, while alloy ZLH 972 was easy to weld and had good efficiency. These results are surprising in view of the high zinc content of alloy ZLH 972, and the fact that alloy IA 6 was the only one that contained aluminum. All three alloys contained a small amount of thorium which may have aided in preventing crack formation. Since all three alloys were welded with parent metal filler rods and stress relieved during aging, stress-corrosion cracking is expected to be negligible.

The weldability of II4 alloy was again studied during the last month of the program for confirmation of the earlier results. Weldments were made from three inch wide strips of as-rolled II4 alloy by the heli-arc technique, using II4 alloy strips for welding rods and bottled argon as the inert gas atmosphere. Steel back-up plates were used to minimize the heat-affected zone. These plates were made with a 1/4 inch diameter groove which allowed the molten metal to penetrate 1/4 inch below the weld plates and, at the same time, chilled the molten metal to obtain a finer grain size and to reduce contamination.

Examinations of the welds showed that the weld metal was clean except for the metal that was in the grooves. This metal was overchilled which, along with the oxide film forming on the molten weld metal, has the effect of producing folds in the metal. In the final test specimen, these folds acted as very severe notches. When the beads were removed by machining, tensile values were obtained from a few tests made on this welded material, which was solution heat treated for three hours at 625°F. The data are reported in Table 1. The results were found to be comparable to the properties of parent metal heat treated in the same manner, and confirm the earlier results that this alloy can be MIG or TIG welded with much greater than the 80% efficiency goal of the contract.

## 2.5 Coatings Development

In order to obtain the response of these alloys to existing coatings at minimum cost to the government, material was initially sent to commercial vendors for application of any coating they considered applicable. At the

same time metallic coatings and modified corrosion coatings were developed and applied in the AMF laboratory. The results of the overall effort, including both negative and favorable, are reported below.

### 2.5.1 Commercial Coatings

At the AMF laboratory, MacDermid MD678, a stannate coating, was applied to ZLH 972 and IA 6 for subsequent testing. The coating was easy to apply to the former alloy, but considerable difficulty was encountered in applying it to IA 6, and the final coating was not satisfactory. Allied Mag 15, a hexavalent chromium conversion coating, and the NASA modified zincate coating were successfully applied to alloy ZLH 972 and exhibited good surface quality. In addition, all three alloys were given an 8% phosphoric acid treatment, but an adherent coating did not develop.

Alloy ZLH 972 was easily cleaned prior to coating by using an alkaline cleaner and a chromic-nitrate pickle. This treatment did not clean the other two alloys and a new cleaning procedure had to be developed for them. The best precoating treatment developed for these alloys consisted of degassing with acetone, immersing the specimens for three minutes at 180°F in MacDermid Metex E 314 alkaline cleaner, followed by immersion in the MacDermid Mag D-CP for three minutes at ambient temperature.

After establishing good cleaning procedures, the development of a metallic coating was initiated by applying a prime coating of electroless nickel. Good adherent coatings were obtained by keeping the bath at a pH of 10.5 and immersing for 15 minutes at 120°F. Longer immersion times and vigorous stirring of the bath resulted in thicker deposits which did not adhere to the surface of the specimens.

The NASA modified zincate coating, NASA Technical Brief 65-10294, October 1965, was also tried as an intermediate coating for electrodeposited gold and nickel. A thin layer of the zincate coating was applied to specimens of each alloy. Normally a flash coating of cyanide nickel would be applied over the zincate coating before electroplating, but this step was omitted in order to obtain a brighter final deposit. The specimens were taken from the zincate bath, rinsed, and immersed directly into a Harshaw proprietary bright nickel plating bath. The final deposit had an exceptionally bright surface.

Initial attempts to coat a layer of copper on the zincate coating resulted in a "burned" deposit. This was done in a pH 10, cyanide-fluoride copper bath, at 135°F, and using 15 asf with mechanical bath agitation. These results

suggested that a lower current density was required for adequate deposition. Successful plating was accomplished at a current density of 8 asf. The cyanide copper proved to be a good base for final bright electrodeposits; a bright nickel and a bright copper over-coating were successfully applied.

Bright nickel plating was accomplished in a proprietary Watts type bath, obtained from the Harshaw Chemical Company, at 40 asf, 140°F, and pH 4.5, using air agitation. Bright copper plating was accomplished in a proprietary, Udylite Company of Detroit, acid copper bath at 85°F, 15 asf and with mechanical agitation. No adverse reaction occurred between the specimens and the acid copper bath because of the protection offered by the primary coatings. Some work was done on coating the specimens directly in an alkaline copper bath without any preliminary coating. While the results were very encouraging, the specimens were not completely covered with the coating and no optical measurements could be made.

The spectral total reflectance of bright nickel, bright copper, and buffed specimens of uncoated alloy ZLH 972 was measured in the range from 230 to 2650 m $\mu$ , i. e., from the ultraviolet, through the visible, and to the near infrared. Typical results are shown in Figure 47 with all percent reflectance values measured vs. MgO as a standard. The reflectance of the bright copper coating was exceptionally good, especially for a coating that was neither polished nor buffed. The copper coatings, as measured, had some blistering, which could be eliminated by adjusting the plating conditions.

A requirement for the alloys under development in this program was that they must be coatable by standard means, although development of a new coating was not required. Electroplating the alloys was found to be an easy task. This was done by applying an initial low temperature (120°F) electroless nickel plate and flash plating it with copper prior to gold plating. The composition of the electroless nickel bath is as follows:

50 g/l	NiSO <sub>4</sub> · 6 H <sub>2</sub> O
25 g/l	NaH <sub>2</sub> PO <sub>2</sub> · H <sub>2</sub> O
25 g/l	Na <sub>4</sub> P <sub>2</sub> O <sub>7</sub>

The first two compounds were mixed with water at 150°F prior to dissolving the sodium pyrophosphate. Water was added to make one liter, and NH<sub>4</sub>OH added to the solution until a pH of 10 was obtained. No special surface preparation was found necessary prior to nickel plating, which took a total of two minutes to obtain uniform coating. Copper flashing was found necessary



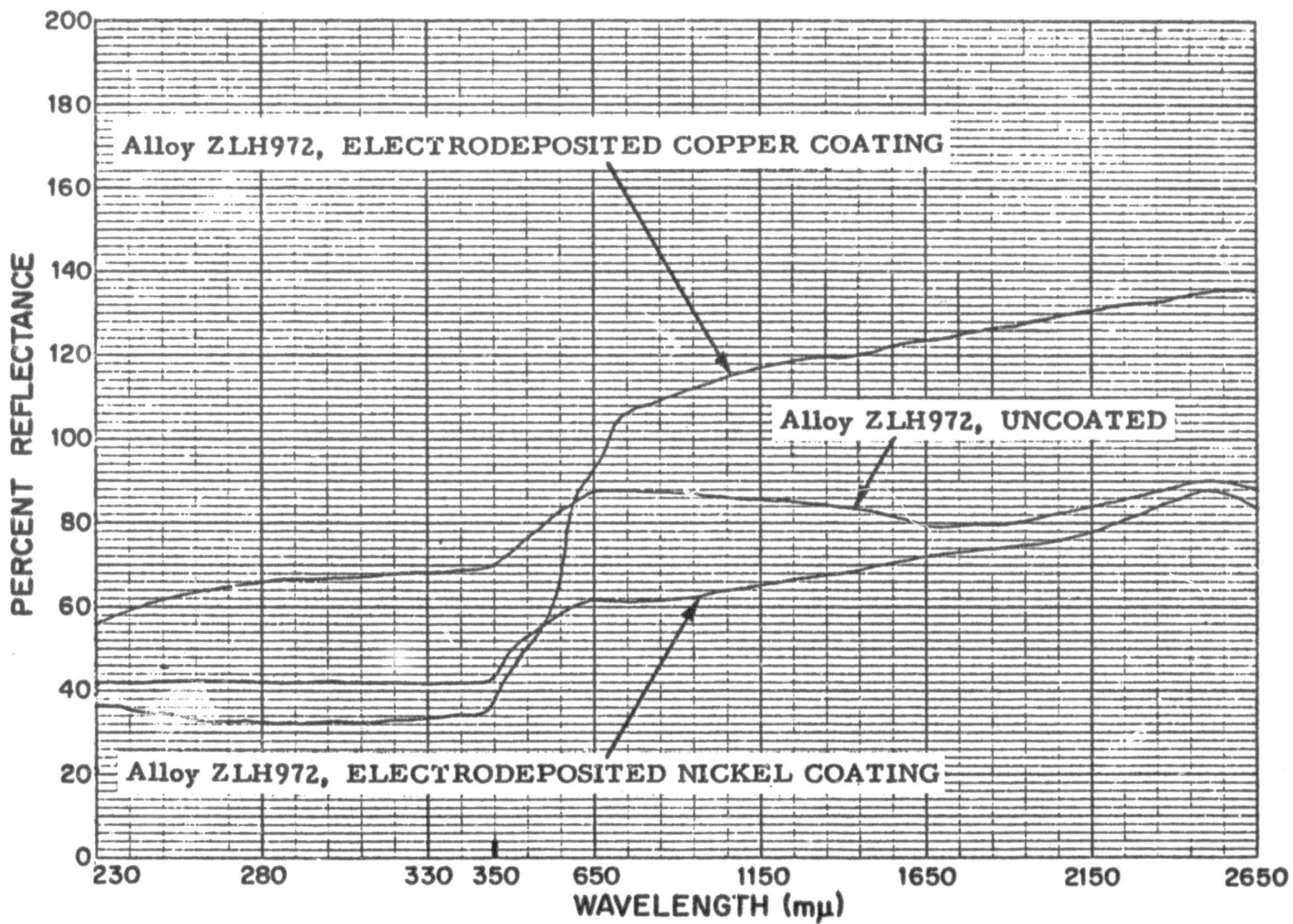


Fig. 47 Spectral Total Reflectance (vs. MgO) of Coated Magnesium-Lithium Alloy ZLH 972 from the Ultraviolet to the Infrared Region



for obtaining a pit-free layer for the final metal coating. No corrosion was observed on the gold coated specimens after four months of exposure to the atmosphere. The gold coating was applied in a cyanide bath, and it was found necessary to completely cover the specimen with electroless nickel before copper flashing or a black deposit would result.

A very thin and hard plastic coating was successfully applied to a specimen of alloy II4 pilot ingot material. The surface of the coated panel remained bright and shiny after one month's exposure in a metallography laboratory and in a humidity cabinet. The coating is called Sealtemt #630, a product of Rector Engineering Company of Washington, D. C. It is essentially a polyurethane coating which cross links any surface moisture, during air drying, to stifle corrosion. The coating contains xylol, cellosolve acetate (Union Carbide), and urethane; the first two eliminate a blushing problem which might cause blistering at the interface, and promote good flow characteristics to keep the coating as thin as possible. The coating air dries in four hours at 70°F and 50% relative humidity with a Sward Hardness (NBS) of 25. After three days the hardness is 36 and after seven days it is 40.

Another coating, an epoxy, called Castaband #250, which is very flexible in liquid nitrogen and inert to a hard vacuum, was studied. There was no problem in applying this coating to the pilot ingot material.

Specimens were successfully zincated by the MacDermid Corporation and then copper flashed for subsequent plating. This company also tried to anodize II4 ingot material, but were not successful.

## 2.5.2 Coatings Developed in AMF Laboratory

As previously stated the purpose of this phase of the program is to develop a coating to protect the metal from marine atmospheric corrosion and, if possible, serve the dual purpose of controlling the temperature of a vehicle when exposed to the extremes of darkness and bright solar energy in aerospace service. On this basis two coatings were developed to serve these functions, one is a dull black coating with high solar absorption, which is also corrosion resistant; and the other is a highly reflectant outer coating which can be applied to the black primary coating when needed.

### 2.5.2.1 Corrosion Resistant Chemical Conversion Coating, FSC-1

This coating is more conveniently applied while the alloy stock is being hot rolled to wrought sheet. The procedures ultimately developed for (1) the optimum initial application during hot rolling, (2) for application finished bare wrought sheet, and (3) for repair of handling scratches, welded or other

coating damaged areas has been summarized in NASA New Technology disclosure on FSC-1 coating of specified magnesium-lithium alloys, shown on the following pages.

In order to test the corrosion resistance of the black chromate conversion coating to sea air exposure, coated panels were taped to a wooden frame and placed 80 feet from the ocean at an AMF test site in Waterford, Connecticut.

Commercially coated specimens were also tested along with the panels coated at the AMF laboratory; these coatings included MacDermid D17, Allied Mag 15, and more recent specimens of all the alloys coated by AMCHEM Products, Inc. of Detroit, Michigan. The latter company reported that the alkali cleaning, deoxidizing (etching) and activating stages normally used to prepare magnesium alloys for coating were not required for alloy II4. Instead, the specimens were simply immersed in their 62-20 Mg-phosphating solution for two minutes at 80°F followed by a water rinse. The resultant coatings were adherent and had a dark green (almost black) color on alloys II4 and ZLH972 and a lighter green color on alloy IA6. The coating on alloy IA6 was spotty and did not appear to completely cover the whole specimen.

After exposure to the Marine Atmosphere for one month the specimens were rinsed in tap water and returned to the Alexandria Laboratory for examination. A picture of three typical specimens are shown in Figure 48. The specimen coated with D17, shown at the top of the picture, had isolated pits which were very deep and the Mag 15 specimen showed very little resistance to a marine atmosphere. The black chromate conversion coating applied at the AMF Laboratory, which is being designated as FSC-1, stood up well in this atmosphere. The corrosion effects were uniform and did not appear deep enough to affect the substrate material. An uncoated control specimen was severely corroded and could not be photographed.

#### 2.5.2.2 High Reflectance Coating Technology

Since the chromate conversion coating, FSC-1, applied during rolling was found to be corrosion resistant and a good base for paint, emphasis in the coatings program was directed towards the development of a highly reflective outer coating which could be applied to the black conversion coating. More than 120 specimens were coated with various combinations of vehicles and pigments including one formulation received from the NASA Goddard Space Flight Center. A brief summary of these coatings is given in Table 4.

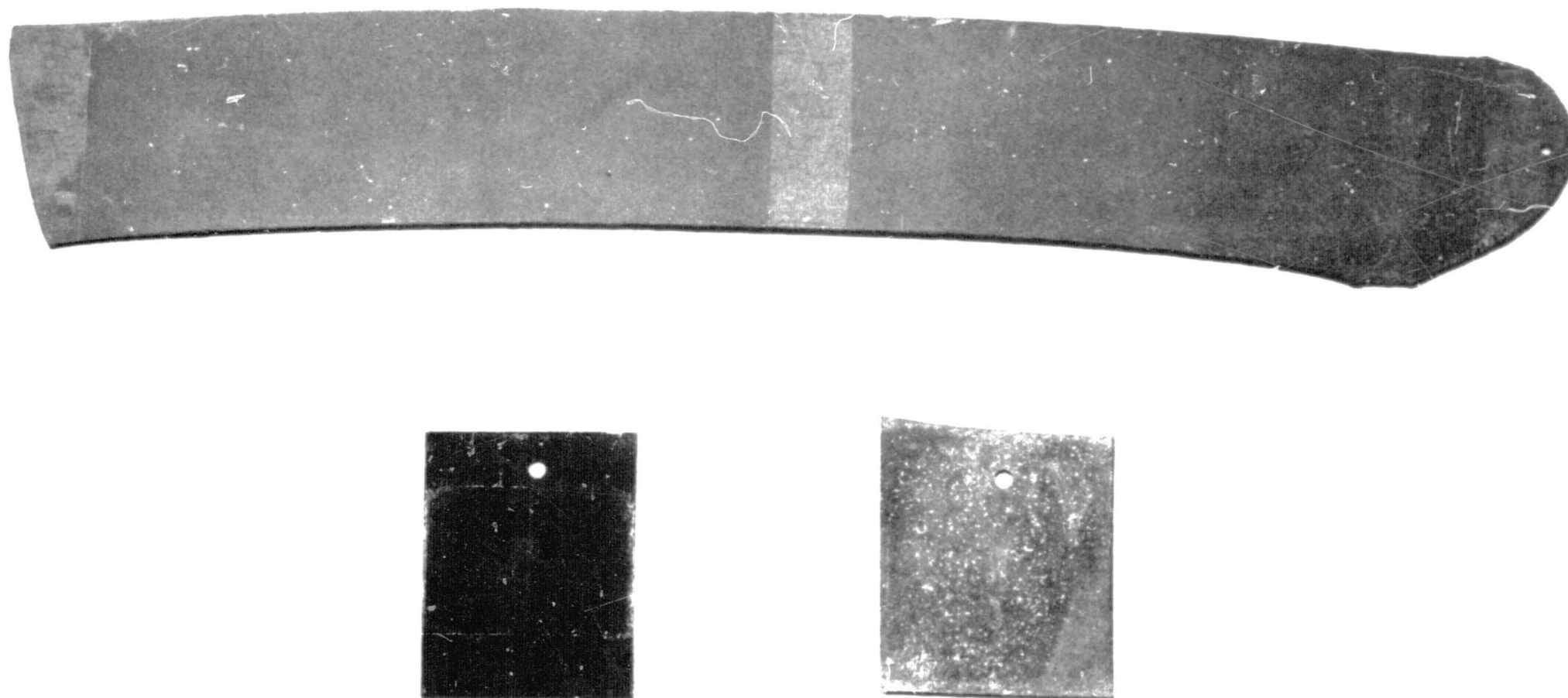


Figure 48. Coated specimens after one month exposure to a marine atmosphere. The large specimen at the top of the picture was coated with Mac Dermid D 17, the specimen at the lower left was coated with FSC-1, and the specimen at the lower right was coated with Allied Mag 15. The D 17 specimen had few but very deep pits, the FSC-1 specimen showed shallow and uniform corrosion, and the Mag 15 specimen showed severe pitting.

TABLE 4

SUMMARY OF HIGHLY REFLECTANT COATINGS DEVELOPMENT

A.	<u>Vehicle</u>	<u>Vendor</u>	<u>Composition</u>
	P-S-7 (Potassium Silicate)	Sylvania	35.0% Solids $K_2O:SiO_2$ (11% $K_2O:24\% SiO_2$ )
	Zerifax	Footo Mineral	$Li_2O:Al_2O_3$ (4.2% $Li_2O:$ 17.3% $Al_2O_3:76.10\%$ $SiO_2$ )
	Thermal Grain #3	Footo Mineral	$Li_2O:Al_2O_3:SiO_2$ (7.18% $Li_2O: 26.8\% Al_2O_3:$ 63.4% $SiO_2$ )

The lithium aluminum silicates were used as both vehicles and pigments.

B.	<u>Pigment</u>	<u>Vendor</u>	<u>Size</u>
	ZnO	New Jersey Zinc. Co.	0.4 $\mu$
	TiO <sub>2</sub>	Dupont	-150 + 170 Mesh
	ZrO <sub>2</sub>	Cabot	-170 + 200 Mesh

C. Coating and Preliminary Results

1. P-S-7 + ZnO - Coating very fluid but good results obtained with 100g PS7 + 58g ZnO + 50 cc H<sub>2</sub>O.
2. P-S-7 + TiO<sub>2</sub> - best results with 100g PS7 + 92g TiO<sub>2</sub> + 50cc H<sub>2</sub>O.
3. P-S-7 + ZrO<sub>2</sub> - Could not be suspended in water.
4.  $K_2SiO_3$  + TiO<sub>2</sub> +  $Al_2O_3$  (13.7g + 5 cc H<sub>2</sub>O) Coating obtained from NASA Goddard,  $\alpha/\epsilon = 0.1$ .
5. Thermal Grain #3 - Tan colored coating resulted - omitted further development.
6. Zerifac - These coatings would not cure at any temperature up to 200° F.
7. 50g Zerifac + 50g TiO<sub>2</sub> + 150 cc H<sub>2</sub>O - Good coating, cured at room temperature.

The pigments tabulated in Table 4 were used just as they were received from the vendor without additional ball milling or blending for added uniformity. For each case highly reflectant coatings were applied over the black chromium conversion coating in alloy II4. The selected coating formulations were based upon typical low  $\alpha/\epsilon$  coatings commonly used for thermal control of space vehicles.

These formulations involved ZnO, TiO<sub>2</sub> and ZrO<sub>2</sub> as pigments and potassium silicate (PS-7)\* or lithium aluminum silicate (Zerifac) as vehicles. In particular, three coatings were evaluated in this phase of the program, i. e. (1) PS-7+ZnO, (2) PS-7 + TiO<sub>2</sub>, and (3) Zerifac (ZR) + TiO<sub>2</sub>.

Solar absorptance values,  $\alpha_s$ , were calculated from spectral reflectance measurements in the 0.23 to 2.65  $\mu$  range, performed using a Beckman DK-2A Spectroreflectometer. Measurements were performed relative to freshly prepared MgO standards. Conversion to absolute reflectance was accomplished using literature values for the spectral reflectance of MgO. The calculation was based on the expression:

$$\alpha_s = \frac{\int_{0.23 \mu}^{2.65 \mu} \alpha_\lambda E_\lambda d\lambda}{\int_{0.23 \mu}^{2.65 \mu} E_\lambda d\lambda}$$

where  $\alpha_s$  is the Solar absorptance,  $\alpha_\lambda$  is the spectral absorptance,  $E_\lambda$  is the spectral energy distribution of solar radiation above the earth's atmosphere, and  $\alpha_\lambda = 1 - r_\lambda$ , where  $r_\lambda$  is the absolute spectral reflectance. The integrals were evaluated graphically by measuring the area under the graphed functions of  $E_\lambda$  and  $\alpha_\lambda E_\lambda$ .

The spectral reflectance curves for the coatings of ZnO-potassium silicate, TiO<sub>2</sub>-potassium silicate, and TiO<sub>2</sub>-lithium aluminum silicate are presented in Figures 49-51.

---

\* PS-7, potassium silicate, was supplied by Sylvania Electrical Products, Inc., Towanda, Pennsylvania, and is characterized by its high purity. The chemical composition is 11.0% K<sub>2</sub>O and 24.0% SiO<sub>2</sub>. Water was added, as necessary, to prepare a sprayable formulation.

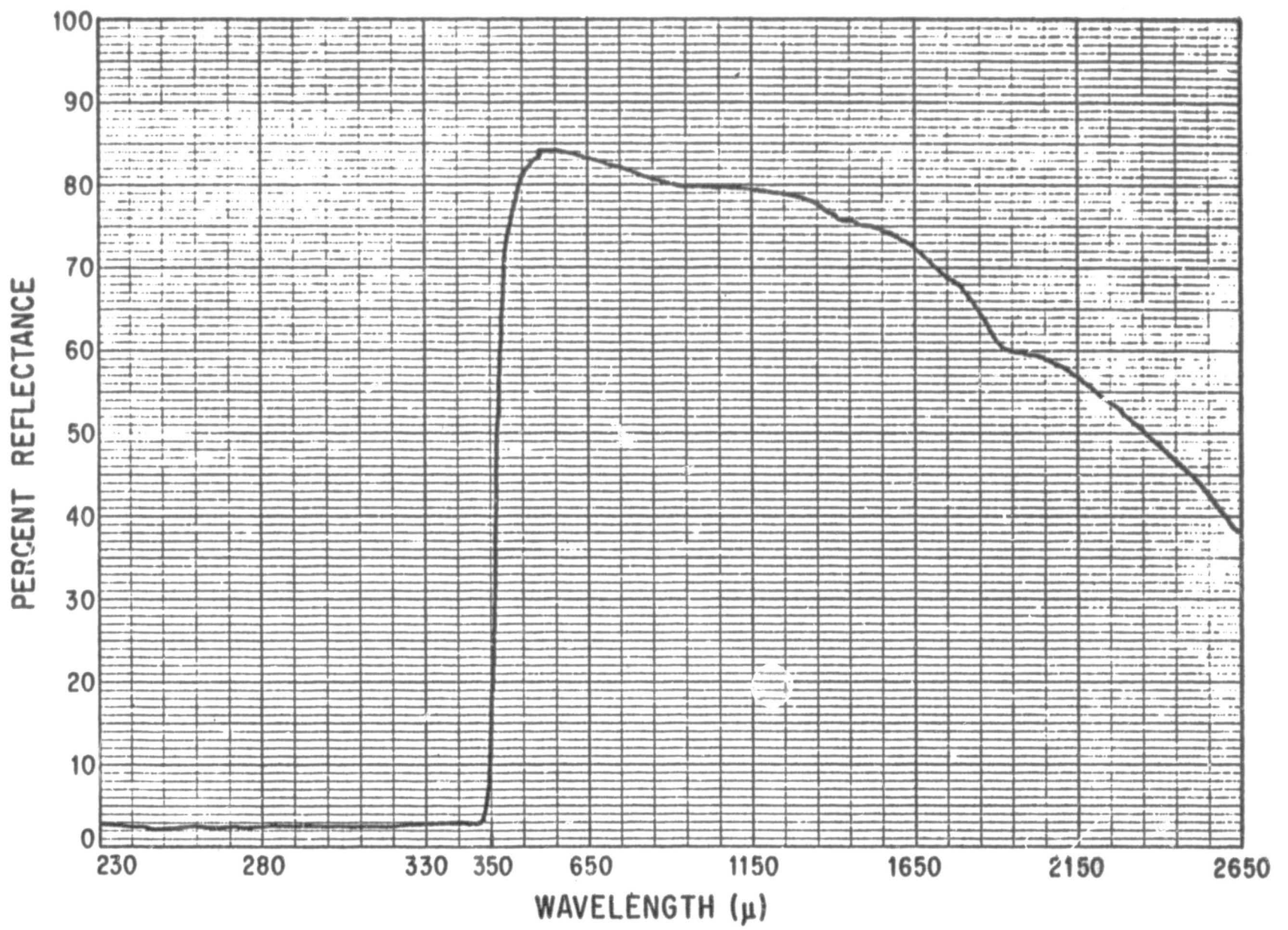


Figure 49. Spectral Total Reflectance of ZnO-Potassium Silicate

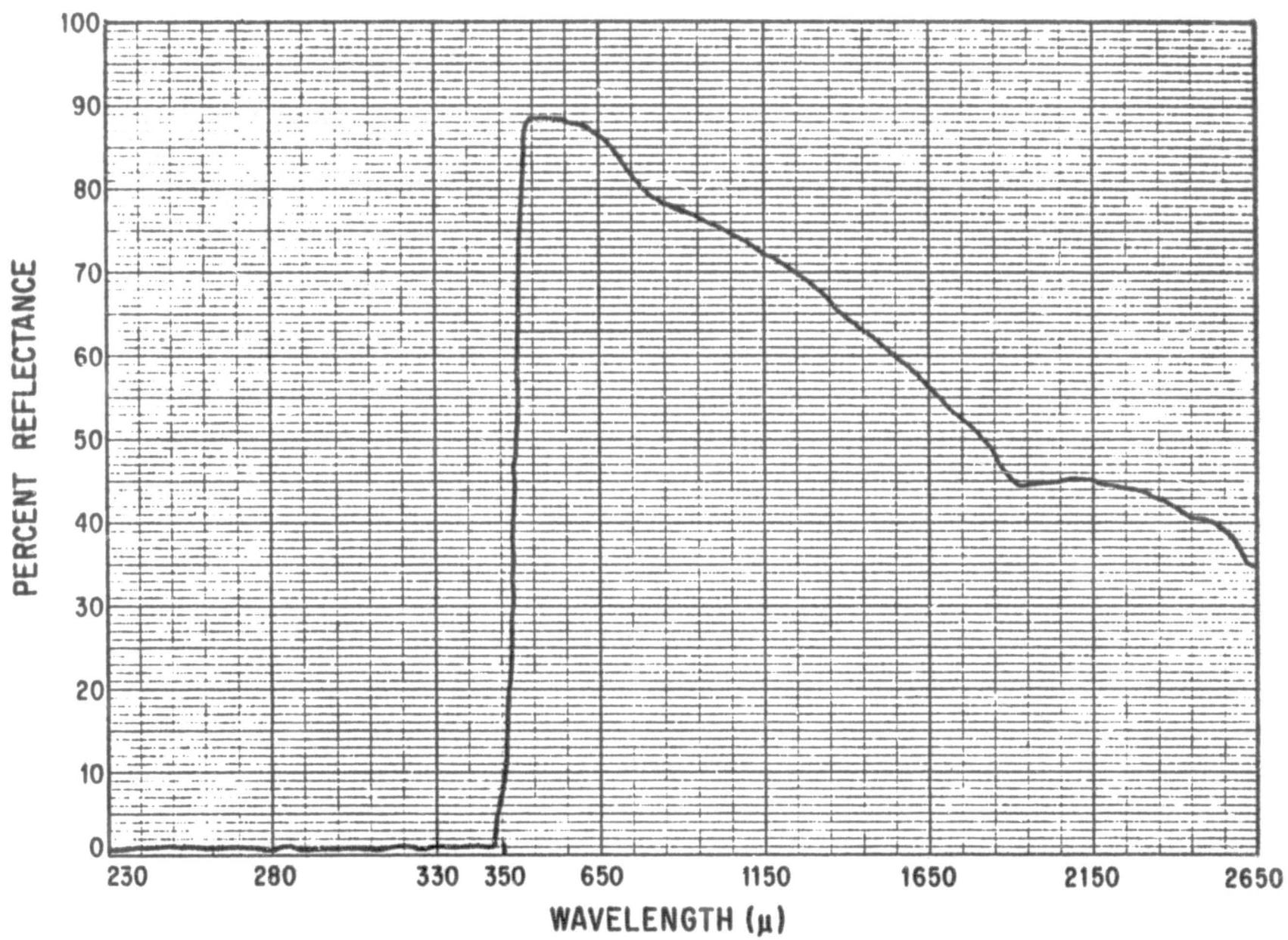


Figure 50. Spectral Total Reflectance of  $TiO_2$ -Potassium Silicate



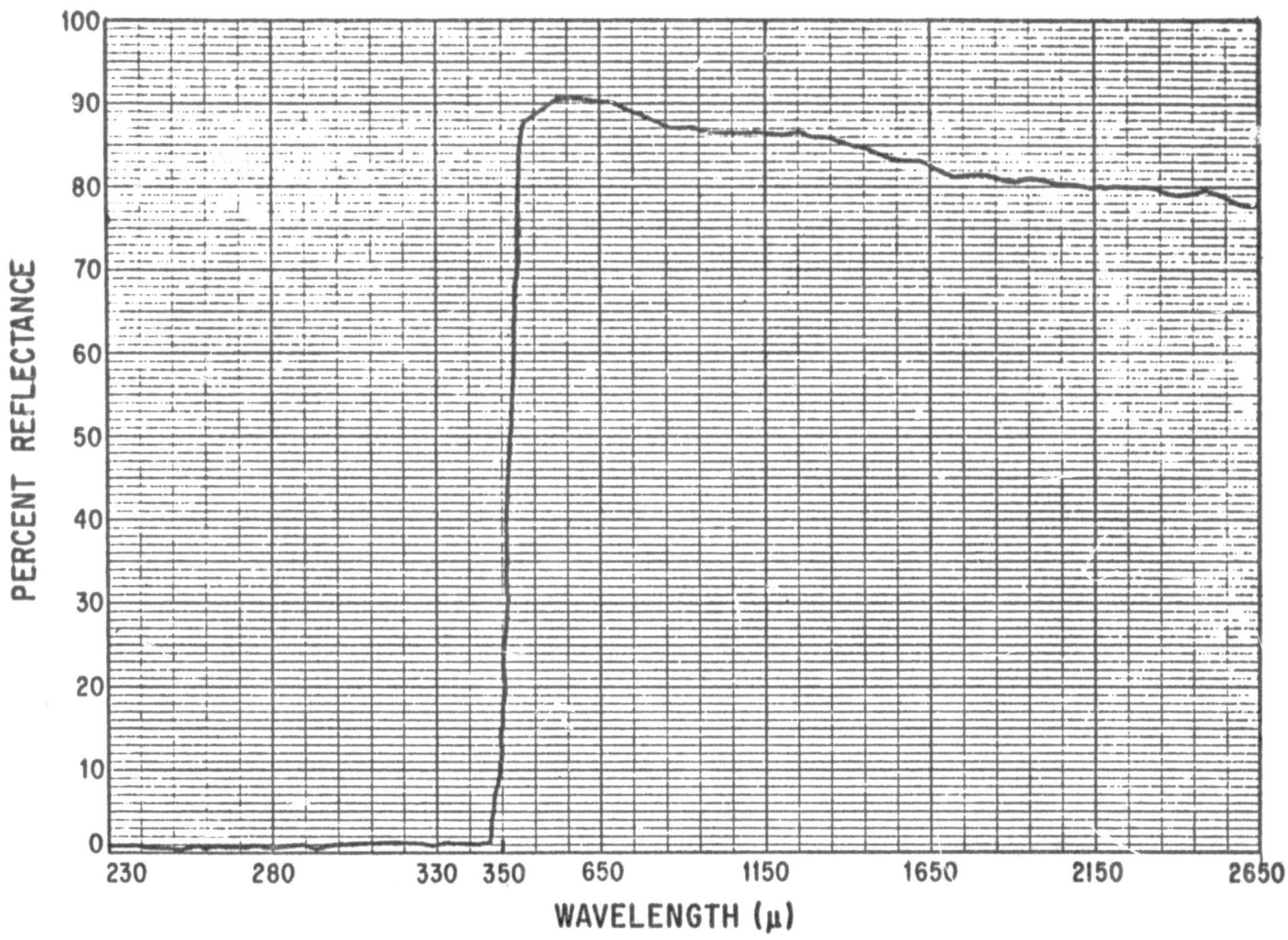


Figure 51. Spectral Total Reflectance of  $TiO_2$  - Lithium Aluminum Silicate

The values of solar absorptance calculated from these curves are 0.27, 0.29 and 0.20. For comparison, the reported values\* of solar absorptance for ZnO-potassium silicate coatings range between 0.13 and 0.27. It should be realized that the main interest for the presently prepared coatings were in their compatibility with the black corrosion-protective layer, rather than in attaining the lowest possible value of solar absorptance. With slight additional research it should be possible to consistently prepare coatings with solar absorptance values below 0.20, even though applied over a black primary coating.

In addition, we have measured the spectral reflectance in the 1 - 15 $\mu$  region (Figure 52) for the TiO<sub>2</sub>-potassium silicate coating to enable approximate calculation of the total emittance. The absolute reflectance was measured using a Blackbody Reflectometer Apparatus\*\* constructed at AMF. The total normal emittance,  $\epsilon_{tn}$ , was calculated from the spectral reflectance,  $r_{\lambda}$ , according to the expression:

$$\epsilon_{tn} = \frac{\int_{1\mu}^{15\mu} \epsilon_{\lambda} W_{\lambda} d\lambda}{\int_{1\mu}^{15\mu} W_{\lambda} d\lambda}$$

where  $\epsilon_{\lambda}$  is the spectral emittance, which equals  $1-r_{\lambda}$  and  $W_{\lambda}$  is the spectral energy distribution for a blackbody at 400°K (the approximate temperature of the sample surface). The integrals were evaluated graphically in a similar manner to that described for the solar absorptance calculations. The calculated total emittance for this sample was 0.56, giving an  $\alpha/\epsilon$  value of 0.29/0.56 or 0.52.

---

\* G. A. Zerlaut, Y. Harada and E. H. Tompkins, "Ultraviolet Irradiation of White Spacecraft Coatings in Vacuum", p. 391, in Symposium on Thermal Radiation of Solids" S. Katzoff (Editor), NASA SP-55, (1965).

\*\* E. A. Schatz, G. H. Alvarez, T. L. Burks, C. R. Counts III, F. J. Dunkerley "High Temperature, High Emittance Inter-metallic Coatings", Part II, ML TDR 64-179, July 1964, AD 472439.

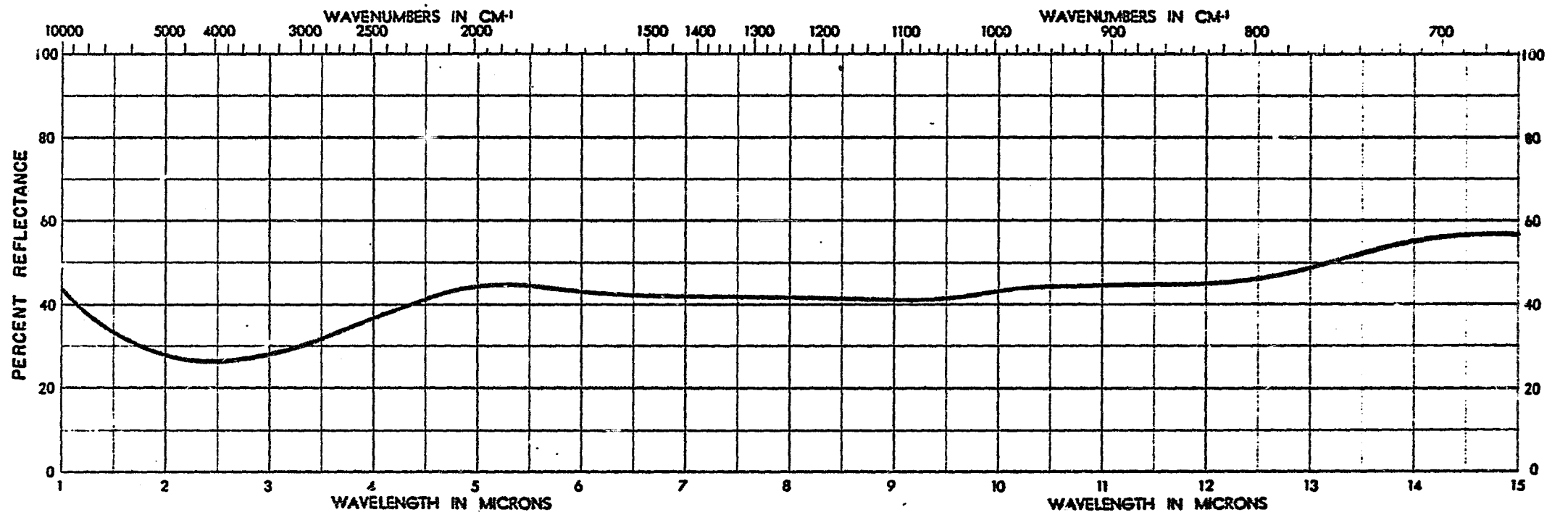


Figure 52. Absolute Spectral Reflectance of a  $\text{TiO}_2$ -Potassium Silicate Coating

The absolute spectral reflectance in the 1-15 $\mu$  region for TiO<sub>2</sub>-potassium silicate was repeated because of experimental difficulties encountered with the first measurements and the absolute spectral reflectance for ZnO-potassium silicate and TiO<sub>2</sub>-lithium aluminum silicate coatings were obtained in the same region. These curves are shown in Figure 53.

The calculated total emittance for these coated specimens were:

	<u><math>\epsilon_{tn}</math></u>	<u><math>\alpha/\epsilon</math></u>
ZnO - Potassium Silicate	0.76	0.36
TiO <sub>2</sub> - Potassium Silicate	0.78	0.37
TiO <sub>2</sub> - Lithium Aluminum Silicate	0.76	0.26

where  $\epsilon_{tn}$  is the total normal emittance as defined above.

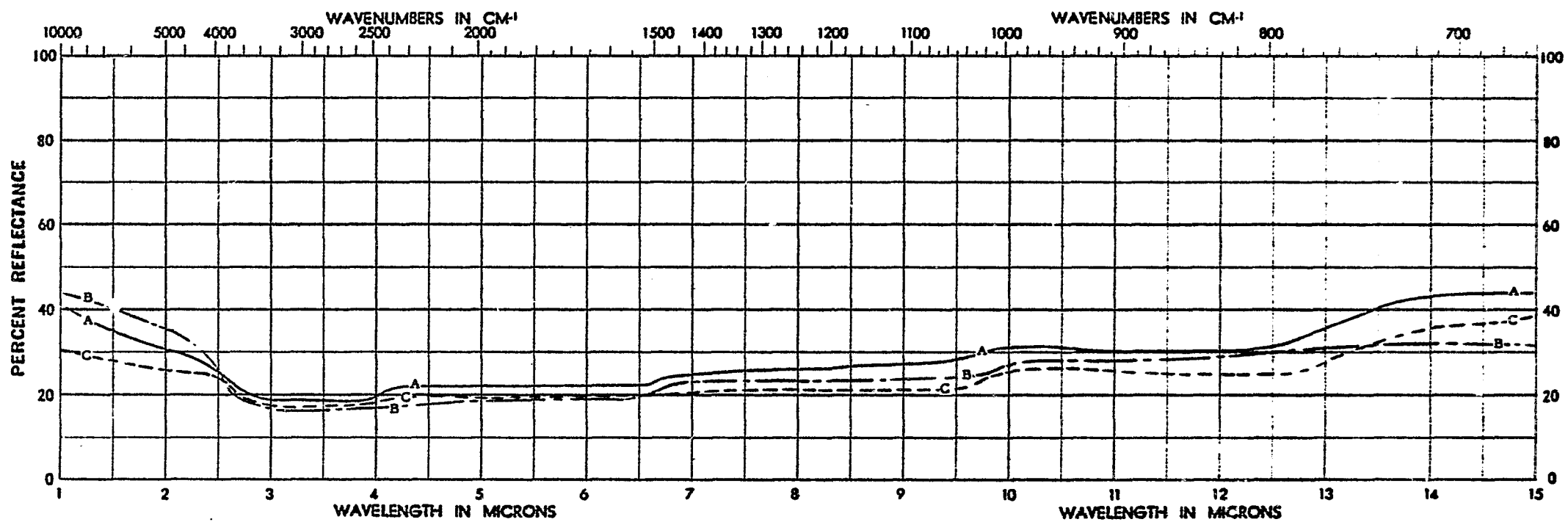


Figure 53. Absolute Spectral Reflectance of  $\text{TiO}_2$  - Potassium Silicate,  $\text{TiO}_2$  - Lithium Aluminum Silicate, and  $\text{ZnO}$  - Potassium Silicate Coatings

- Curve A -  $\text{TiO}_2$  - Lithium Aluminum Silicate Vehicle
- Curve B -  $\text{ZnO}$  - Potassium Silicate Vehicle
- Curve C -  $\text{TiO}_2$  - Potassium Silicate Vehicle

## 2.6 X-Ray Diffraction Studies

X-ray diffraction patterns were obtained early in the program for the three alloys scaled-up and studied throughout this program. Flat, polished specimens were placed in a rotating specimen holder which was part of the Norelco x-ray diffraction equipment used for these studies. The specimens were rotated at a speed of two degrees per minute and irradiated with  $\text{CuK}\alpha$ .

The x-ray data obtained for the three wrought, pilot ingot materials are tabulated in Table 5, A through G, along with a pattern obtained for pure magnesium. The maximum intensity occurred at a  $2\theta$  angle of 36.10 to 36.15 degrees for alloy IA6 and did not change as a function of solution heat treating time or as a function of aging time. The maximum intensity occurred at the 101 plane, as it did for pure magnesium, with a corresponding d value of 2.485 Å which also did not change significantly with heat treatment.

The maximum intensity also occurred at the 101 plane for alloy ZLH 972 with a corresponding d value of 2.491 Å. This alloy is actually a modification of alloy II 4 D which contained 8% zinc and 7% lithium. The pattern obtained for alloy II 4 D (not shown) was similar to the one obtained for the unmodified alloy II 4 shown in Table 5E. For this alloy the maximum intensity occurred at a  $2\theta$  value of 35.1 degrees after rolling and prior to heat treatment with a corresponding d value of 2.556. Upon solution heat treating and aging, the pattern changed significantly. The maximum intensity occurred at a  $2\theta$  value of 51.35 degrees with a corresponding d value of only 1.779 Å. This plane has tentatively been identified as 003 indicating that the mechanism of aging is vastly different in alloy II 4 compared with the other two major alloys developed in this program. More exhaustive x-ray studies, although outside the scope of this program, would undoubtedly be most helpful in obtaining a better understanding of the microstructural constitution of these alloys in variously processed and heat-treated states, the nature of age hardening reactions, and many other aspects of their physical metallurgy.

## 2.7 Machinability

To determine the machinability of alloy II4, the constant-pressure machinability experimental set up described in NASA CR-79, June 1964,\* was modified slightly as follows: Constant pressure producing the feed, and

---

\* T. G. Byrer, E. L. White, and P. D. Frost, "The Development of Magnesium-Lithium Alloys for Structural Applications", NASA CR-79, June 1964

X-RAY DATA

A. Pure Magnesium 99.9999

2θ	d value	Intensity %	hkl
69.9	1.36	8.65	201
68.5	1.369	27.8	112
63.1	1.473	11.15	103
47.8	1.903	22.25	102
36.6	2.452	100	101
34.4	2.607	79	002
32.1	2.788	49.4	100

B. Alloy 1A 6, Rolled at 260°F, Solution Heat Treated 1 Hour at 600°F and Aged 20 Hours at 200°F

2θ	d value	Intensity %	hkl
87.8	1.112	11.7	
80.75	1.190	10.9	
76.55	1.244	17.5	
73.2	1.293	12.1	
68.3	1.373	32.0	112
64.8	1.439	85.7	
64.0	1.455	15.4	
57.75	1.596	13.6	110
54.6	1.681	22.5	
52.0	1.758	53.0	
48.4	1.881	14.3	
44.75	2.025	37.0	
37.8	2.380	39.5	
36.85	2.442	26.6	
36.15	2.485	100	101
38.15	2.553	22.8	
32.35	2.767	27.6	100
32.95	3.875	67.8	

C. Alloy 1A 6, Rolled at 260°F, Solution Heat Treated 3 Hours at 600°F and Aged 1 Hour at 200°F

2θ	d value	Intensity %	hkl
76.6	1.244	10.4	
73.05	1.295	13.0	
69.5	1.352	10.4	
68.3	1.373	20.0	
64.9	1.436	70.0	
64.15	1.452	17.4	
57.8	1.570	14.6	
54.6	1.681	22.8	
52.0	1.758	72.0	
48.5	1.877	14.1	
44.7	2.027	24.6	
43.7	2.089	14.4	
40.2	2.243	18.4	
37.85	2.380	30.0	
37.0	2.429	26.2	
36.15	2.485	100	101
35.1	2.556	32.0	002
32.4	2.763	21.6	100
26.5	3.333	28.0	
24.35	3.655	32.4	
23.0	3.867	74.2	

D. Alloy 1A 6, Rolled at 260°F, Solution Heat Treated 3 Hours at 600°F and Aged 20 Hours at 200°F

2θ	d value	Intensity %	hkl
87.7	1.120	14.7	
76.5	1.245	14.9	
73.0	1.296	15.3	
68.3	1.373	23.3	112
64.8	1.439	51.5	
64.2	1.451	21.7	
57.7	1.598	18.2	
54.55	1.682	33.7	
51.9	1.762	87.0	
48.4	1.881	20.2	102
44.65	2.029	29.4	
40.15	2.246	23.7	
37.8	2.380	37.7	
36.95	2.443	30.0	
36.10	2.488	100	101
35.1	2.556	38.8	002
32.3	2.771	38.8	100
26.4	3.376	36.4	
24.2	3.677	45.5	
22.85	3.892	89	

E. Alloy 114 As Rolled at 450°F

2θ	d value	Intensity %	hkl
87.7	1.113	7.2	
83.05	1.163	14	
74	1.281	11	
68.95	1.362	15.5	112
64.95	1.436	46	
65.15	1.452	37.5	
57.8	1.595	11.5	110
55	1.669	17	
52.1	1.755	47	
48.5	1.893	21.5	102
45.05	2.012	22.5	
42	2.151	13.5	
40.1	2.248	16.2	
38.1	2.365	15.5	
37	2.429	54	
36.15	2.485	29	101
35.1	2.556	100	
32.45	2.759	18.5	
30.75	2.907	21.7	
26.75	3.333	22.7	
23.2	3.834	80.7	
20.75	4.281	29.8	

F. Alloy 114, Rolled at 750°F, Solution Heat Treated 3 Hours at 600°F and Aged 20 Hours at 200°F

2θ	d value	Intensity %	hkl
87.1	1.118	32.7	
68.8	1.363	32.7	201
64.2	1.451	42	
63.4	1.467	30.7	103
57.1	1.613	58.5	
54.3	1.689	37.5	
51.35	1.779	100	003
39.4	2.287	27	
36.3	2.475	48.5	101
35.45	2.537	63	
34.4	2.607	46.8	002
22.35	3.978	42.2	

G. Alloy ZLH 972, Rolled at 450°F, Solution Heat Treated 1 Hour at 800°F and Aged 1 Hour at 200°F

2θ	d value	Intensity %	hkl
87.6	1.114	8.75	
76.6	1.244	7.5	
73.7	1.285	8.45	
70.55	1.335	8.75	
69.25	1.357	11.75	
68.75	1.365	13.7	112
64.8	1.439	20	
64.0	1.455	16.9	
60.3	1.535	8.0	
57.75	1.596	20	110
54.9	1.672	47.2	
51.9	1.762	100	
48.4	1.881	20.2	102
44.95	2.017	25.7	
38.05	2.365	51.8	
36.85	2.439	67.5	
36.05	2.491	93.8	101
34.9	2.571	34.3	
32.3	2.771	25.3	100
26.65	3.346	30.0	
23.05	3.858	40.6	



controlled by a weight-and-pulley system that turned the carriage feed-control, was actually measured directly at the tool with a spring scale.

The lateral movement of the carriage was measured by a roller chain-and-sprocket assembly attached to the carriage. Rotation of this assembly turned a cogwheel which, in turn, closed an electrical circuit after each 0.1 inch of carriage travel to record the length of travel. The number of revolutions of the spindle during each 0.1 inch of carriage travel was indicated on a revolution counter directly geared to the spindle.

The following set of conditions was used to machine the specimens:

Spindle speed	- 200 RPM
Bar Diameter	- 0.75 inches
Depth of Cut	- 0.050 inches
Tool Geometry	- 5-degree back rake angle 3-degree front relief angle

A seven pound weight on the pulley resulted in a force at the tool bit of 20-ounces which, when machining the II4 alloy, resulted in a feed rate of 11.6 revolutions of the spindle for every 0.1 inch of carriage travel, i. e., a feed rate of .0086 inches per revolution. This machinability is considerably better than that reported by Byrer et al in NASA CR-79 for alloy LA141, but the machinability tests were within 5% of those reported by Byrer et al; it must be concluded that the higher machinability ratings obtained here for II4 alloy are most significant.

## 2.8 Electrical Resistivity

Electrical resistivity measurements were made on flat cleaned sheet material and on extruded tubing. All measurements were made with a Gray Instrument Company Kelvin Bridge model No. E3272 which is readable to six places, has an accuracy of  $\pm 0.1\%$ , and a range of 0-20 ohm. Copper knife edges were made for contacts and at least 10 readings were made at different locations on the specimens. The results of these measurements are tabulated below:

<u>Alloy</u>	<u>Type of Specimen</u>	<u>Electrical Resistivity at 68°F</u>
II4	Sheet	11.78 microhm - cm
II4	Tubing	18.5 microhm - cm
IA6	Tubing	20.8 microhm - cm

These results compare favorably with other wrought magnesium sheet material, e. g., AZ31B (9.2 microhm-cm), AZ61A (12.5 microhm-cm) and HM31A (6.6 microhm-cm).

## 2.9 Thermal Conductivity

Specimens of II4 alloy, 1" diameter x 6" long were employed in a steady state heat flow thermal conductivity devised by Dr. Walter Norew, University of North Carolina at Charlotte, Charlotte, North Carolina. The measuring system consisted of the probe of radius,  $r_o$ , made up of a resistance heater of length,  $L_h$ , and a carefully calibrated copper-constantan thermocouple. The specimen was drilled to receive the probe and time-temperature values recorded as the temperature of the resistance heater was gradually increased. The same procedure was used on cooling, except that care had to be taken to insulate the specimen to assure slow steady-state cooling.

Pure copper was used to calibrate the apparatus and evaluate the constants in the relationship, from which the thermal conductivity,  $T$ , were calculated directly, i. e.,

$$T = CT(Q_s/L_h)/4\pi k \ln (4D/r_o^2) t$$

where  $C$  = constant;

$r_o$  = radius of probe;

$Q_s$  = measured heat flow in the specimen;

$k$  = thermal conductivity;

$D$  = thermal diffusivity, =  $k/c$ , where  $c$  is the heat capacity per unit volume of the material;

$t$  = time;

$L_h$  = length of resistance heater.

Values obtained at two average test temperatures are:

at 125°F  $K = 27.2$  BTU/hr./ft./°F;

at 167°F  $K = 31.1$  BTU/hr./ft./°F.

Based on the National Bureau of Standards values for the pure copper used to calibrate the apparatus, these values are estimated to be accurate within  $\pm 3\%$ .

## 2. 10 Extrusion of Thin Wall Tubing

The purpose of these studies was to compare the workability of the three alloys by extruding 1 inch O.D. thin walled (0.025 inch) tubing. In preparation for extruding, 2 1/8 inch diameter rods were machined from the three pilot ingots and used directly, (without any pretreatment) as extruding billets.

Extrusion trials were conducted on a million ton hydraulic press at an AMF facility in York, Pennsylvania. Initially, the billets were heated to temperatures of 600<sup>o</sup>F, 700<sup>o</sup>F and 800<sup>o</sup>F in an air circulating furnace prior to inserting them in a porthole die. No lubrication was used and ram speeds of 1 to 2 ipm were employed initially. None of the alloys extruded successfully under these conditions and the results in each case were characterized by an inability of the longitudinal edges of the pipe to weld together.

The initial extrusion studies showed that extrusion parameters developed for other magnesium-lithium alloys such as LA 141 could not be used successfully to extrude the higher strength alloys under development in the current program. Consequently, the critical extrusion parameters were thoroughly studied in the laboratory on a smaller, and more convenient, 20 ton hydraulic press. The preliminary studies showed that heating the billets to 700<sup>o</sup>F and using slower ram speeds were necessary for extrusion and that neither lubrication nor elaborate provisions for protecting the metal from oxidation were required.

After successfully extruding short 6 inch tubing in the 20 ton press, further attempts were made to extrude longer tubing in the larger press. The billets were heated in situ along with the porthole die without using inert argon cover gas for oxidation protection.

Alloy II4 and alloy IA 6 were successfully extruded under the following conditions:

Extrusion Temperature	-	725 <sup>o</sup> F
Die Temperature	-	500 <sup>o</sup> F
Ram Speed	-	0.025 ipm
Tubing Run-out Speed	-	2.24 fpm
Pressure on Billet	-	42,500 psi
Extrusion Ratio	-	61:1

Alloy ZLH 972 could not be successfully extruded in the large press indicating that, on the basis of present knowledge, this alloy could not be extruded by a commercially feasible practice.

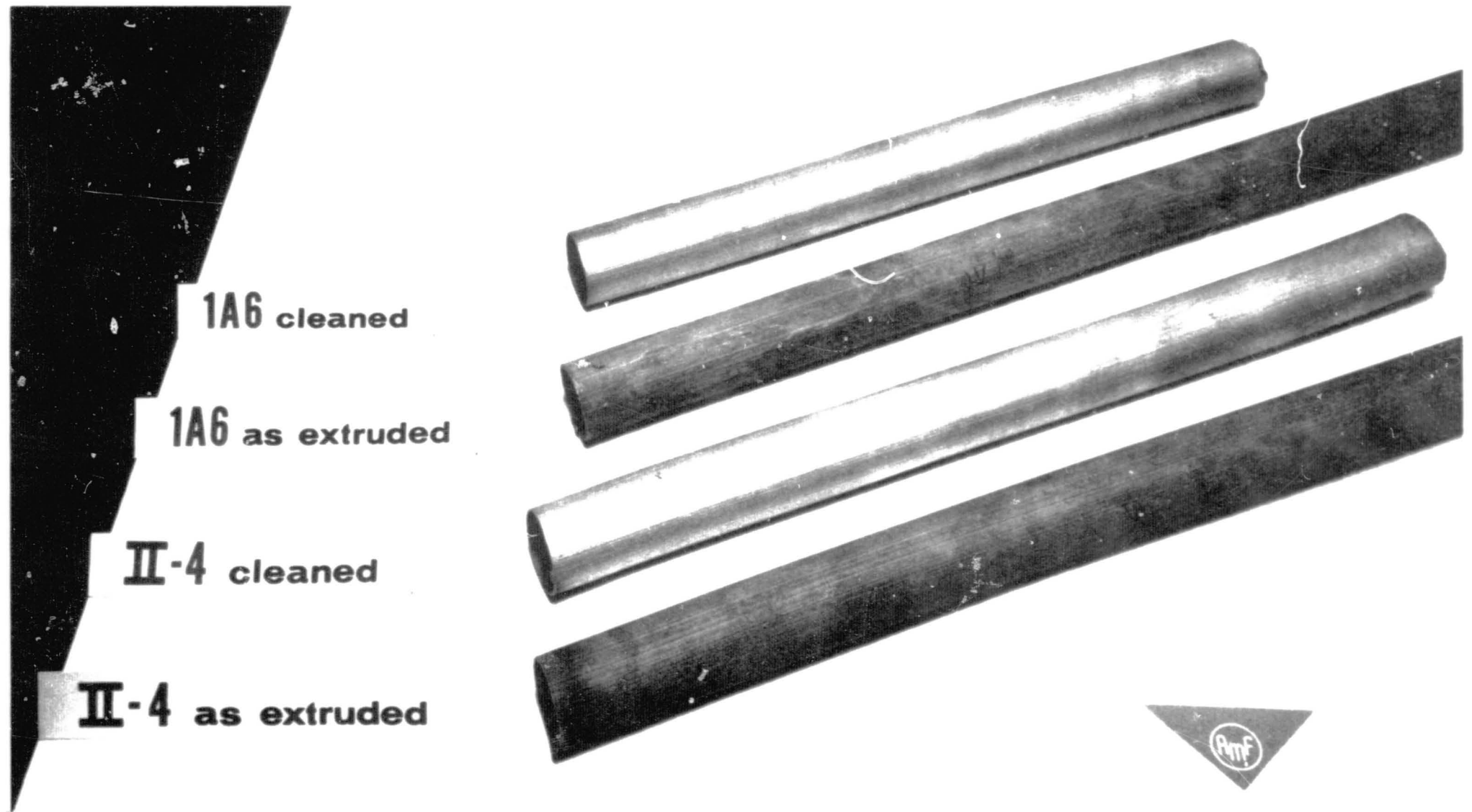


Figure 54. Tubing of alloys II4 and IA 6 extruded at 725<sup>o</sup>F with a die temperature of 500<sup>o</sup>F and ram speed of 0.025 ipm. Pressure on the billet was 42,500 psi and the extrusion ratio was approximately 61:1.

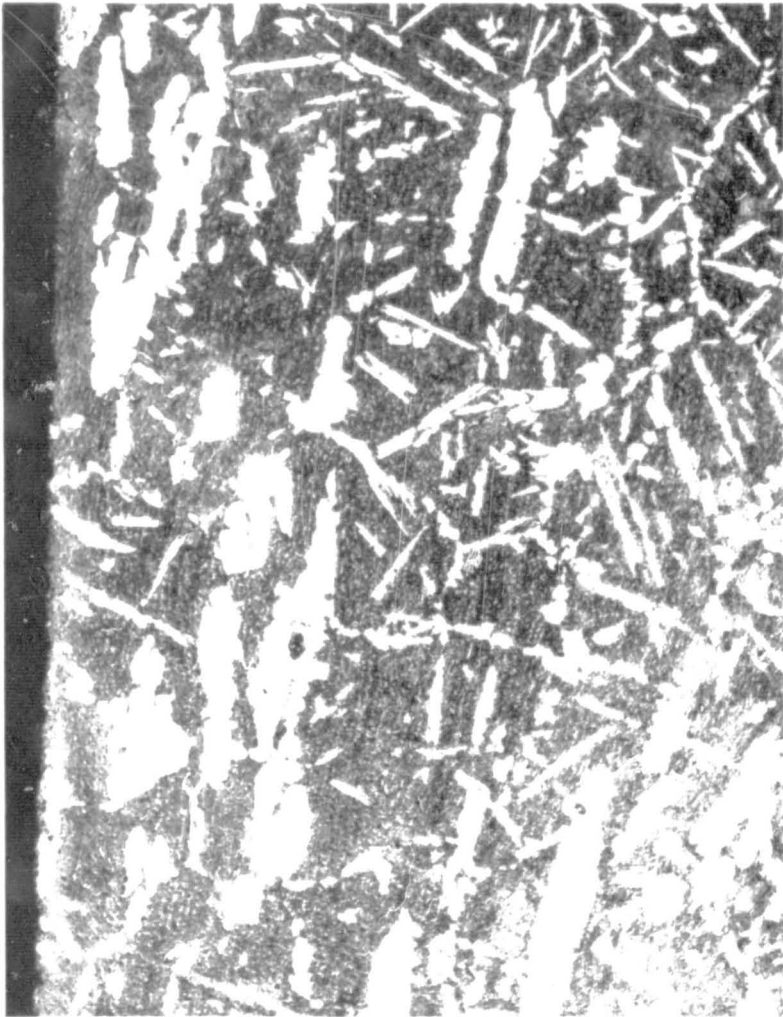


Figure 55 A

Alloy II4, 100X

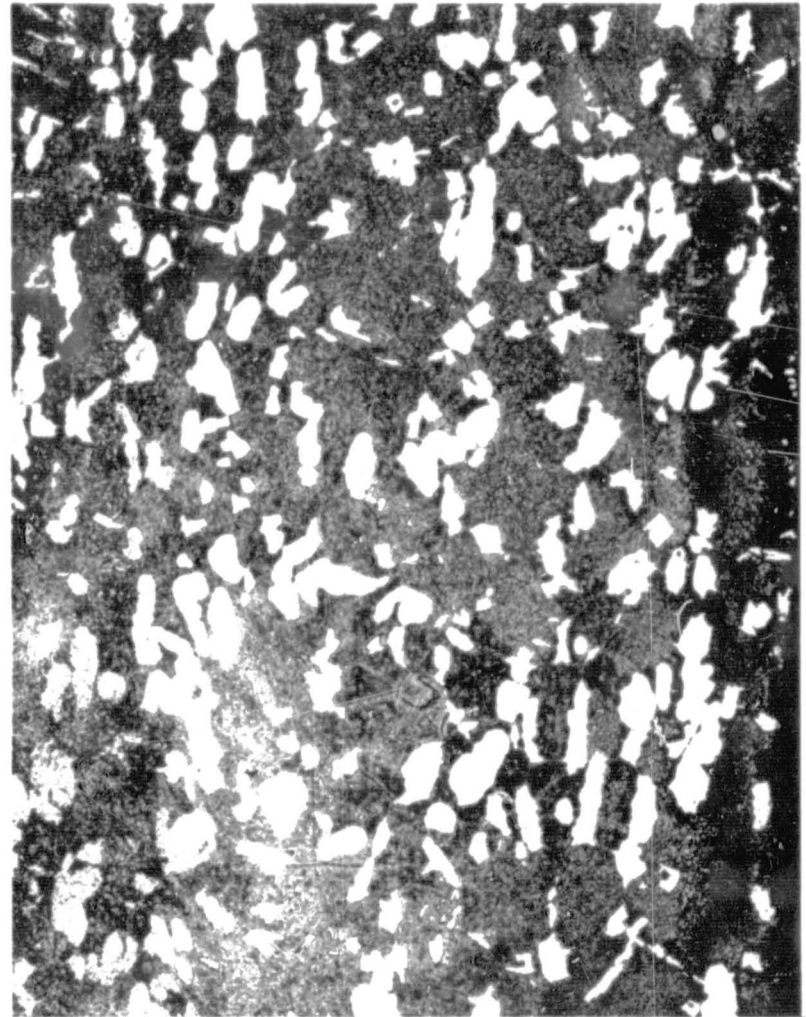


Figure 55 B

Alloy 1A6, 100X

Figure 55. Photomicrographs of extruded tubing of Alloys II4 and 1A6 showing the structure in the extruding direction. The high extruding temperature, 725°F, has resulted in segregation of lithium in both alloys and is more pronounced in Alloy 1A6. The average tensile strength of the extruded II4 material is 42,000 psi and the average tensile strength of the extruded 1A6 material is 27,500 psi.

The length of successfully extruded tubes was limited to four feet because of limitations on the available space in the extrusion press. Chemical analyses of the extruded material showed that approximately 1/2% of lithium was depleted from the first 1/2 inch extruded from the die and that the remaining portion of the tubing maintained the nominal composition of the original billet. The small amount of depletion was probably caused by oxidation and was not considered to be serious enough to warrant oxidation protection. A picture of two extruded tubes and two other sections cut from these tubes is shown in Figure 54. The outer surface of the tubing appeared rough because the die itself was in need of polishing and not because of any lithium depletion or other forms of corrosion which could be detected by conventional metallographic techniques, e. g., see Figures 55A and 55B.

Tensile specimens were machined from the tubes and tested in an Instron Tensile Testing Machine at ambient temperature. Careful machining had to be employed in order to avoid introducing notches in this very thin material and a special holder was made to grip the rounded surface. The average mechanical properties of the tubing were found to be:

Alloy IA 6 27,600 psi UTS, 22,000 psi YS (0.2% offset), 18.8% El in 2";

Alloy II 4 42,500 psi UTS, 35,000 psi YS (0.2% offset), 13.2% El in 2".

The low strength values obtained for alloy IA 6 were attributed to the high extrusion temperature rather than to the introduction of notches or to any difficulties attributed to holding the specimens in place during testing. The strength obtained for alloy II 4 was considered good although the variation in the data reduced the average tensile strength to below the 45,000 psi goal for the program.

The photomicrographs of the extruded material which are shown in Figures 55A and 55B show a segregated  $\beta$  structure indicating that higher strength and perhaps greater ductility could have been obtained if the material was extruded at a lower temperature but, unfortunately, this did not appear feasible.

Alloy ZLH 972 was brittle at the operating temperature, which, in addition to the welding difficulties, prevented the metal from extruding. This result confirms the high temperature brittleness effect encountered while hot rolling alloy ZLH 972 at 650°F to 800°F. The high temperature brittleness of this alloy was, therefore, confirmed and no further attempts were made to extrude it.

## 2.11 Final Tensile Properties

As a final phase of the program several 50 lb. lots of IIA alloy were prepared with the optimum melting and heat fabrication practices developed

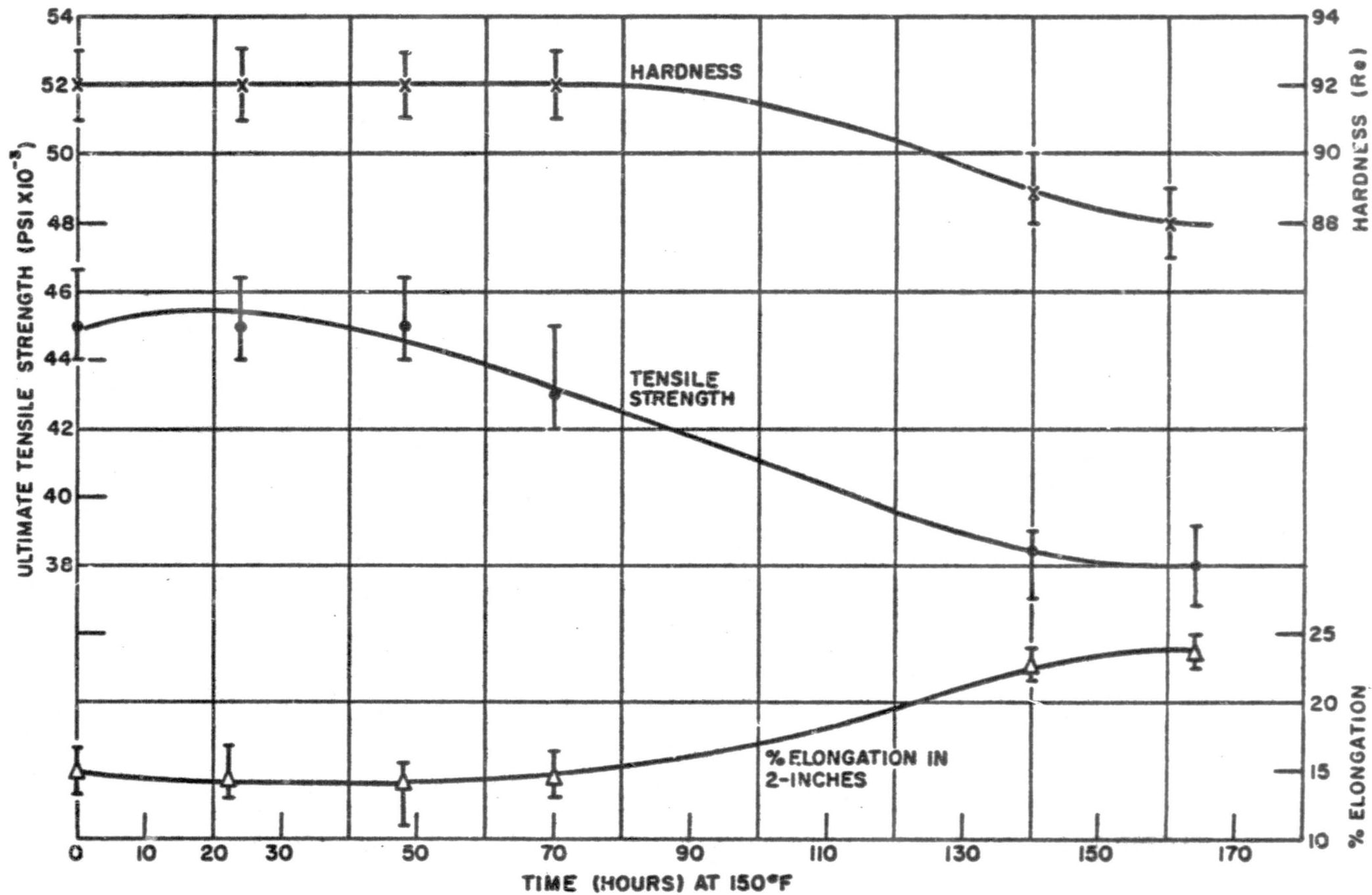


Figure 56. Properties of As-Rolled Alloy II4 After Exposure to 150°F for Various Time Intervals

in the course of this thirty-three month program. This material was then submitted to various heat treating practices and tested in tension at cryogenic to ambient temperatures; the alloy was also tested for thermal stability and all these data are summarized in the section below.

#### 2. 11. 1 Final II4, As-rolled Properties and Thermal Stability

The as-rolled tensile strength of the newest II4 material (heat number 4-9-1 rolled at 675°F with two final skin passes at 450° was found to be 45,000 psi after a total reduction of 85% which was exactly the average tensile strength obtained earlier in the program for material processed from heat number 4-8-2B.

After confirming the earlier test results, the stability of the as-rolled II4 material was tested by heating tensile specimens in a 150°F oil bath for various lengths of time and then testing them in an Instron Tensile Testing Machine at ambient temperature. The results of these tests are shown in Figure 56.

The as-rolled material was found to be stable at 150°F for 50 hours, but the average tensile strength dropped to 43,000 psi after 70 hours of exposure. These results are very similar to the results obtained earlier in the program when II4 tensile specimens, made from heat No. 4-8-2B material, were exposed for 72 hours at 150°F. At that time an average tensile strength of 43,500 psi was obtained after this lengthy exposure time and it was thought that the material was very stable considering that the thorium content of the 4-8-2B material was less than 1%. However, the new material, i. e., heat No. 4-9-1, had a thorium content of 1.5%, indicating there is little difference between the stabilizing effects of 1.5% and 1% thorium when the starting condition of the alloy is the as-rolled condition. Extending the total exposure time to 164 hours resulted in a reduction in tensile strength from 45,000 psi to 38,000 psi and a corresponding increase in elongation (within 2 inches) from 15% to 24%. Figure 56 indicates that the tensile strength is stabilizing at the minimum of 38,000 psi and the hardness, as measured on four separate specimens, did not change after 320 hours of exposure to 150°F.

#### 2. 11. 2 Mechanical Properties of Heat Treated Material

The results obtained thus far indicate that the II4 alloy can be used successfully in the as-rolled condition and that a sheet metal producer may safely ship and stock the material in warehouses in this condition without fear of degradation of the mechanical properties under ordinary service conditions where the temperature does not exceed 150°F. However, a manufacturer may wish to heat treat the material and earlier results have indicated the alloy will respond to heat treatment; therefore, to complete the alloy development, heat treating studies were continued.



Flat sheet specimens were solution heat treated at 625°F, 650°F, and 675°F for three hours in an argon atmosphere and then quenched by pushing them out of the hot zone of the furnace into a chamber cooled by running water. Earlier results have shown that the alloy is not sensitive to the rate of quench. The hardness of the material immediately after the quench was usually Re 88 but would increase to its permanent as-quenched hardness after approximately four hours at ambient temperature. This initial change in hardness is believed to be a reflection that quenched-in point defects serve as low activation energy nucleation sites for precipitation and accompanying hardening at low temperatures.

After the solution heat treatment, tensile specimens were machined from flat sheet material and either tested immediately or aged at 150°F. The results of testing material which was solution heat treated at 625°F is shown in Figure 57. The strength of the material in the T-4 (solution heat treated) condition was slightly low (42,800 psi) and, as is usually the case for these materials in the T-4 condition, the % elongation within 2 inches was low. The response to aging at 150°F was very sluggish as shown by the % elongation vs. time curve in Figure 57 which increased very slowly to about 5% after 94 hours at temperature. The average tensile strength also increased to a little more than 46,000 psi and the hardness remained essentially unchanged. Solution heat treating at 600°F results in the formation of a very fine precipitate of MgLi<sub>2</sub>ZnX, where X is Ag for the II 4 alloy, around the periphery of the ductile β phase. This precipitate is evidently stable at 150°F and a higher aging temperature, e.g., 200°F, is required to raise the elongation to 15% as was done earlier in the program.

Solution heat treating the II 4 alloy at 650°F resulted in a quicker response to aging at 150°F as shown in Figure 58. With this higher solution heat treating temperature the elongation rose to 15% after 30 hours at 150°F and the ultimate tensile strength remained unchanged for at least 50 hours although it seems to be declining after 70 hours.

Solution heat treating the II 4 alloy at 675°F resulted in very brittle material which showed little response to aging at 150°F as shown in Figure 59. The fractured surface of these specimens showed some evidence of grain growth which accounts for the poor ductility of the material after a 675°F solution heat treatment. No amount of aging will improve the ductility enough to overcome the effect of grain growth; 650°F will therefore be recommended as a safe upper temperature limit for solution heat treating.

### 2. 11. 3 Cryogenic Testing of II 4

Cryogenic tensile values are summarized in Table 6. The as-rolled tensile strength is exceptionally high at -320°F with some usable ductility (4% elongation). Stress relieving the specimens for 2 hours at 150°F did not improve the ductility and heat treated specimens tested in both liquid nitrogen

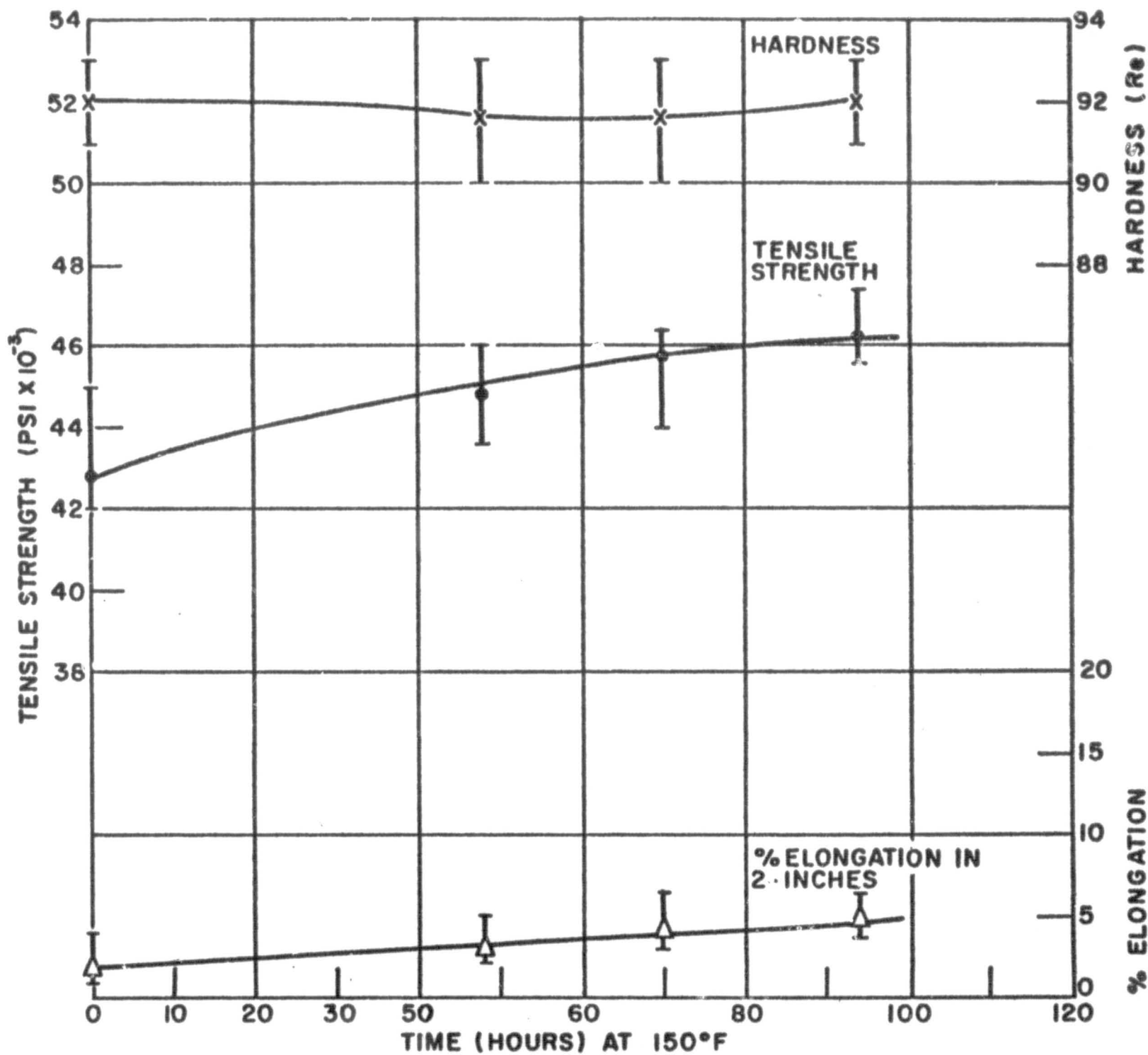


Figure 57. Properties of Alloy II4 Solution Heat Treated Three Hours at 625°F and Heated at 150°F for Various Time Intervals

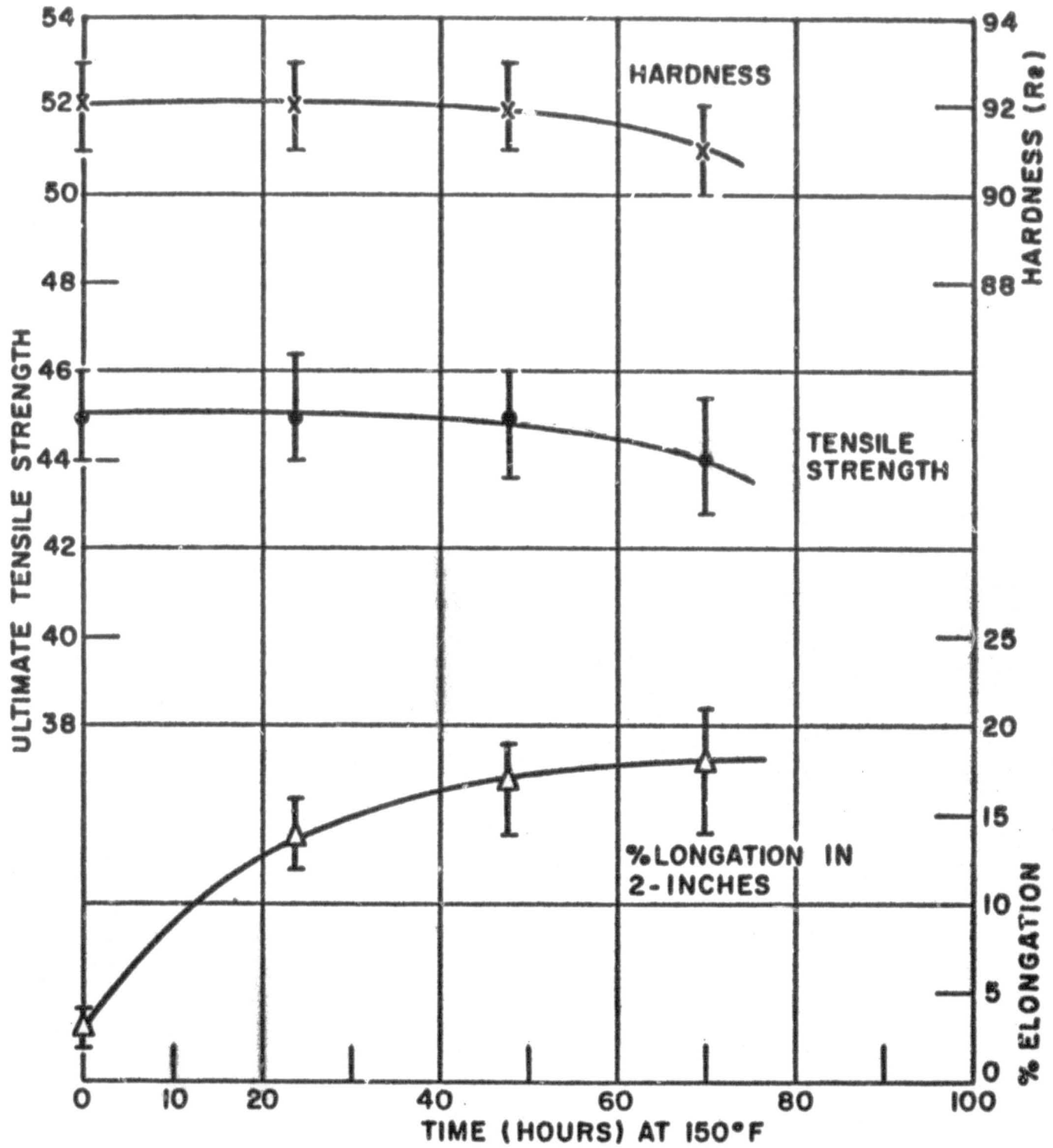


Figure 58. Properties of Alloy II4 Solution Heat Treated Three Hours at 650°F and Heated at 150°F for Various Time Intervals

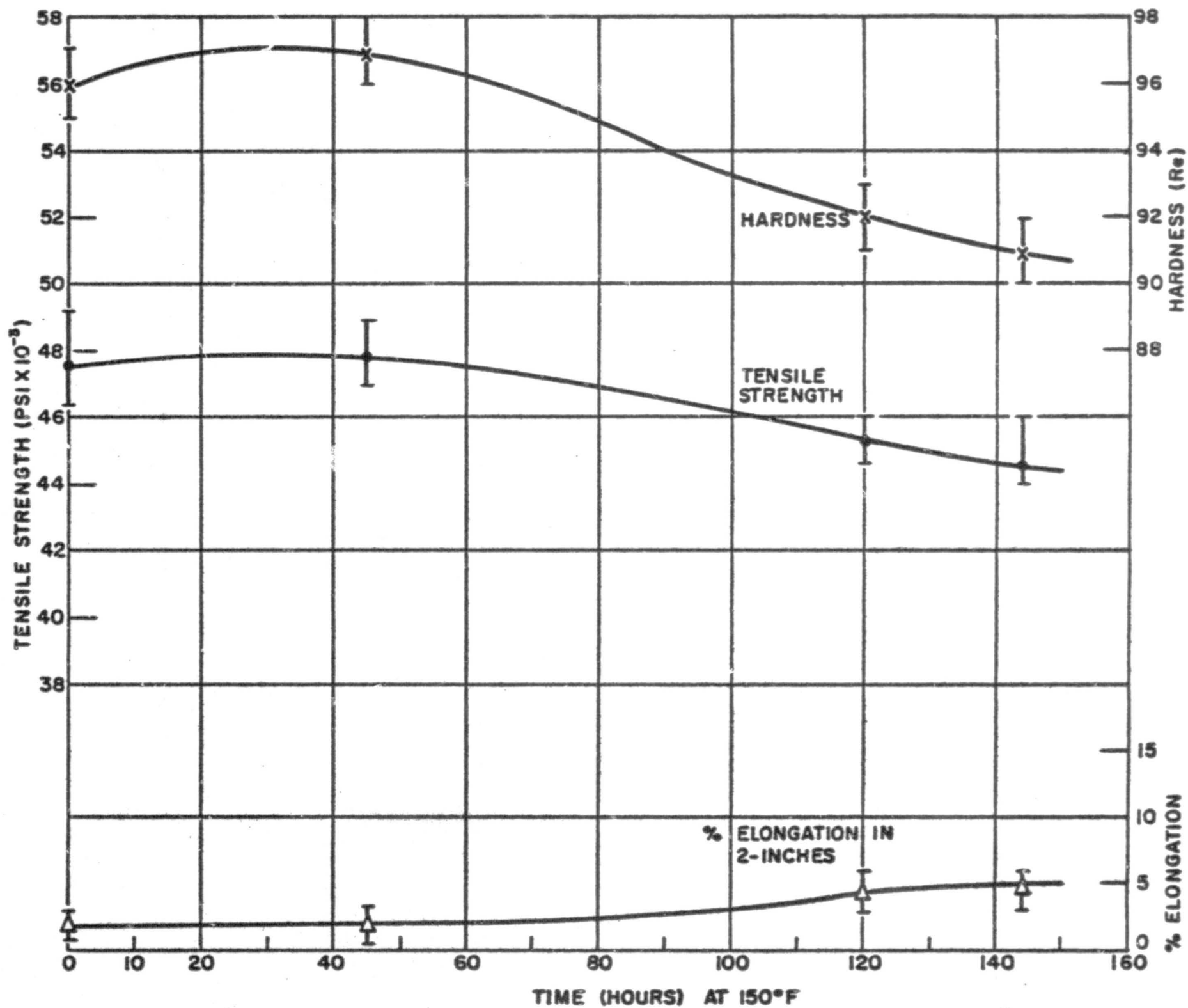


Figure 59. Properties of Alloy II4 Solution Heat Treated Three Hours at 675°F and Heated at 150°F for Various Time Intervals

TABLE 6

## SUMMARY OF THE TENSILE PROPERTIES OF II 4 ALLOY

Heat No.	Rolling	S. H. T.		Aging		UTS psi	0.2% YS psi	El. % in 2"	Hardness Re	Testing	Remarks
	Temp. °F	Temp. °F	Time Hrs.	Temp. °F	Time Hrs.					Temp. °F	
4-8-2B	675					48800	43500	2.4	95	68	95% Reduction
4-8-2B	675					45000	37000	15.0	90	68	85% Reduction
4-9-1	675/450					45000	38800	15.0	93	68	85% Reduction
4-9-1	675/450			150	24	45000	37800	14.6	92	68	
4-9-1	675-450			150	48	45200	38000	14.3	92	68	
4-9-1	675/450			150	70	43000	37000	14.9	92	68	
4-9-1	675/450			150	140	38500	32800	23.0	89	68	
4-9-1	675/450			150	164	38000	32300	24.0	88	68	
4-9-1	675/450	625	3	-	-	42800	39000	2.0	92	68	
4-9-1	675/450	625	3	150	48	44800	40000	3.0	91.6	68	
4-9-1	675/450	625	3	150	70	45900	40000	4.0	91.6	68	
4-9-1	675/450	625	3	150	94	46400	41000	5.0	92	68	
4-9-1	675/450	650	3			45000	41000	3.0	92	68	
4-9-1	675/450	650	3	150	24	45000	38000	14.0	92	68	
4-9-1	675/450	650	3	150	48	45000	37800	17.0	92	68	
4-9-1	675/450	650	3	150	70	44000	37000	18.0	91	68	
4-9-1	675/450	675	3	-	-	47500	42000	2.0	96	68	
4-9-1	675/450	675	3	150	45	47800	42000	2.0	97	68	
4-9-1	675/450	675	3	150	120	45200	40000	4.2	92	68	
4-9-1	675/450	675	3	150	144	44800	40000	5.0	91	68	
4-9-1	675/450	-	-	-	-	61000	55000	4.0	92	-320	
4-9-1	675/450	-	-	150	2	58500	52000	2.0	92	-320	
4-9-1	675/450	675	3	-	-	45500	39000	2.4	92	68	Transverse weld >97% weld efficiency
4-10-1	675/450	-	-	-	-	54500	47000	7.0	90	-452	Cross Rolled
4-10-1	675/450	-	-	-	-	62000	53000	4.0	92	-452	
4-10-1	675/450	-	-	150	100	58500	50500	8.5	90	-320	
4-10-1	675/450	650	3	150	100	59000	51000	8.0	92	-452	
4-10-1	675/450	650	3	150	100	56000	47000	2.0	90	-452	Transverse weld >94% weld efficiency

and liquid helium are seen to very substantially exceed the low temperature strength requirements as well as meeting the minimum ductility goal of 8%.

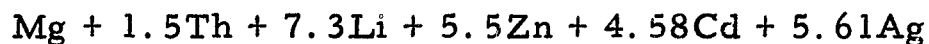
### 3.0 REFERENCES

1. T. G. Byrer, E L. White, and P. D. Frost, "The Development of Magnesium-Lithium Alloys for Structural Applications", page 20 of the Final Report on Contract NAS 8-5049.
2. J. B. Clark, "The Mechanism and Kinetics of Age Hardening Mg-Li Alloy Systems", WADC TR-57-405.
3. W. R. D. Jones and G. V. Hogg, "The Stability of Mechanical Properties of Beta Phase Magnesium-Lithium Alloys", J. Inst. of Metals 85, 1956-57, 255.

## APPENDIX I

### TECHNIQUES USED FOR CHEMICAL ANALYSES

The chemical composition of the ingot that is being saved for processing and delivery to the George C. Marshall Space Flight Center is as follows:



Chemical analyses play an extremely important part in this alloy development program. Therefore, with due respect to this phase of the program, the techniques which have been used to determine the chemical composition of the pilot lot ingots and the final wrought products are presented and discussed herein.

The methods used for the analyses of silver, thorium, lithium, zinc, aluminum and zirconium required dissolving the alloy in hydrochloric acid. The same dissolved sample could therefore be used for all these analyses.

#### Silver Determination

Approximately four gram samples of the Mg alloys were dissolved in about 30 ml of concentrated HCl. The acid must be added gradually in small amounts to prevent a violent reaction, otherwise part of the sample may be lost by sputtering and spraying. In certain alloys it was also necessary to add  $\text{H}_2\text{O}_2$  and to boil until the sample completely dissolved. The solution was then very concentrated in HCl. Upon dilution to about 250 mls. with  $\text{H}_2\text{O}_2$ , AgCl precipitated. The solution was allowed to stand overnight to coagulate the fine particles, filtered through a weighed Gooch crucible, and dried for about one hour at  $110^\circ\text{C}$ . The percent silver in the alloy was calculated from the weight of the AgCl (Ref. 1 p. 979). The filtrate was diluted to exactly one liter and saved for the Th, Li, Al and Zr determinations.

#### Thorium Determination

In the determination of the percentage thorium, an aliquot of the dissolved sample was used containing an estimated 2.5 mg of Th. The disodium salt of o-(2-hydroxy-3, 6-disulfo - 1 naphthylazo) benzenearsonic acid forms a colored complex with thorium, whose peak absorbance is around 545  $\text{m}\mu$ . At this wave length, the absorbance was proportional to the amount of thorium in solution. Absorbance measurements were made upon standard  $\text{Th}(\text{NO}_3)_4$  solutions and upon the unknown solutions with a Beckman DU Spectrophotometer. The absorbance readings of the standard solution, of

---

1. N. H. Forman (editor) Scott's Standard Methods of Chemical Analysis, Vol. 1 Sixth Edition, D. Van Nostrand Co., Inc., Princeton, New Jersey (1962).



which the exact thorium content was determined by gravimetric means, were plotted against the thorium concentration of the solution to prepare a calibration curve. The concentration of the Th in this curve ranged from 0 mg/100 mls to 1.25 mg /100 mls. Upon comparing the absorbance readings of the unknown samples to the data from the calibration curve, the amount of thorium in the samples was able to be calculated (Ref. 1 p. 626).

### Lithium Determination

Flame photometry was used to determine the percentage of lithium in the samples. Standard lithium solutions, ranging from 0 ppm Li to 10 ppm Li, were excited in an oxygen-acetylene flame and measured at 671 m $\mu$ . with a flame photometer attachment to the Beckman DU Spectrophotometer. The emission of the unknown samples was compared with the measurements of the standard solutions enabling the calculation of the percent lithium (Ref. 1 p. 602).

### Zinc Determination

In neutral or weakly alkaline solutions zinc forms a reddish purple complex with dithizone. The complex is soluble in CCl<sub>4</sub> and has a peak absorbance at about 540 m $\mu$ . The procedure followed was to add about 0.4 ml of the dissolved magnesium sample to a mixture of (a) 20 ml. of pH 5 ammonium oxalate-sodium acetate buffer solution, and (b) 20 ml. of dithizone in CCl<sub>4</sub>. The buffer solution also contained sodium thiosulfate and potassium cyanide to prevent interference from bismuth, cadmium, copper, lead, nickel and cobalt. The zinc complex was transferred to the CCl<sub>4</sub> layer by shaking in a separatory funnel. The zinc concentration was determined by absorbance measurements of the CCl<sub>4</sub> layer using the Beckman DU Spectrophotometer. Comparison was made to a calibration curve obtained using standard zinc solutions. The use of separatory funnels in the determination resulted in a reproducibility of about 10% (Ref. 2, p. 3713).

### Aluminum Determination

An aliquot of the dissolved sample was used which contained about 0.02g of aluminum. The Al was then precipitated as Al(OH)<sub>3</sub> by adding ammonia and NH<sub>4</sub>Cl. The NH<sub>4</sub>Cl maintained the pH below 10, thereby preventing the precipitation of Mg, Mn, Zn and Zr. The Al(OH)<sub>3</sub> was collected on Whatman No. 40 filter paper, and then washed into a beaker and dissolved in 50:50 HCl. Tartaric acid was added to prevent reprecipitation of Al(OH)<sub>3</sub>, and the solution was made just basic using ammonia, and then made just acidic using 10:90 acetic acid. Fifty milliliters of 8-hydroxyquinoline in acetic acid, and 50 ml. of ammonium acetate solution are added to the aluminum solution maintained at 70-80°C. Aluminum oxinate [Al(C<sub>9</sub>H<sub>6</sub>ON)<sub>3</sub>] precipitated out, was retained on a Gooch crucible, dried at 130-140°C, and weighed. (Ref. 2, p. 103).

- 
2. A. Mayer and W. J. Price Chemical and Spectrographic Analysis of Magnesium and Its Alloys, Magnesium Elektron LTD, Manchester, England (1954).

### Soluble Zirconium Determination

Zirconium forms a colored complex with alizarin red S at a pH of 0.6 to 0.7. Absorbance measurements were performed at 510 m $\mu$  using the Beckman DU Spectrophotometer. A calibration curve was prepared using a standard zirconyl chloride solution. (Ref. 1, p. 631.)

### Maganese Determination

For the determination of manganese and cadmium, the HCl sample solutions could not be used. The analyses required dissolving the samples in H<sub>2</sub>SO<sub>4</sub>.

Approximately 2g. samples of the alloy were dissolved in about 50 mls. of H<sub>2</sub>SO<sub>4</sub> and 5 mls. of HNO<sub>3</sub>. Samples of pure Mn metal were also dissolved in acid for calibration purposes. In these acid solutions, potassium periodate was added to oxidize the manganese to permanganate ion which has a peak absorbance of 545 m $\mu$ . The percent manganese was obtained from photometric measurements performed with the Beckman DU. (Ref. 1, p. 612.)

### Cadmium Determination

A one gram sample of the alloy was dissolved in sulfuric acid. Hydrogen peroxide was decomposed by boiling and silver was displaced with pure iron wire to prevent interference. After filtering, phenyltrimethyl ammonium iodide was added to form an insoluble cadmium complex which was retained on a fine Gocch Crucible. The precipitate was dissolved with ammonium hydroxide and HCl was added to form HI. The hydriodic acid was volumetrically titrated with potassium iodate solution till a carbon tetrachloride layer was decolorized. The amount of cadmium in the sample was calculated from the volume of KIO<sub>3</sub> and the weight of alloy used. (Ref. 2, p. 805.)

### Alternate Zinc Determination (Potentiometric Method)

An alternate method for zinc analysis, which is limited however because of silver and cadmium interference, involved the potentiometric titration of the alloy dissolved in sulfuric acid. The zinc was titrated with potassium ferrocyanide solution using platinum and calomel electrodes. Silver interference was avoided by adding HCl and filtering to remove AgCl. (Ref. 1, p. 630.)

### Magnesium Determination

The alloy was dissolved in concentrated HCl, and the solution neutralized with NaOH using methyl red indicator. Ten mls. of a Na<sub>2</sub>S solution was added to precipitate interfering metals such as aluminum, zinc, cadmium and manganese. The magnesium was then precipitated using 1N NaOH, filtered through Whatman #40 filter paper, and titrate one-tenth of the volume of the filtrate with 0.1N HCl to the methyl red end point. The difference between the

1N NaOH and the 0.1N HCl used for back-titration was equivalent to the 1N NaOH used to precipitate the magnesium. (Ref. 1, p. 636.)

## APPENDIX II

### Chemical Analyses

The chemical analytical techniques used throughout the program were summarized in Quarterly Progress Report Number 8, 15 January 1967, and is repeated in this final summary report, Appendix I. The results of chemical analyses which were recently completed and which were not reported previously are tabulated below in Table 1.

TABLE 1

#### COMPOSITION OF EXPERIMENTAL MAGNESIUM BASE ALLOYS

<u>Alloy</u>	<u>Heat No.</u>	<u>%Th</u>	<u>%Li</u>	<u>%Zn</u>	<u>%Ag</u>	<u>%Al</u>	<u>%Mn</u>	<u>%Cd</u>	<u>%Zr</u>
ZLH972	Z-6-4	1 to 0.6	6.1	7.0					
ALH972 Top	Z-3-3	0.3	7.3	8.0					
ZLH972 Bottom	Z-3-3	0.4	6.6	8.7					
ZLH972	Z-1-1	0.89	-	8.6					
IA6 Top	6-5-1	0.0	14.2	2.2		3.3			
IA6 Bottom	6-5-1	1.2	13.5	1.7	4.0				
IA6	6-10-2A	0.04	8.2	1.6	3.0		0.07		
II4 Top	4-4-1	1.4	6.7	8.0	6.0				0.04
II4 Bottom	4-4-1	1.1	7.2	8.0	6.1				0.01
II4	4-8-2B	0.5	7.1	5.9	5.5			2.4	0.01
II4	4-9-1		7.3		6.37				
II4	4-10-1		6.9		5.86				
II4	4-11-1		7.3		5.90				

Alloy IA6, heat No. 6-5-1, was reported earlier as being too high in lithium. This observation was based upon metallographic techniques which showed a two phase alloy with an excess of  $\beta$  phase. The reason for the alloy not being single phase with 13-14% Li is not apparent but must be associated with the effect of the other elements (Zn, Ag, Al, Mn) on the structure of the alloy.

There is a small difference between the chemical composition at the top of an ingot compared to that found at the bottom, as might be expected, but there is no indication that the light element lithium has segregated to the top or that heavier elements have settled on the bottom. Alloy II4, heat 4-4-1, shows a slightly higher lithium content of 7.2% near the top than that of 6.7% near the bottom. The difference in the zinc content of the alloys was not significant.